CRYSTAL CHEMICAL STUDIES ON THE GROWTH SIZE PROBLEM OF Y ZEOLITE

Der Naturwissenschaftlichen Fakultät der

Gottfried Wilhelm Leibniz Universität Hannover

Zur Erlangung des Grades

Doktorin der Naturwissenschaften

Dr. rer. nat.

genehmigte Dissertation

von

Nada Salman

geboren am 21. Oktober 1976 in Hreissoun, Syrien

November 2006

ABSTRACT

Synthesis of (if possible large sized) pure zeolite Y crystals of high Si : Al ratio (n_{Si}/n_{Al}) was performed in the first part of the present work. Therefore, the reproducibility of important procedures, given in the literature was checked and modifications like the use of a nucleation solution were worked out to obtain pure phase products with high n_{Si}/n_{Al}. The characterization showed that no high silica zeolite Y crystals of sizes bigger than 1 µm could be prepared and a systematical decrease in size with increasing n_{Si}/n_{Al} was found.

For a better understanding of the relation of growth behavior and the n_{Si}/n_{Al} ratio of the products an investigation of Y-type formation mechanism was performed in a further experimental section. A control of the mother liquor during gel aging and crystal growth was found to be an effective tool for directing the crystallization process with respect to crystal size and morphology. Substitution experiments of the mother liquor in a broad n_{Si}/n_{Al} range gave valuable information how the species in the solution are responsible for formation of the final type of zeolite. The influence of the alkalinity was also investigated in this experimental series. It was found that an increase of alkalinity led to an increase or to a decrease of n_{Si}/n_{Al} of the finally crystallized Y zeolite according to the initial batch condition and silica source. An increase in n_{Si}/n_{Al} (2.43) of the final Y zeolite was observed if the substitution of mother liquor by sodium hydroxide occurred directly after aging at RT while a decrease in n_{Si}/n_{Al} (2.15) of the final product happened if the mother liquor was substituted by sodium hydroxide after the nucleation stage of the initial batch. In all cases, however, this procedure prevented the formation of undesired admixtures during the heating period of the batch up to the temperature of zeolite Y crystallization.

Steaming procedure was investigated for further understanding of the relations between the nature of FAU synthesis gel and the homogeneity or heterogeneity of the crystalline framework with different n_{Si}/n_{Al}, as well. Three characteristic ranges of composition possessing significant differences have been observed from the steaming behavior. For ratios n_{Si}/n_{Al} of 1 to 1.5 the framework completely hydrolyses during the hydrothermal treatment denoting a total structure collapse which is, therefore, related to pure zeolite X following Breck´s original definition. An intermediate range has been experimentally selected to be of $1.7 \leq n_{Si}/n_{Al} \leq 2.2$. Samples of such compositions reveal a partial dealumination and amorphization during steaming which can be related to the existence of X/Y phase mixtures. The ratio $n_{Si}/n_{Al} = 2.428$ defines a critical value. Infinite silicon chains must occur over the whole framework for $n_{Si}/n_{Al} > 2.428$. This leads, therefore, to a new definition of zeolite Y for $n_{Si}/n_{Al} > 2.428$. It can be concluded that only FAU type zeolite with $n_{Si}/n_{Al} > 2.428$ can be optimally dealuminated with a minimum content of amorphous phase.

As the starting synthesis experiments even all the other experimental research of the present work showed that no zeolite Y crystals of sizes bigger than 1 µm could be prepared. Therefore, the obtained FAU zeolites showed a systematical decrease in size with increasing n_{Si}/n_{Al}. Consequently, all syntheses reported in literature about the synthesis of large Y zeolite crystals after Breck definition ($n_{Si}/n_{Al} > 1.5$) but with n_{Si}/n_{Al} lower than 2.428 should be considered as X/Y type mixture zeolites.

Temperature and time effects during steaming experiment on Y zeolite of $n_{Si}/n_{Al} = 2.7$ have been discussed. At temperatures below 573 K a framework dissolution takes place as a consequence of the attack of water molecules (chemical reaction). At temperatures above 973 K a thermal reaction is dominant leading to a total collapse of Y framework. Between 673 K and 573 K a significant framework dealumination takes place and the degree of dealumination becomes higher with temperature increase within this range. The optimal temperature for dealumination is found to be at 873 K. Effect of steaming time is more dominant at higher temperatures (up 973 K). Normally the effective time range is between 1 and 3 hours. Up 3 hours a low steaming effect with time increase is observed for all series.

Keywords: Zeolite-synthesis, formation mechanism, Dealumination

ZUSAMMENFASSUNG

Im ersten Teil der vorliegenden Arbeit wurden Experimente zur Synthese großer Kristallite von Zeolith Y mit hohem Si:Al Verhältnis (n_{Si}/n_{Al}) durchgeführt. Dabei wurde zunächst die Reproduzierbarkeit einiger, in der Literatur angegebener Rezepturen überprüft. Anschließend wurden diese modifiziert, z.B. durch Verwendung von Keimbildungslösungen, um phasenreine Produkte mit hohem n_{Si}/n_{Al} Verhältnis zu erhalten. Bei allen Syntheseexperimenten konnten jedoch, keine siliziumreichen Y-Zeolithe mit Kristallitgrößen > 1 μm hergestellt werden. Um die Ursachen dafür zu klären, wurden spezielle experimentelle Untersuchungen zum Bildungsmechanismus von Zeolith Y aus alumosilikatischen Gelen durchgeführt. Die Kontrolle der Mutterlaugen während des Alterns der Gele und während der Kristallisation erwies sich als wichtiges Instrument zur Klärung des Kristallisationsverhaltens, insbesondere der Beziehungen von Kristallitgröße und Morphologie in Abhängigkeit vom Verhältnis n_{Si}/n_{Al}. Experimente unter Substitution der Mutterlauge durch Lösungen mit unterschiedlichem (n_{Si}/n_{Al}) zeigten hier den Einfluss der Spezies in der Lösung auf die Struktur, Zusammensetzung und Kristallitgröße des gebildeten Produktes. Der Einfluss der Alkalinität wurde ebenfalls untersucht. Es zeigte sich, dass zunehmende Alkalinität der Mutterlauge sowohl zu höherem n_{Si}/n_{Al} als auch zu niedrigerem n_{Si}/n_{Al} führen kann, je nach Zustand des Ausgangsansatzes und der zur Gelfällung verwendeten Silicatquelle. So wurde ein Anstieg des n_{Si}/n_{Al} Verhältnisses von Y Zeolith (n_{Si}/n_{Al} 2.43) beobachtet, wenn die Mutterlauge direkt nach der Gelalterung bei Raumtemperatur durch NaOH ersetzt wurde. Hingegen führte der Ersatz unmittelbar nach dem Keimbildungsstadium zu einem Produkt mit geringerem n_{Si}/n_{Al} von 2.15. In allen Fällen verhinderte die Substitution aber die Bildung von Fremdphasen während der Aufheizperiode des Ansatzes auf die Kristallisationstemperatur.

Um weitere Hinweise auf den Zusammenhang zwischen der Natur des Gels und dessen Einfluss auf die Homogenität oder Heterogenität der Gerüststruktur des Produktes zu erhalten, wurde die hydrothermale Stabilität der Zeolithe („Steaming-Verhalten") in Abhängigkeit vom n_{Si}/n_{Al}–Verhältnis untersucht. Dabei wurden drei charakteristische Bereiche der Zusammensetzung mit jeweils unterschiedlichem „Steaming-Verhalten" gefunden.
Im n_{Si}/n_{Al} Intervall von 1.0 - 1.5 findet eine vollständige Zersetzung der Zeolithstruktur infolge der Hydrolyse der Al-O-Si-Bindungen während der Hydrothermalbehandlung statt. Dieses Verhalten entspricht dem von Zeolith X-entsprechend Breck´s klassischer Definition entsprechend dem Si/Al-Verhältnis der Faujasit-Struktur (FAU). Ein intermediärer Bereich konnte zwischen $1.7 \leq n_{Si}/n_{Al} \leq 2.2$ bestimmt werden. Solche Proben zeigten sowohl partielle Dealuminierung als auch partielle Amorphisierung. Dieses Verhalten ist ein Hinweis auf die Existenz heterogener X/Y Phasengemenge. Alle Proben mit einem höheren n_{Si}/n_{Al} zeigten wiederum ein anderes „Steaming-Verhalten". Sie konnten optimal dealuminiert werden mit minimalen amorphen Anteilen. So konnte gezeigt werden, dass ein n_{Si}/n_{Al} Verhältnis von 2.428 einen kritischen Wert darstellt, denn für $n_{Si}/n_{Al} > 2.428$ existieren erstmals unendlich ausgedehnte Silicatketten im zeolithischen Strukturgerüst. Dieser Umstand könnte auch zu einer neuen Definition für Y-Zeolith benutzt werden: Y Zeolithe sind Zeolithe vom FAU-Typ mit $n_{Si}/n_{Al} > 2.428$. Nur diese zeigen ein optimales „Steaming-Verhalten".

In allen hier durchgeführten Synthesen konnte siliziumreicher Zeolith Y mit einer Kristallitgröße über 1 μm nicht synthetisiert werden. Vielmehr wurde eine Abnahme der Kristallitgröße mit zunehmendem n_{Si}/n_{Al} Wert festgestellt. Demzufolge sollten alle großen Kristallite vom FAU-Typ, die in der Literatur nach Breck`s Definition ($n_{Si}/n_{Al} > 1.5$) als Y Zeolithe beschrieben werden, bis hin zu einem n_{Si}/n_{Al} von 2.428 als Mischung aus X/Y Typ Zeolithen angesehen werden.
Abschließend wurde der Einfluss von Temperatur und Behandlungszeit auf das „Steaming-Verhalten" von Y Zeolith mit einem n_{Si}/n_{Al} Wert von 2.7 untersucht. Unterhalb einer Temperatur von 573K fand Auflösung statt (Hydrolyse), bei hoher Temperatur (973 K) hingegen thermische Zersetzung (Kollabieren des Strukturgerüstes). Im Bereich zwischen 673K und 573K erfolgte die Dealuminierung des Gerüstes, deren Grad mit zunehmender Temperatur in diesem Intervall anstieg. Als optimale Bedingung für die Dealuminierung wurde eine Temperatur von 873 K festgestellt. Der Effekt der Dauer der Behandlung wirkte sich bei hoher Temperatur merklich aus, am effektivsten waren Zeiten zwischen 1 und 3 Stunden. Längere Zeiten führten zu einer Verringerung des „Steaming Effekts".

Schlagwörter: Zeolithsynthese, Bildungsmechanismus, Dealuminierung

LIST OF CONTENTS P

LIST OF TABLES

LIST OF FIGURES

.

1. Introduction

Zeolites are porous tectosilicates usually of a three dimensional aluminosilicate framework structure with micropores or channels. The framework cavities are occupied by cations and water molecules. The first description of a natural zeolite had been accomplished by A. Cronstedt in 1756 [1]. The earliest systematic investigations on zeolite syntheses were started by R. M. Barrer and co-workers in the late 1940`s [2] but very soon zeolites have been widely used as molecular sieves, adsorbents, ion exchangers and catalysts in petrochemistry [3]. A great variety of natural and synthetic structure types is known up to now. Some synthetic zeolites have a natural counterpart, like the famous X and Y-type zeolites which have the structure of the mineral faujasite (FAU) [4]. Faujasite zeolites have a broad range of Si/Al ratio (n_{Si}/n_{Al}) from 1.0 (LSX-type) over 1.2 (13X) up to 2.4 – 3.0 (Y-type). For a special use dealuminated Y zeolites with n_{Si}/n_{Al} up to 100 were prepared. Figure 1 shows well shaped octahedral faujasite crystals grown on phillipsite [5].

Fig. 1. Faujasite crystals grown on phillipsite. Crystal size is ~ 1.5 mm, ref. [5].

The typical chemical composition of faujasite is given in [6] by the form:

$$(Ca^{2+}, Mg^{2+}, Na^+_2)_{29}(H_2O)_{240} [Al_{58}Si_{134}O_{384}] \quad (1)$$
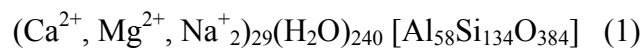
The faujasite structure is formed by the connection of tetrahedral TO_4-units (T-atoms: Si , Al) via oxygen bridges forming polyhedral cages called sodalite cages or β-cages. Every sodalite cage is built up through the connection of 24 T atoms. Finally, the three dimensional faujasite framework is formed by linking of sodalite cages through 6-6 secondary building units also termed double six-ring (D6R) units [6]. Channels along [111] crystal direction were formed this way with 12-ring "openings" of 7.4 x 7.4 Å. The connection of the sodalite cages by the

D6R-units leads to formation of super-cages, called α-cages. Because of the tetrahedral co-ordination, the Al atom is negatively charged. The cations compensate the negative charge of the zeolite framework. Water molecules are arranged as cage-filling atoms or molecules mainly inside the α-cages and some also inside the sodalite cages. A sodalite cage and the FAU framework are shown in figure 2.

a   b
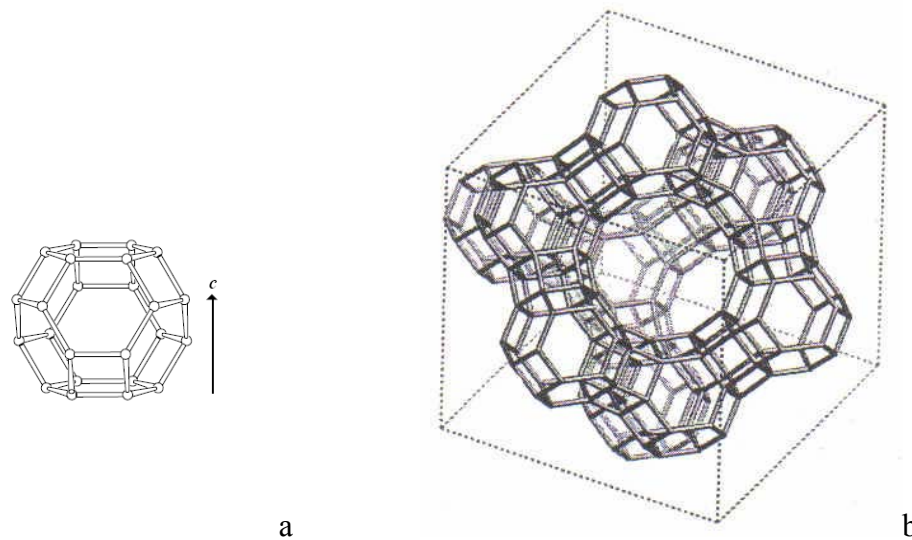
Fig. 2. Linking of T- atoms form the sodalite cages (a) which are linked in turn through D6R forming the FAU framework (b), ref. [6].

The crystal system of FAU is cubic and with the space group Fd-3m. The framework density is 13.3 T/1000Å^3. The cell parameter of a typical faujasite with the chemical composition (1) is a =24.345Å. Figure 3 shows a projection of the faujasite framework along the [010] direction [6].

Synthetic X-, Y- type zeolites are traditionally synthesized from aluminosilicate gels in an alkaline medium at hydrothermal conditions as has been previously described in many works, e.g. [2] and [7]. The size of the crystals with different n_{Si}/n_{Al} values synthesized in such way usually varied from $\leq 1\mu m$ up to few micrometers. This size characterizes, in most cases, the particle size (as measured by SEM, see 2.4.3.) because especially zeolite Y is polycrystalline consisting of crystallites of 50 – 200 nm (as estimated by XRD, see 2.4.1.). A typical composition of a synthetic Y-type zeolite is given by [7]:

$$Na_{56}[Al_{56}Si_{136}O_{384}]\, 250\, H_2O \quad (2)$$
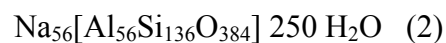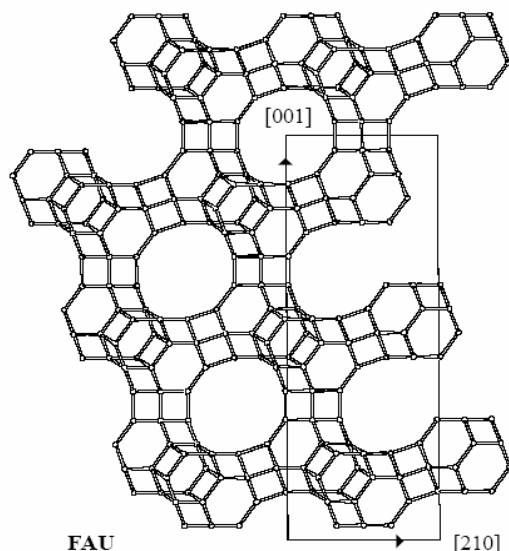
Fig. 3. Projection of the faujasite framework along [010], ref. [6].

The direct synthesis of X-, Y-type zeolites from gels has been discussed in huge number of works starting with the early works of Barrer [2], Breck [4] and Zhdanov [8-9], who accomplished particular investigations in fields of zeolite chemistry, structures and applications followed by kinetic studies on gel formation and synthesis of Y zeolite performed by Fahlke et al. [10-11], Thilo et al. [12] and Flanigen [13] as well as the significant works of Lechert et al. [14-20] on the mechanism of nucleation and crystal growth of X and Y zeolite and the role of the pH value and gel aging in controlling the crystallization process and many other works [21-30]. Additionally there are variant investigations concern the appointment of various spectroscopic methods for solid phase (gels, crystalline powders) and liquid phase (mother liquors and supernatants) analyses like ^{29}Si MAS NMR spectroscopy [31-32], IR Spectroscopy [33-34] and Raman spectroscopy [35].

Whereas most of the technical applications of FAU zeolites need materials of only 1 μm grain size like the fluid catalytic cracking (FCC) process (made by spray drying of spheres of zeolite mixtures dispersed in an inorganic oxide matrix [36-38]), large particles with dimensions over 100 μm are of specific academic interest for understanding the synthesis mechanism. There are several publications in literature on syntheses of large scale X- and Y crystals but most of them, however, are not available for industrial uses.

Developed procedures on the synthesis of large crystals of faujasite have been pointed out using several techniques such as templating with organic cation or complexes [39-41]. Large X type crystals up to 140 μm of n_{Si}/n_{Al} of 1.36 has been synthesized by Charnell [39] using

triethanolamine as complexing or stabilizing agent. However, P (gismondine structure type-GIS) zeolite existed as a second phase in the final product. This procedure has been later used and modified by Ferchiche et al. [40]. These authors were comprised fumed silica, as silicate source (Cab-O-Sil M-5), with sodium aluminate and the template bis(2-hydroxyethyl)dimethylammonium chloride (TCl) in an aqueous triethanolamine (TEA) cosolvent. The final products contained mixtures of large FAU octahedral of ~175-245 μm with $n_{Si}/n_{Al} = 1.71$ and polycrystalline spheres of GIS type. The same procedure was repeated by Berger et al. [41] and faujasite crystals of crystal size between 10-100 μm were obtained with $n_{Si}/n_{Al} <1.8$ and with formation of P zeolite as the main product. After Breck's definition [4] of X- ($n_{Si}/n_{Al} <1.5$) and Y- ($n_{Si}/n_{Al} > 1.5$) types the FAU crystals synthesized by [40] and [41] were considered as Y type crystals.

The formation of P type zeolite of the GIS (gismondine) structure as by-product or main product was the main problem in the previously mentioned procedures. It is known that the crystallization of P starts in the late stage of synthesis of X and Y zeolites and its level increases when the gel is crystallized for long periods [42]. Consequently, attempts were carried out to avoid crystallization of multi-phases from the batch employed for FAU zeolite synthesis. Kacirek et al. [42] have shown that adding of seed crystals to an initial gel before crystallization may reduce the formation of P as an impurity phase in faujasite type zeolite product. This procedure was repeated again in [41] using seeds of zeolite Y. Whereas the final product was FAU phase of 30-40 μm in size with 1-5 % of P phase when seeds with n_{Si}/n_{Al} of 3.35 and 3-4 μm were used, a FAU phase of 30-100 μm with higher amount of P phase (15 %) was produced when seeds with n_{Si}/n_{Al} of 1.54 and 10 μm were used with a broader size distribution.

Lechert et al. [14] used a nucleation gel aged for 4 days at RT with a nuclei radius of ~ 100 nm as seeding agent. The result shows that the nucleation gel is more effective than the seed crystals with a radius of 230 nm. The liquid phase produced over this nucleation gel after aging was also used by Lechert et al. [14], with an average nuclei radius in the solution of ~ 50 nm, as well as by Robson [43]. The results show that FAU type zeolite has been produced in a shorter time, i.e. the nucleation solution used was more active than both the seed crystals and the nucleation gel. However, the exist of a small amount of P zeolite as an impurity phase in FAU synthesis in which the upper liquid was used, has been referred in [43]. Other attempts of synthesis of large X and Y crystals have been reported by [44], [45] and [46].

Synthesis of Y crystals of high n_{Si}/n_{Al} and large crystal size suitable for dealuminated-structure applications (catalysts) was also the aim of many works. Dealumination procedure have been developed starting from works of Zhdanov, Kiselev, Barthomeuf and co-workers [47-50], Breck and Flanigen [51-52] and Dempsey [53], Lohse and Engelhardt and co-workers [54-57]. There are also works concerning the ion-exchange treatment [58-59] and characterization of the dealuminated structure using different methods like IR spectroscopy [60] and adsorption methods [61] or the characterization depending on cation exchange capacity and standard chemical analysis [62]. Data of XRD and IR methods [63-65] can be calibrated by ^{29}Si and ^{27}Al MAS NMR, which were used successfully for investigation of basic building units distribution in faujasite framework [66-73].

Despite all those experimental studies on X- and Y-type zeolites formation many questions concerning the relations between synthesis parameters, chemical composition and the resulting crystal size are still open. Therefore three aims of the present work have been pointed out.

Firstly, the synthesis of (if possible large sized) pure Y-type crystals of high n_{Si}/n_{Al} suitable for specific applications as hydrophobic adsorbent in gas separation processes or more thermally stable FAU molecular sieves. Therefore, the reproducibility of the procedures of Charnell [39], Ginter et al. [7] and Ferchiche et al. [40] was checked and modifications on these procedures were performed to avoid crystallization of multi-phases and to increase the n_{Si}/n_{Al} (if possible). Using the nucleation solution (see 2.1.1.) in this work as a structure-directing agent for synthesis of Y zeolite was successful for avoiding (or minimizing) the formation of impurity phases, increasing the degree of crystallinity of the sample and producing FAU zeolites with higher n_{Si}/n_{Al} values.

Secondly, a control on the mother liquor during gel aging and crystal growth as an effective tool for directing the crystallization process with respect to crystal size and morphology. Therefore, further syntheses were performed to get a deeper insight into the structural and compositional changes of the aluminosilicate gel and the mother liquor during aging as well as during crystallization period. For this the solution over the solid phase was separated at different synthesis stages and analysed by ICP-OES method (see 2.4.7.)

Finally, finding out the reason of different growth behaviour of FAU type zeolites as a function of their silica content. For this aim, investigations on the structural distinction of the synthetic X-, Y-type zeolites with n_{Si}/n_{Al} between 1.2–2.7 through their different thermal and chemical behaviour under hydrothermal treatment were performed. Important structural differences such as the length of silicate chains as well as the heterogeneities of the aluminium distribution could be derived from the different steaming behaviour of the samples.

2. Experimental

2.1. Synthesis

Synthesis of FAU zeolites was performed using aluminosilicate gels of the general mole composition : xSiO$_2$: yAl$_2$O$_3$: mNaOH: nH$_2$O; where x = 1-10, y = 0.5-1, m = 1- 4.76 and n = 140 - 454. The gels were prepared by mixing silicate solution with aluminate solution and aging at room temperature for 24 hours before crtstallization. The synthesis temperature varied from 65°C up to 100°C under autogenous pressure. The containers used for synthesis were either teflon liners (ca. 2 cm in diameter, 10 cm height) put inside steel autoclaves or polypropylene bottles 60 ml or 250 ml (Fig. 4).

a   b

Fig. 4. Containers used in the syntheses. a) Teflon liner with the steel autoclave b) Polypropylene bottles (PP), 60 and 250 ml.

Triethanolamine (TEA) was added in some synthesis either alone as a stabilizer of FAU phase or combined with bis(2-hydroxyethyl)dimethylammonium chloride (TCl) organic template.

Table 1. Chemicals used in the syntheses.

Substance	Company	Specification No.
Sodium silicate solution	Merck	1.05621.2500
Silicic acid	Merck	1.00657.1000
Sodium metasilicate	Fluka	2299129
Sodium aluminate anhydrous	Riedel-deHaën	13404
Sodium hydroxide pellets	Merck	1.06467.9010
Triethanolamine (TEA)	Merck	1.08379.0250
bis(2-hydroxyethyl)dimethylammonium chloride (TCl)	Merck-Schuchardt	8.03052.0250
13XP-IR	Köstro- Lith	30201

On the other hand, nucleation solutions used for nucleating the FAU batches were prepared separately (see 2.1.1.) and used as a "structure-directing agent" in some syntheses either as a single additive or combined with templates. After synthesis the final products were washed with distilled water and dried either for 24 hours at 90 °C or for 1 hour at 120 °C. The sources of materials used in these syntheses are given in table 1.

2.1.1. Preparation of the "nucleation solution" as a crystallization agent

An aluminosilicate gel of high silicate and alkaline concentration: $13Na_2O: 0.5Al_2O_3: 16SiO_2: 224H_2O$ has been prepared and aged at room temperature for 1 to 6 weeks. An upper solution started to appear after 3 days and it increased in volume with increasing time. The gel was then separated into a precipitated solid part and a liquid part above it. The clear liquid part was used in nucleating the starting batches for faujasite zeolite synthesis (Fig. 5).
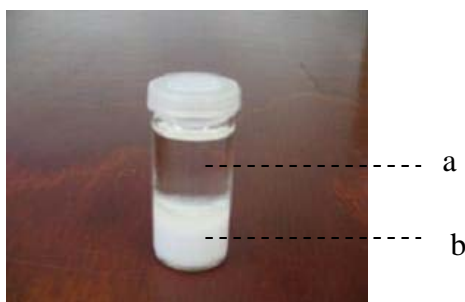
Fig. 5. An aged gel at room temperature for 6 weeks shows two separated phases: A precipitated solid phase (a) and a clear upper solution (b) which was used as a "structure directing agent".

2.1.2. Synthesis according to Ginter et al. [7]

The procedure after [7] was repeated for synthesis of Y-type zeolite. The starting materials were sodium silicate solution, solid sodium aluminate and sodium hydroxide pellet. The batch consisted in a combination of two gels; a seed gel of the composition: $10.67Na_2O: Al_2O_3: 10SiO_2: 180H_2O$ aged at room temperature for one day, and a feedstock gel of the composition: $4.30Na_2O: Al_2O_3: 10SiO_2: 180H_2O$. The overall gel of the composition: $4.62Na_2O: Al_2O_3: 10SiO_2: 180H_2O$ was then formed by mixing of the feedstock gel with 16.50g of the seed gel at room temperature for 20 minutes under high shear and aged at 100°C for several hours. Polypropylene bottle 60 ml was used for the synthesis. After the thermal treatment the product has been washed with distilled water and dried at 90°C for 24 hours.

2.1.3. Modified synthesis of Ginter et al. [7]

The procedure described in [7] was modified by adding ca. 5 % (of the total batch) of a nucleation solution (see 2.1.1.) to the overall gel of the composition: $4.62Na_2O$: Al_2O_3: $10SiO_2$: $180H_2O$. The gel was thermally treated directly after hand-shaking at 100°C and autogenous pressure for 2, 3, 5, 7 and 24 hours.

2.1.4. Synthesis according to Charnell [39]

The synthesis was prepared as described in [39]. The silica source was sodium meta silicate. A gel of the composition Na_2O: Al_2O_3: $2.8SiO_2$: $140H_2O$ was used. Triethanolamine was added to the aluminate solution as template. Both silicate and aluminate solutions have been filtered before mixing. Polypropylene bottle 60 ml was used as batch container. After synthesis at 80°C for 5 weeks the product was washed and dried for 24 hours at 90°C.

2.1.5. Modified synthesis of Charnell [39]

Applying TEA as a stabilizing agent in synthesis of large crystals of FAU structure type was the main step taken from procedure [39] with other modifications regards the synthesis conditions. The solutions have been not filtrated before mixing. The syntheses run in steel autoclaves and not in polypropylene containers as mentioned in [39]. Synthesis time was 7 and 14 days. Two different compositions were used, one of the composition: Na_2O: Al_2O_3: $5SiO_2$: $140H_2O$ and the other of higher silicate concentration: Na_2O: Al_2O_3: $10SiO_2$: $140H_2O$ for crystallization of X- and Y-types, respectively, according the starting composition.

2.1.6. Synthesis according to Ferchiche et al. [40]

Triethanolamine as a stabilizer and the template bis(2-hydroxyethyl)dimethylammonium chloride (TCl) were added to the aluminosilicate gel of the composition: $4.76Na_2O$: Al_2O_3: $3.5SiO_2$: $454H_2O$: $0.6T_2O$: $5TEA$ under alkaline condition as described in [40]. The silica source was silicic acid. Polypropylene bottles were used as batch containers. The aluminate solid was added to a hot sodium hydroxide solution. After cooling down the solution was filtered to avoid the sodium aluminate nano-crystals which are known to act as seeds in zeolite synthesis [40]. Afterward, the templates were added together to this solution forming a stock solution which has been filtered again and added to the silicate solution. The formed gel

was then hand-shaken for some seconds at room temperature and divided into four bottles which were sealed and aged at 95°C for 2 to 3 weeks. The final products have been washed with distilled water and dried at 90°C for 24 hours before characterization.

2.1.7. Modified synthesis of Ferchiche et al. [40]

The modifications on procedure [40] were consisting in adding a combination of template and nucleation solution to the prepared gel. The initial gel was prepared as described in [40]. 3 ml of the nucleation solution was then added to the gel. The batch was put at 90°C for 24 hours. The synthesis temperature was then reduced down to 65°C for further 19 days crystallization time. Amounts of nucleation solution of 1 ml were added to the batch in the rate of 1ml/day. After crystallization the sample has been washed and dried for 24 hours at 90°C. During crystallization period probes of the batch were taken and measured directly with IR method (see 2.4.2.). Such investigation provided a kinetic view over the whole crystallization process.

Another modification was performed by increasing the silicate concentration of the batch in order to increase the n_{Si}/n_{Al} of the final FAU. Therefore, another trial was prepared with the same starting composition of [40] and using same organic templates. The modification was done by adding nucleation solution and varying the synthesis time and temperature.

2.1.8. Synthesis of aluminosilicate gels of different additives prepared for the kinetic experiments

Four batches of aluminosilicate gel composition with n_{Si}/n_{Al} value of 1.7 were prepared. A nucleation solution was prepared separately. During the thermal treatment at 95°C for 0.5 hours to 21 days. Four kinetic experiments were performed using IR spectroscopy in different cases described in the following:
1. An aluminosilicate gel without any additives.
2. An aluminosilicate gel using the nucleation solution as a crystallization agent for Y-type zeolite synthesis.
3. An aluminosilicate gel using TEA as a stabilizer and TCl [bis(2-hydroxyethyl)dimethylammonium chloride] as an organic template.
4. An aluminosilicate gel using the nucleation solution together with TEA and TCl.

2.1.9. Special experiments for further investigation of high silica Y-type formation mechanism

2.1.9.1. Procedure I

Effect of mother liquor on the final crystallized phase has been worked out through this procedure. Two batches of different mol compositions (A and Y batches) have been prepared according the procedure described by Fahlke et al. [74].

Preparation of A type batch of $n_{Si}/n_{Al} = 1$

An aluminosilicate gel of the composition: 2 SiO_2 : 1 Al_2O_3 : 3.5 Na_2O : 170 H_2O was prepared by dissolving of 8.16 g sodium hydroxide in 175 ml distilled water. 13 g of solid sodium aluminate were then added to the sodium hydroxide solution and mixed until dissolving. 30 ml of sodium silicate solution was then added to the sodium aluminate solution. The overall gel was Mixed for 30 min. and aged for 24 hours at room temperature.

Preparation of Y type batch of $n_{Si}/n_{Al} = 4.5$

An aluminosilicate gel of the composition: 9 SiO_2 : 1 Al_2O_3 : 3 Na_2O : 120 H_2O was prepared by dissolving 14.45 g of solid sodium aluminate in 52.5 ml distilled water. 150 ml of sodium silicate solution were added to the sodium aluminate solution. The gel was mixed for 15 minutes and aged at RT for 24 hours. After aging, the formed upper liquids (mother liquors) over both batches were separated from the solid parts (gels) by centrifugation and exchanged, i.e. the mother liquor of Y batch was added to the gel of A batch and that of A batch was added to the gel of Y batch. The new batches were thermally treated at 80°C. This process allowed the observation of the influence of liquid phase components on the crystallization pathway of both batches.

2.1.9.2. Procedure II

The control of Mother liquor by increasing or decreasing the alkalinity concentration of Y batch of the composition after aging at RT and/or after synthesis at hydrothermal conditions was applied on Y batch of the composition 9 SiO_2 : 1 Al_2O_3 : 3 Na_2O : 120 H_2O prepared after [74]. The gel preparation was consisting in solving 8g of sodium hydroxide in 45 g distilled water. 11.4 g of sodium aluminate were added to the sodium hydroxide solution. 90 g

of silica sol (by weight) were mixed with the sodium aluminate solution. The gel was mixed for 30 minutes and aged at room temperature for 22 hours.

The mentioned procedure was repeated many times with variation of the alkalinity content and the crystallization time. All batches were aged at room temperature for 22 hours. The liquid phase was separated from the gel by centrifugation after aging or/and before aging. Addition of the excess of sodium hydroxide solution was either before or after aging of the initial gel at RT or during synthesis at hydrothermal conditions after 2, 24 or 48 hours. The experimental details are summarized as following:

Sample 1-16-1

After ageing for 22 h at RT the mother liquor was separated and 1.47 g of NaOH was added to 25 g of mother liquor (by weight) and given back to the batch. Synthesis time of 3 days at 90°C has been applicated on this sample.

Sample 1-16-3

After ageing for 22 hours at RT, the sample was aged at 90°C for 2 hours. The mother liquor was separated from the gel.

Sample 1-16-4

After ageing for 22 hours at RT the mother liquor was substituted by an equal amount of sodium hydroxide solution 1.55M (the same molarity of the primary batch). The batch was then aged at 90°C for 3 days.

Sample 1-16-5

After ageing for 22 hours at RT the batch was aged at 90°C for 2 days. Afterward, an excess amount of sodium hydroxide solid was added to the mother liquor. The batch was then aged at 90°C for other 1 day.

Sample 1-16-6

After ageing for 22 hours at RT the batch was aged at 90°C for 2 hours. Mother liquor was then separated from the gel and substituted by an equal amount of distilled water. The sample was aged at 90°C for 3 days.

Sample 1-16-8

After ageing for 22 hours at RT the mother liquor was substituted by an equal amount of sodium hydroxide solution 1.55M. The batch was then aged at 90°C for 3 days.

Sample 1-17-1

Two batches of the composition : 9 SiO_2 : 1 Al_2O_3 : 3 Na_2O : 120 H_2O have been prepared.

Batch 1: After ageing for 22 hours at RT the gel was aged at 90°C for 24 hours.

Batch 2: After ageing for 22 hours at RT the gel was aged at 90°C for 2 hours.

The two batches were mixed and the new gel was aged at 90°C for 2 other days.

Sample 1-17-2

After ageing for 22 hours at RT the batch was aged at 90°C for 2 hours. Mother liquor has been separated and substituted by an equal amount of sodium hydroxide solution 1.55M. The sample was aged at 90°C for 3 days.

2.2. Ion-exchange experiments

2.2.1. The maximum degree of NH_4^+ : Na^+ exchange of Y zeolite

NaY zeolite with n_{Si}/n_{Al} of 2.66 was Na^+ : NH_4^+ exchanged in 0.1 M of NH_4Cl salt solution. The ion-exchange process run at room temperature in 9 integral steps for 1 hour/ step. The ion-exchanged sample was analysied by BET method (see 2.4.8.).

Another ion-exchange experiment was done for same Y sample using $(NH_4)_2SO_4$ salt solution of 0.1 M. The experiment was carried out for 3 hours in term of 1h/ step. The solution was then analysed by ICP OES method (see 2.4.7.).

This NH_4Y sample was hydrothermally treated at 775 K, 5 h and 1 bar water vapor and a second ion-exchange was applied, afterthere, at RT in $(NH_4)_2SO_4$ salt solution of 0.1M in term of 3 steps (1 h/step) using 100 ml salt solution / 1 g zeolite. The solution at the end of the second ion-exchange process was analysed by ICP OES method (see 2.4.7.).

2.2.2. Preparation of the proton form of FAU (H-FAU) type of different n_{Si}/n_{Al} values

The proton form of FAU (H-FAU) type of the self-prepared samples was obtained from the ammonium form (NH$_4$-FAU) which was previously prepared by NH$_4^+$: Na$^+$ exchange at room temperature using (NH$_4$)$_2$SO$_4$ salt solution of 0.1 M in term of three steps for 1 hour/ step using the ratio 100 ml salt solution/1 g zeolite. Templated samples were calcined at 550°C for 1.5 hours before the exchange process to get out the organic phase. H-FAU modification was formed by the thermal treatment of NH$_4$-FAU at 533 K for 1 hour in air or in steam. At the end of Na$^+$: NH$_4^+$ exchange course the samples were slightly washed and dried at 120°C for 1 hour.

2.3. Steaming experiments

2.3.1. Steaming of the self-prepared H-FAU zeolites with and without intermediate treatment

The self-prepared samples according to [7], [39] and [40] were structurally modified using steaming procedure. NH$_4$-FAU modification was first prepared as described in 2.2.2..

The samples were located in a Bed-form quartz holder specially designed for steaming procedure. The holder was put in the steaming apparatus. temperature of 773 K was then applied for 5 hours under 1 bar water pressure. The steam was produced by the principle of water distillation as an open system. The flow of water steam started with reaching 473 K to 573 K and the H-FAU modification was first obtained. At the end of steaming procedure the furnace was switched off and the apparatus was cooled down.

To study the effect of the intermediate hydrothermal treatment on the degree of amorphization and dealumination with respect to the related n_{Si}/n_{Al}, two FAU samples with n_{Si}/n_{Al} of 2.66 and 2.23 were thermally and chemically treated in the following order: - Ion-exchange Na$^+$: NH$_4^+$ in (NH$_4$)SO$_4$, 0.1 M, 3 steps, 1h/step. - Steaming at 773 K, 5 hours and 1bar H$_2$O. - Ion-exchange Na$^+$: NH$_4^+$ in (NH$_4$)SO$_4$, 0.1 M, 3 steps, 1 hour/step. - Calcination at 823 K, 1.5 hours - Steaming at 773 K, 5 hours, 1 bar H$_2$O.

Another series of FAU type samples of variant n_{Si}/n_{Al} values (2.66, 2.46, 2.25, 2.16 and 2.0) were hydrothermally treated at 873 K and 7 hours under 1bar water pressure. This experiment was performed for estimation of the extra-framework species occur after steaming using molybdate method (2.4.5.) and ^{29}Si MAS NMR spectroscopy (2.4.6.).

2.3.2. Steaming of HY zeolite at elevated temperatures with variation of time

Commercial NaY (Grace Davison) with n_{Si}/n_{Al} of about 2.66 and ~ 1 µm in size was used for the experimental studies. The HY modifications were obtained as described in 2.2.2.. These samples were then treated at hydrothermal conditions of wide range of temperatures (473 K to 1073 K) in steps of 100 K/ step each for different times (from 0.5 hour up to 20 hours) in steam of 1 bar pressure. The steam was produced by the principle of water distillation as an open system. The flow of water steam started with reaching 473 K to 573 K. The samples were located in a heated quartz tube. At the end of the hydrothermal treatment the samples were set at room temperature for cooling down. The dealuminated Y samples were dried at 393 K for 1hour.

In another series, the dealuminated Y (DAY) type zeolites with n_{Si}/n_{Al} between 2.0 and 2.66 were prepared (for further investigation) by steaming the HY at 873 K for 7 hours under 1 bar water pressure.

2.4. Characterization methods

2.4.1. X-ray powder diffraction (XRD)

X-ray powder diffraction has been used for structure characterization of the studied zeolites. The measurements were recorded on Bruker AXS D4 Endeavor, Cu K$\alpha_{1,2}$-radiation, Ni-Filter, Bragg-Brentano geometry. The reflection was scanned at 2 Theta range between 5.00° and 80.01° in steps of 0.030 counting 4.0 sec/ step. The zeolite powder was first carefully milled and filled in a disc-like sample holder and put in the diffractometer for measurement after setting the desired parameters. This method allows the identification of the structure type, the calculation of crystallinity degree of the zeolite as well as detection of the multi phases in the sample, if any.

Structure determination has been performed using two different software. Whereas DIFFRAC Plus Topas 3.0 (Bruker AXS) software was used for determination of the cell parameter (a_0) of the samples with multi-phases, the degree of crystallinity and the average crystal size (in nm), STOE WinXPOW 1.08 software was used for determination of a_0 of pure-phase samples. The term "particles" was used to mention the grains which were seen and measured directly from SEM-image and these particles were compared with that termed in the literature as crystals. In this sense, two values described the size of the obtained zeolite particles; the average crystal size estimated from XRD analysis and the maximum particle size (given in µm) measured directly from SEM.

2.4.2. Fourier transform infrared spectroscopy (FTIR-spectroscopy)

FTIR spectroscopy was used as an effective tool for further characterization of zeolite structure by which the local building units of zeolite framework could be detected. The IR spectra have been recorded on Bruker IFS/66 spectrometer in the middle infrared range between 300 and 5000 cm^{-1}. Three types of atomic vibration modes can be observed using this method; symmetric stretching mode (v_s T-O-T) at the approximated range 650-820 cm^{-1}, asymmetric stretching mode (v_{as} T-O-T) at 900-1250 cm^{-1} and bending mode (δ O-T-O) at 420-500 cm^{-1}. The double six-ring as a characteristic feature of faujasite type zeolite exists in the frequency range between 500-650 cm^{-1} [52]. The sample preparation consists in mixing 1 mg of zeolite powder with 200 mg of KBr. This mixture was then pressed in pellet under 10 tons for 2-3 minutes before measurement.

2.4.3. Scanning electron microscopy (SEM) and energy dispersive X-ray analysis (EDX-analysis)

SEM was used for observation of the morphology and the crystal size distribution of the studied particles. A thin focussed beam of electrons with energy of 10 to 50 keV is directed to the surface. The intensity of the secondary electrons produced by the primary beam are measured by a detector. As the primary beam starts to move (to scan) above the sample the secondary electron signal, as a function of the momentary spots of the electron beam, becomes visible. Thus a three dimensional object of high resolution could be visible due to the output of the secondary electrons. During the contact of the electron beam with the sample a characteristic X-ray radiation is produced. The element specific energy of the secondary

radiation is used for qualitative analysis of the sample. A lithium doped Si-semiconducting crystal serves as a detector during this energy dispersive X-ray analysis (EDX-analysis). The crystal size distribution and the morphology of the as-synthesized and commercial X-, Y- type zeolite crystals have been obtained using HITATCHI S – 530 microscopy. For some samples JSM 6700F microscopy has been used. The qualitative X-ray analysis for the scanned samples has been taken using Kevex EDX system.

2.4.4. Water adsorption

The water sorption capacity of the studied zeolites (as-prepared and hydrothermally treated) was gravimetrically measured as following: The weights of empty glasses with lids were taken, then ca. 150-300 mg of the zeolite have been weighted and put into the glasses. The open glasses with zeolites were put in a furnace and heated up to 450°C for 3 hours in order to get a water-free zeolite. A standard zeolite sample of known water adsorption value was taken to prove the measurement accuracy. The glasses with zeolites were directly covered by the lids to prevent the rehydration again. Then the covered glasses with zeolites were put into an desiccator (tightly sealed evacuated vessel) for cooling down. After cooling down the total weights were taken again and the dry weights of the samples were calculated. The glasses, thereafter, were put open again in the desiccator which contained $MgCl_2$ solution. This solution acts as a water support for the water adsorption of zeolite. The vapour pressure of the solution has 16 Torr and not 24 Torr as it in water and consequently no condensation of water takes place at glasses. The attraction strength of the micropores (< 1 nm) to water molecules is, however, very strong that an internal condensation can not be reached any more. On the other hand, the mesopores (~ 10 nm) have enough space for the internal water condensation. The desiccator was sealed tightly using special grease and then evacuated. After 24 hours, air was slowly entered to the exicator. The glasses were taken out and the total weight of glasses with samples and lids was taken. Using the empty weight of the glasses, the increase in zeolite weight could be calculated. The samples were put for another 24 hours in the exicator and the weight was taken again. This process was repeated 2-3 times until reaching a value at which the final weight did not change anymore. The same experiment was repeated again to reduce the mistakes in the taken weight values.

2.4.5. Molybdate reaction method

The molybdate method is used for characterization of the degree of condensation of silicate species of the studied material so that the monomeric, dimeric and oligomeric units of silicate in the studied zeolite are detected. For this purpose the zeolite structure is dissolved in acid. In the acidic condition the Si-O-Al bonds are destroyed and the structure decomposes into different silicate species.

The mono silicic acid reacts with the molybdic acid and gives a dodecamolybdato silicic acid complex according the reaction:

$$H_4SiO_4 + 12\ H_2MoO_4 \rightarrow H_4[Si(Mo_3O_{10})_4] + 12H_2O$$
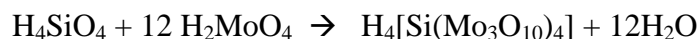
The resulting complex is determined by the yellow colour, measured by UV-VIS spectroscopy (Shimadzu UV-spectrometer 1601) at a wave length of 400 nm. As higher as the condensation degree of silicate combinations as longer the reaction time is. That is because the silicate combinations should first decompose into monomers. For an optimal measurement about 0.5-1.0 mg of silicium should be used. Ca. 3 mg of the studied zeolite was put in a small glass and 50 ml of 0.1M HCl solution was added and stirred for 2 minutes at 0°C where the silicate units were set free but not decomposed. The sample was then filtered using an ultra fine filter, warmed up to 25°C to start the decomposition from oligomeric to diameric silicate and further to the monomeric silicic acid followed by adding 2 ml of 0.1 M ammonium molybdate solution and hand-shaken at the same moment of starting measurement at room temperature. The measurement continues until having a constant maximum.

2.4.6. Magic angle spinning nuclear magnetic resonance spectroscopy of nucleus ^{29}Si (^{29}Si MAS NMR spectroscopy)

The solid-state NMR spectra were recorded at room temperature on a Bruker Avance 400 spectrometer, operating at afrequency of 79.5 MHz for ^{29}Si. A 4 mm double tuned (^{1}H-X) MAS probe (Bruker Biospin) was used to perform MAS NMR measurements at spinning rate of 12 kHz. The ^{29}Si MAS spectra were obtained using single pulse excitation consisting of 4 μs pulses (π/2 pulses) and recycle delays of 120 s to exclude saturation effects. Up to 1400 FIDs were accumulated to obtain reliable signal-to-noise ratio. The ^{29}Si spectra were

externally referenced to liquid Me$_4$Si at 0 ppm. For the line shape analysis of the ^{29}Si MAS NMR spectra the dmfit software package [75] was used.

2.4.7. Inductive coupled plasma optical emission spectroscopy (ICP OES)

The ion-exchanged (Na$^+$: NH$_4^+$) samples as well as the mother liquor of some studied samples reported in this work have been chemically analysed by ICP OES spectrometry using the spectrometer IRIS Intrepid HR Duo (THERMO elemental, UAS). Main components as well as trace impurities down to 1 ppm can be measured quantitatively in the sample with high accuracy. The precision is ca. 3 %. The ICP OES spectrometer was calibrated with simple synthetic solution standards.

2.4.8. BET surface measurements

The sorption capacity of the synthesized zeolites was analysed by nitrogen sorption at 77.4 K (BET-surface) using the NOVA 1200 instrument from Quantochrome. 200 mg of the zeolite were used in each case, all samples were dried for 1 hour at 373 K before measurement.

3. Results and discussion

3.1. The approach to verify syntheses of large size Y zeolite crystals according to literature procedures and the modification of these concepts

3.1.1. Characterization of the products prepared according to Ginter et al. [7] by XRD, FTIR and SEM

Ginter et al. [7] obtained FAU type crystals of a_0 = 24.72 Å with size < 1 μm after 7 hours synthesis time at 100°C. Our results following the same procedure shows an X-ray amorphous phase after 7 h thermal treatment. After 16 hours treatment both FAU and GIS types were crystallized at the same time. The intensity of FAU phase decreased with proceeding the synthesis time where GIS phase became the main product after 24 hours. XRD characterizations of this synthesis series are given in table 2.

Table 2. X-ray data of the samples synthesized according to Ginter et al. [7].

Synthesis			XRD data			
Time	Product	Amount	Average crystal size	Degree of crystallinity	Cell parameter a_0	n_{Si}/n_{Al}
h		%	nm	%	Å	
7	X-ray amorph.	-	-	-	-	-
16	FAU/ P1	26/73	110(9)	99	24.698(5)	2.22
24	FAU/ P1	10/90	156(27)	92	24.708(6)	2.17
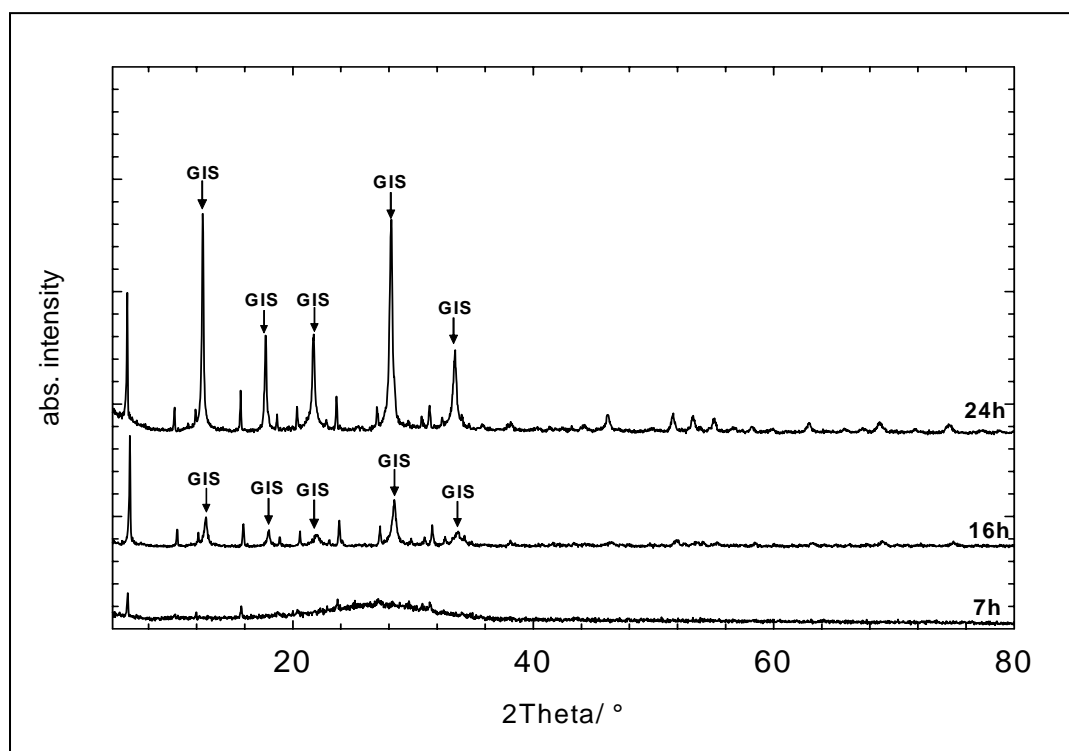
Fig. 6. X-ray diffraction patterns denominate the crystallization of two phases after selected synthesis times (7 h, 16 h and 24 h).

The X-ray pattern of the synthesized sample for 7 hours shows an X-ray amorphous phase with a maximum at about $2\theta = 27$ degree (Fig. 6). Small peaks which belong to FAU phase could also be recognized. After 16 hours aging at hydrothermal conditions the characteristic peaks of FAU phase with an amount of ~ 26 %, average crystal size of 110(9) nm and a_0 of 24.698(5) Å was obtained together with the GIS phase with ~ 73 % and an average crystal size of 35(1) nm. The n_{Si}/n_{Al} of FAU phase is 2.22. The first reflection through the direction <111> of the octahedral FAU crystals has been recorded at $2\theta = 6.4$ degree. The first reflection of P (GIS structure) crystals was observed at $2\theta = 12.5$ degree. The cell parameters of this phase are $a_0 = 10.015(3)$ Å and $c_0 = 10.050(59)$ Å. After 24 hours synthesis the intensity of FAU decreases down to ~ 10 % with an average crystal size of 156(27) nm and a_0 of 24.708(6) Å ($n_{Si}/n_{Al} = 2.17$) while the amount of GIS increases to reach ~ 90 % of the total final product. FTIR was employed for further characterization of the studied zeolite during crystallization (Fig. 7).
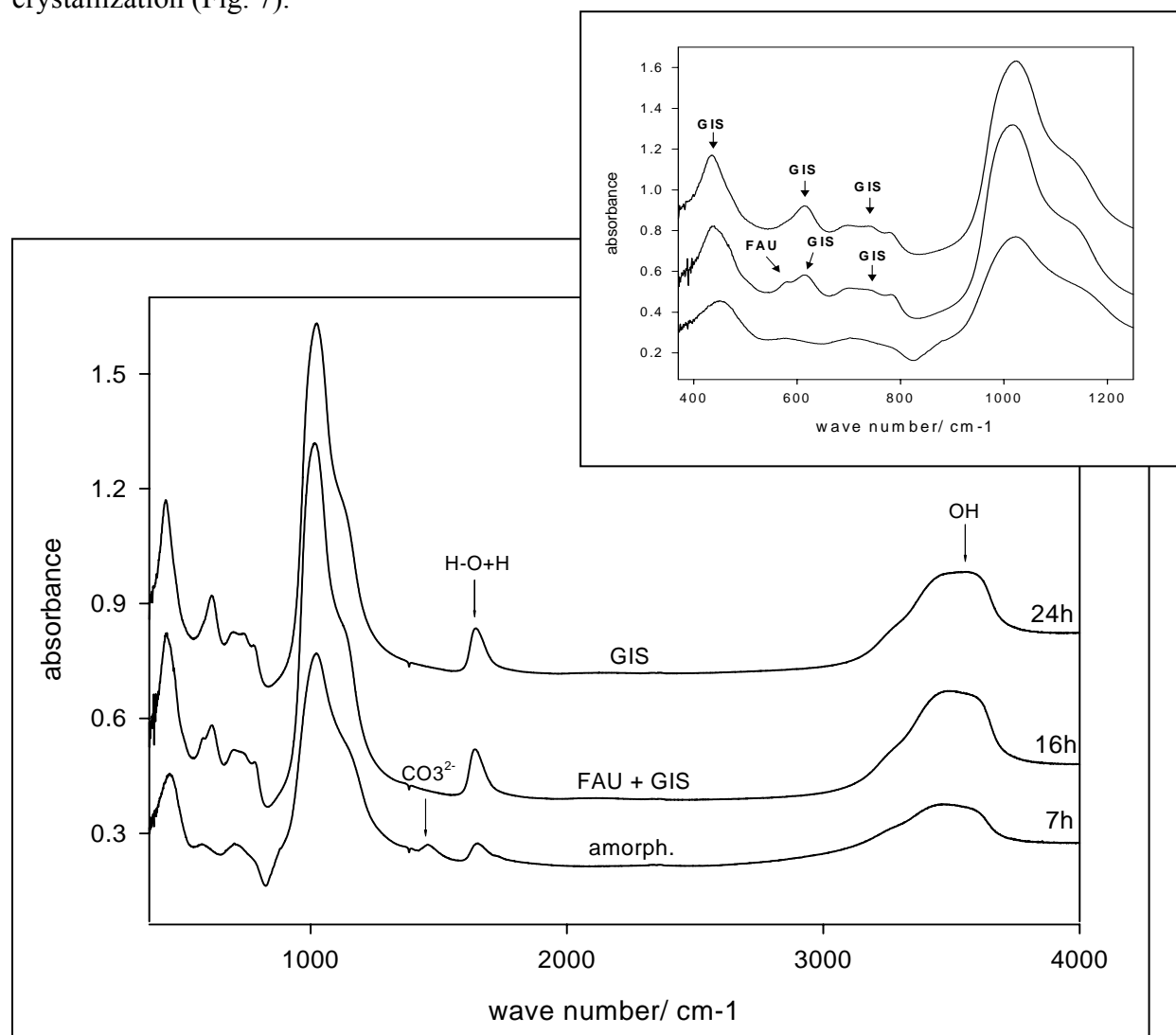
Fig. 7. IR spectra of the gel prepared after [7] (See the expended plot of the 400 cm^{-1}- 1200 cm^{-1} region for details about the phase transition).

The sample of 7 hours synthesis shows a typical spectrum of an amorphous aluminosilicate material with two main peaks at 451 cm^{-1} and 1022 cm^{-1}. A small peak at 1456 cm^{-1} denotes the carbonate (CO_3^{2-}) and the water molecules show two frequency values at 1653 cm^{-1} and 3471cm^{-1}. The spectrum of the sample synthesized for 16 days denotes the crystallization of FAU phase characterized by the D6R at 577 cm^{-1} and GIS phase at 614 cm^{-1}. At 738 cm^{-1} a small peak appears which belongs to P phase. The framework water has two values at 1642 cm^{-1} and 3471 cm^{-1}. After 24 hours synthesis time the intensity of FAU decreases with growing the GIS phase. There are three frequency values denote the P phase, the value at 614 cm^{-1}, at 433 cm^{-1} as well as the peak at 743 cm^{-1} in the range of ν_s T-O-T. There is also an increase of the ν_{as} T-O-T mode which reveals a value at 1024 cm^{-1}. SEM images of these three samples denominate the development of an amorphous phase into a crystalline phase (Fig. 8). After 7h (Fig. 8a) only an amorphous material could be seen. Small particles (~ 1.5 µm in size) appear after 16h (Fig. 8b) which belong to two phases; X and P. The FAU phase decreases again and the GIS crystallizes continuously to be the main phase after 24h with sphere-shaped particles of around 3 µm in size (Fig. 8c).

| a | b | c |
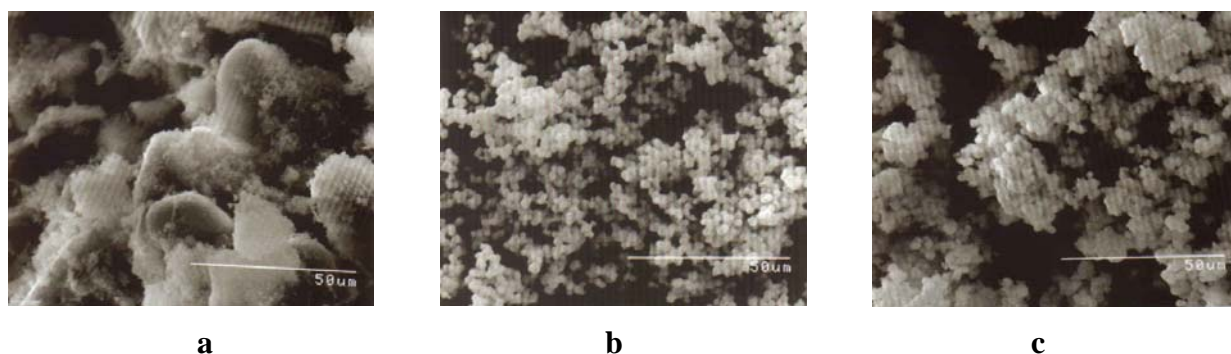
Fig. 8. SEM images of three samples of the same batch composition and different synthesis times, a) after 7 h where only amorphous phase is observed, b) after 16 h where particles of ~ 1.5 µm are produced and c) after 24 h where bigger particles are observed of a diameter of ~ 3 µm.

3.1.2. Characterization of the products prepared after the modified procedure of Ginter et al. [7] by XRD, FTIR and SEM

It has been early reported by Lechert et al. [14] that the liquid part of a separately aged gel causes an increase in the crystallization rate of Y zeolite. According this concept a nucleation solution has been prepared separately from a batch of high silicate and alkali concentration and aged at room temperature for 6 weeks (2.1.1.). The prepared solution was added in a very small amount (5 %) to the starting Y composition. The modified procedure after [7] is

consisting in adding the nucleation solution " as a crystallization agent" to the batch prepared according to Ginter et al. [7]. Results of XRD characterizations of the final products synthesized after the modified procedure are given in table 3. The samples measured after 2 h and 3 h synthesis time at 100°C show an X-ray amorphous phase with a maximum at around 2θ of 27 degree. After 5 h the X-ray pattern shows very small peaks represent the significant diffraction features of the FAU structure. After 7 h the X-ray pattern reveals a single FAU phase (amount ~99 %) with a_0 = 24.69(5) Å (n_{Si}/n_{Al} of 2.23). The degree of crystallinity estimated from XRD data of this sample is ~ 94 % (Fig. 9).

Table 3. X-ray data of samples after the modified synthesis of Ginter [7].

Synthesis			XRD data			
Time	Particle size	Product	Amount	crystallinitiy	Cell parameter a_0^a	n_{Si}/n_{Al}
h	μm		%	%	Å	
2	-	amorph	-	-	-	-
3	-	amorph	-	-	-	-
5	-	amorph	-	-	-	-
7	<1	FAU	99	94	24.69(5)	2.23
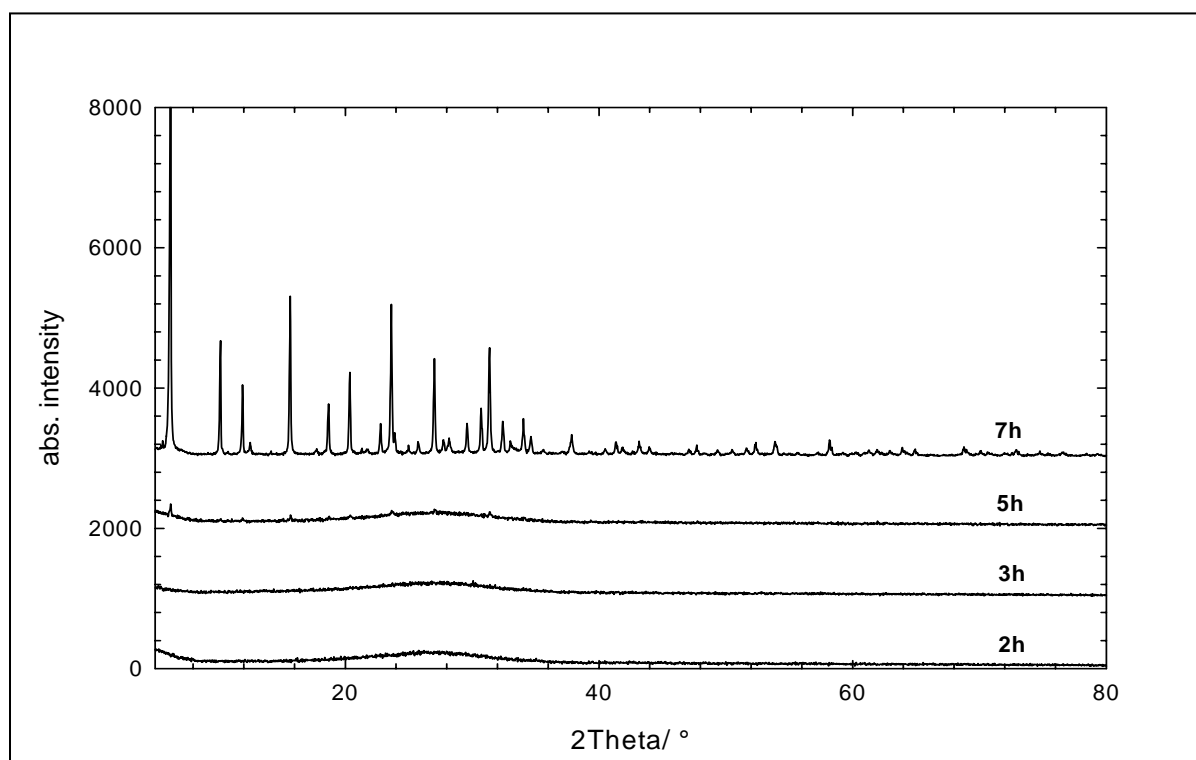
Fig. 9. X-ray diffraction patterns of the modified sample synthesized after [7]. The modification consisting in adding of 5 % of the nucleation solution to the primary batch.

IR spectra of this series show a sudden crystallization step from the amorphous phase into the crystalline phase. Up to 5 h synthesis at 100 °C the sample shows nearly an amorphous phase.

Between 5 h and 7 h a complete crystallization of FAU type zeolite occurs (Fig. 10). The D6R mode of this sample is recorded at 575 cm^{-1} and the v_{as} T-O-T at 1010 cm^{-1}. SEM image shows the crystallization step between 5 and 7 hours at 100 ^{o}C. The particles after 7 h synthesis are less than 1 μm in diameter (Fig. 11a, 11b).

IR spectrum recorded on the mid infrared range between 300 and 5000 cm^{-1} for the sample synthesized for 7h reveals the characteristic IR features of faujasite type zeolite (Fig. 10). The asymmetric stretching mode v_{as} T-O-T has a frequency of 1012 cm^{-1}. The symmetric stretching mode v_s T-O-T occurs at 784 cm^{-1}. The double six-ring as a characteristic building unit was observed at 576 cm^{-1}. The δ O-T occurs at 458 cm^{-1}. A shoulder was observed at a frequency value of 501 cm^{-1} appears in Y type zeolite but not in X type. This shoulder is considered, therefore, as a characteristic feature for Y type.
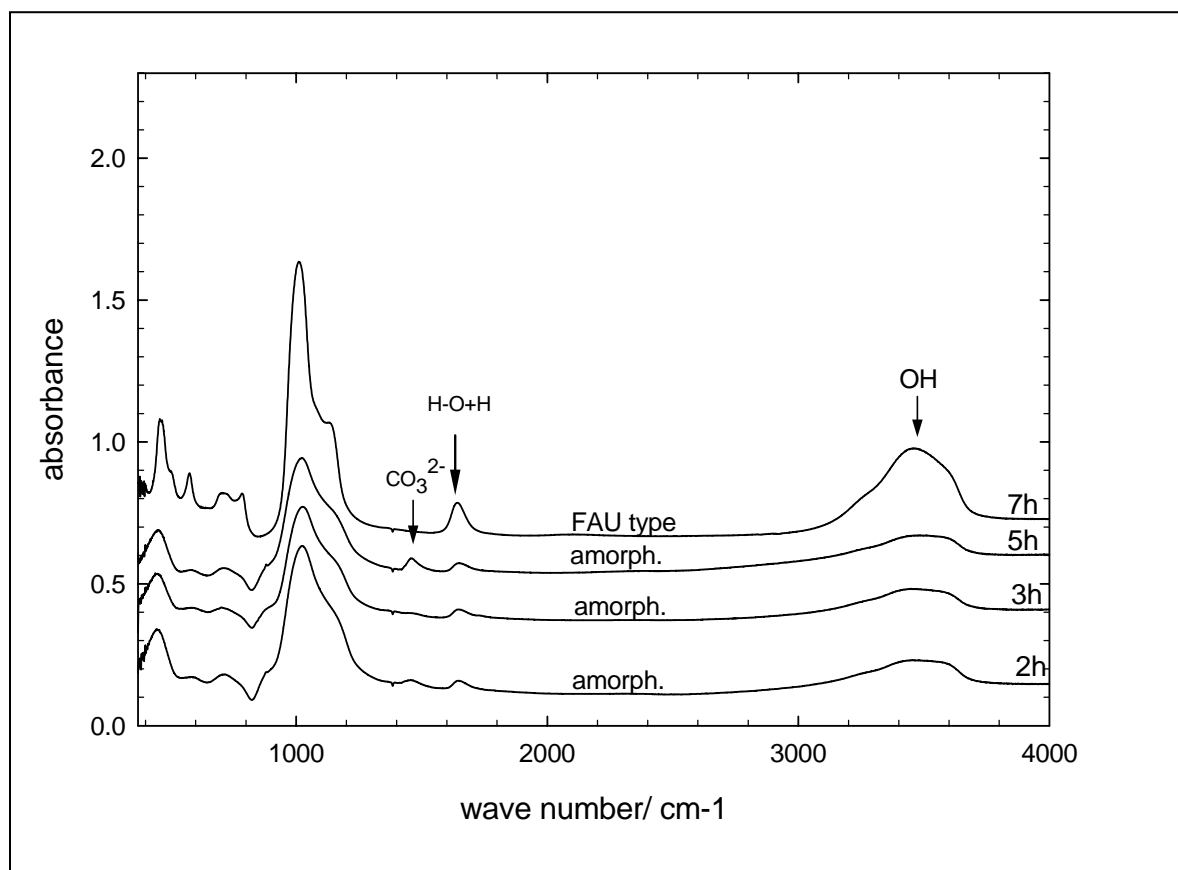
Fig. 10. IR spectra of the modified sample synthesized after [7] at different steps of crystallization, after 2 h, 3 h, 5 h and 7 h.

Another two batches were prepared and the nucleation solution was added to one of them and each was synthesized for 7 h and 24 h. The sample synthesized without nucleation solution

shows an X-ray amorphous pattern after 7 h (Fig. 12a) and a multi-phase after 24 h synthesis (Fig. 12b). The X-ray diffraction pattern for the sample synthesized in the presence of the nucleation solution for 7 h and 24 h (Fig. 12c and 12d, respectively) shows a complete re-crystallization into GIS phase. It seems that the crystallization of two phases at same time is avoided by the effect of the components which exist in the nucleation solution.

a   **b**
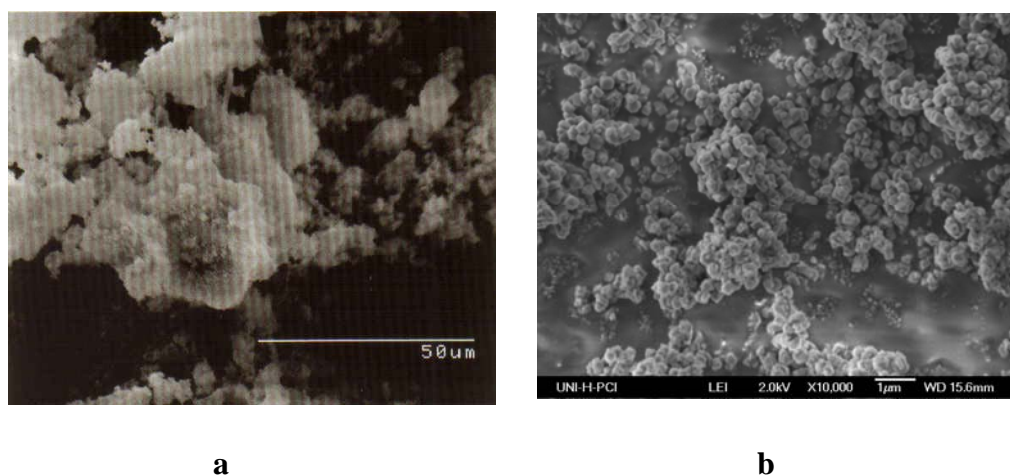
Fig. 11. SEM images of the samples synthesized for a) 5h (amorphous phase) , b) at 7h (crystalline FAU phase).
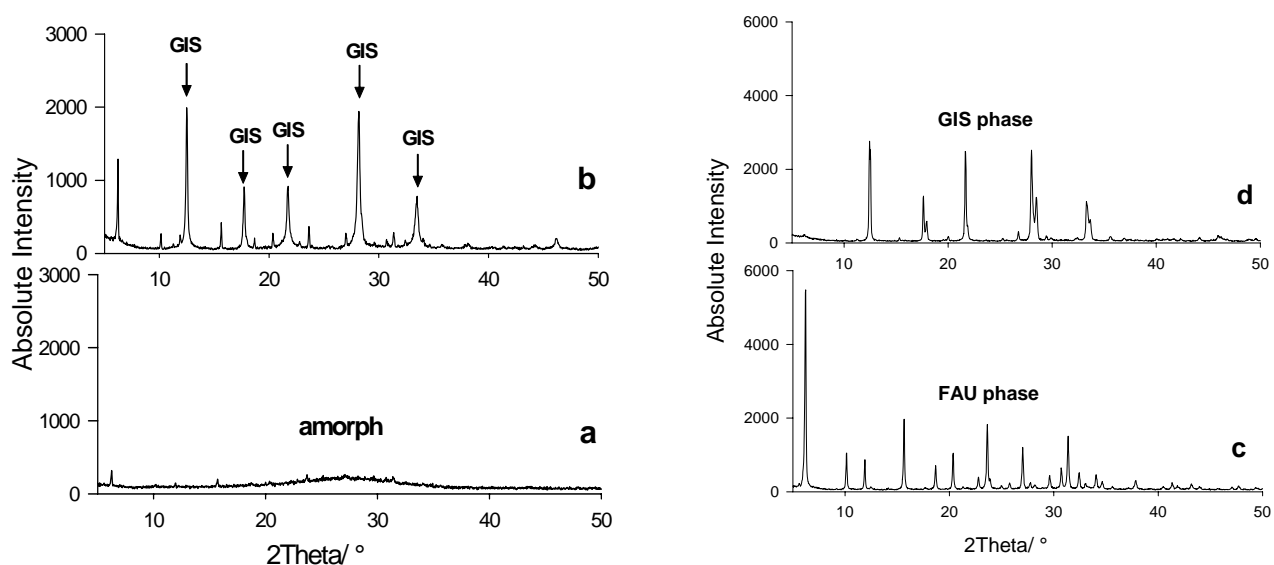
Fig. 12. Comparison of XRD-patterns between two batches prepared after [7] in the presence of nucleation solution synthesized for a) 7 h and b) 24 h, and without nucleation solution synthesized for c) 7 h and d) 24 h.

3.1.3. Characterization of the products prepared according to Charnell [39] by XRD, FTIR and SEM

Charnell [39] has synthesized X type zeolite crystals up to 140 μm in size using triethanolamine (TEA) as stabilizer of FAU phase during crystallization. P zeolite exsited also as by-phase in the final product. This procedure was repeated here and the final product shows a pure X phase but with a maximum particle size of ~ 12 μm. However, some experimental details were not possible like the filtration of silicate and aluminate solutions before crystallization using a 0.2 μm pore size Gelman Acropor AN-200 filter and the type of container used for the synthesis which may explain the difference in the particle size of the final products in both procedures. X-ray pattern of this sample shows a pure phase of FAU structure with a_0 of 24.933(1) Å (n_{Si}/n_{Al} of 1.29) and an average crystal size of 183(6) nm. The degree of crystallinity is ca. 95 % (Fig. 13a). IR spectrum shows further structural details (Fig. 13b). The T-O bending was recorded at 462 cm^{-1} and the double six-ring (D6R) at 565 cm^{-1} characterizes the FAU structure type. The symmetric stretching mode (v_s T-O-T) occurs at 694 cm^{-1} and the asymmetric mode (v_{as} T-O-T) at 978 cm^{-1}. Both D6R and v_{as} T-O-T are sensitive for the concentration of the framework silica of FAU and reveal higher frequency values with increasing n_{Si}/n_{Al}. SEM image of this sample shows a well defined octahedral particles with a maximum size of 12 μm (Fig. 14).
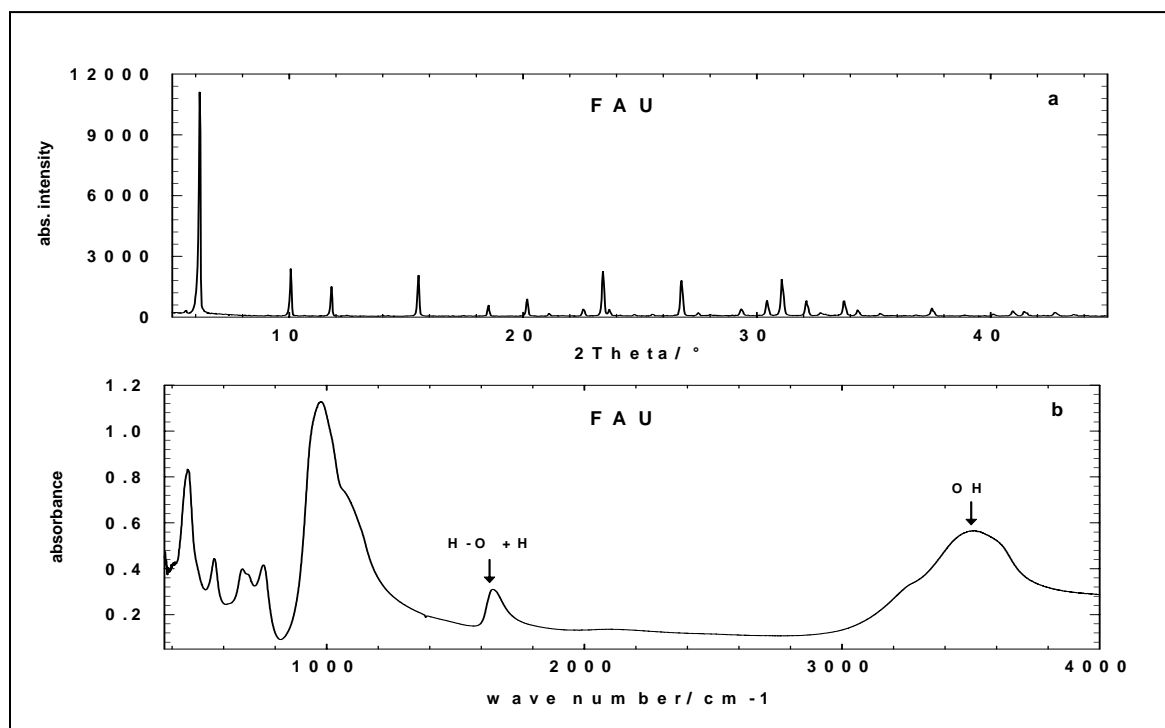
Fig. 13. XRD diffraction pattern (a) and IR spectrum (b) reveal a pure FAU phase of the sample prepared after [39].
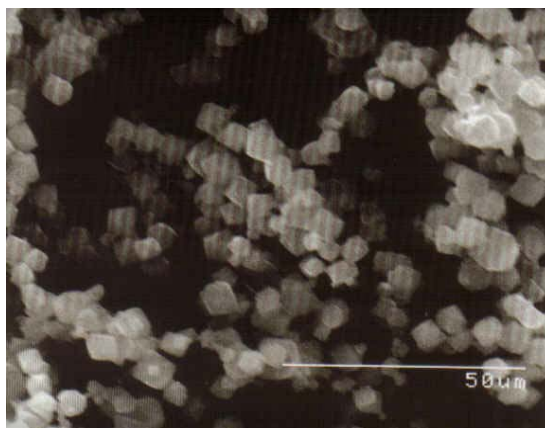
Fig. 14. SEM-image of the sample prepared after [39] of gel composition with $n_{Si}/n_{Al} = 1.4$. The maximum particle size is 12 μm.

3.1.4. Characterization of the products prepared after the modified procedure of Charnell [39] by XRD, FTIR and SEM

This procedure was modified by varying the synthesis conditions in the presence of TEA. Results of X-ray measurements of this series are given in table 4.

Table 4. X-ray data of samples after the modified synthesis of Charnell [39].

Synthesis				XRD data			
n_{Si}/n_{Al} of gel	Time	Product	Amount of FAU	Crystallinity1	Maximum particle size2	Cell constant $a_0$3	n_{Si}/n_{Al}4
	d		%	%	μm	Å	
2.5	7	FAU/ P1	97/ 3	70	5	24.88	1.44
5	7	FAU/ P1	96/ 4	85	5	24.79	1.77
5	14	FAU/ P1	79/ 21	80	3	24.82	1.65

1,2,3,4 determined for FAU phase

X-ray data of the sample of a starting composition with $n_{Si}/n_{Al} = 2.5$ synthesized for 7 days shows a diffraction pattern of FAU structure with n_{Si}/n_{Al} of 1.44 and an average crystal size of 89(3) nm determined by (XRD data). P zeolite crystallizes as an impurity phase with 3 % (Fig. 15a). The degree of crystallinity is about 70 %. IR spectrum shows the FAU structure with D6R at 566 cm^{-1} and the ν_{as} T-O-T at 972 cm^{-1} (Fig. 15b). SEM image shows a maximum particle size of 5 μm (Fig. 16).

The sample of a starting composition of $n_{Si}/n_{Al} = 5$ synthesized for 7 days shows a diffraction pattern (Fig. 17a) of FAU structure with higher n_{Si}/n_{Al} of 1.77. The degree of crystallinity reaches 85 %. P type zeolite exists as an impurity phase with 4 %. The average crystal size determined by XRD is 144(4) nm. IR spectrum shows FAU structure with D6R frequency at

570 cm^{-1} and v_{as} T-O-T at 993 cm^{-1} (Fig. 17b). SEM image gives a maximum particle size of 5 μm (Fig. 18).

The sample of a starting composition with n_{Si}/n_{Al} = 5 but synthesized for longer time (14 days) shows FAU structure of lower n_{Si}/n_{Al} value (~ 1.65) with an average crystal size of 140(4) nm. The degree of crystallinity is about 80 %. The amount of P zeolite increases distinctly in this sample and reaches ~ 21 % (Fig. 19a). IR spectrum shows the FAU structure of D6R frequency at 569 cm^{-1} and v_{as} T-O-T at 993 cm^{-1} (Fig. 19b). SEM image gives a maximum particle size of 3 μm (Fig. 20).
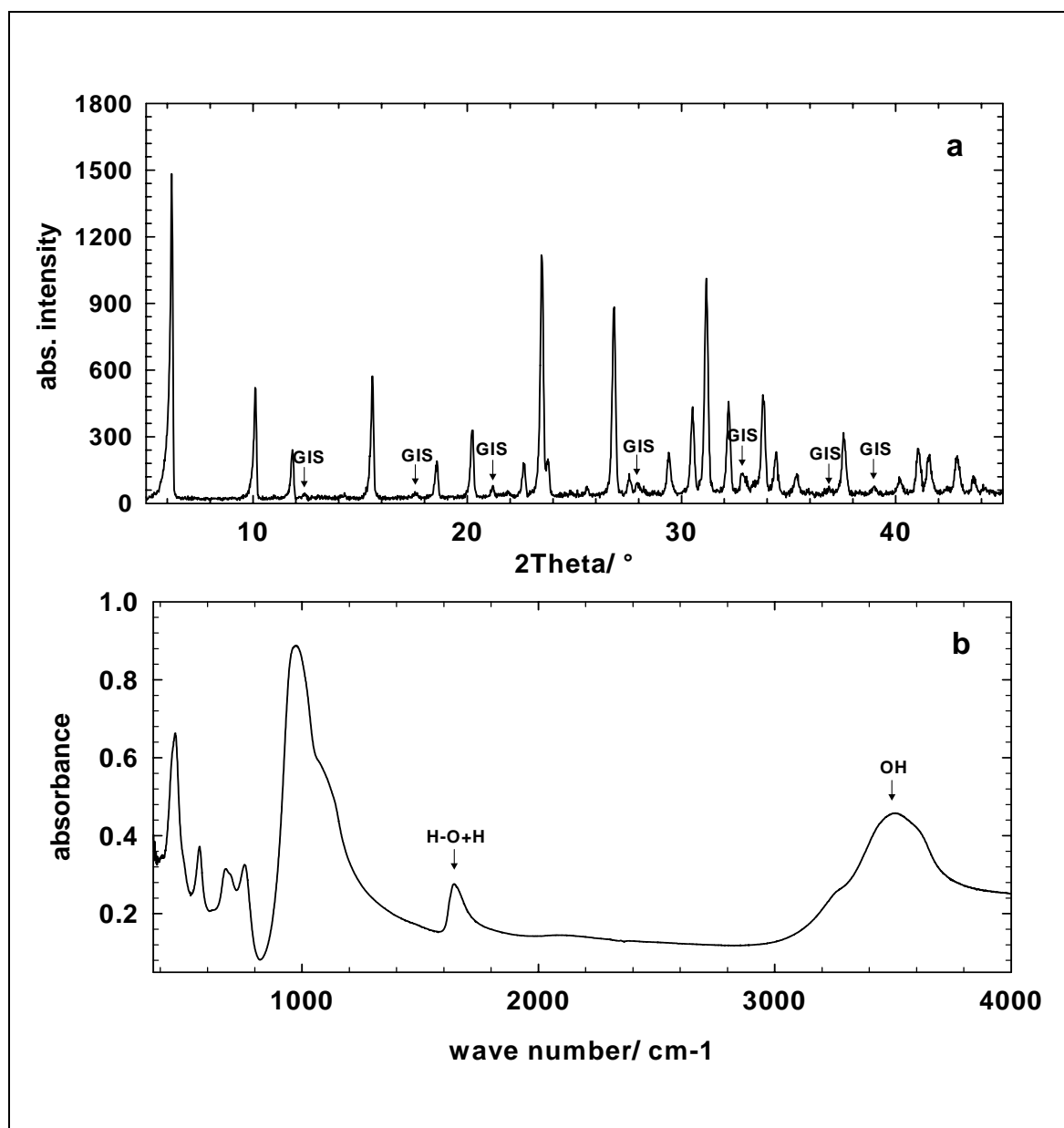
Fig. 15. X-ray diffraction pattern (a) and IR spectrum (b) of the FAU sample of a strating composition with n_{Si}/n_{Al} = 2.5 synthesized for 7 days after the modified synthesis of [39].
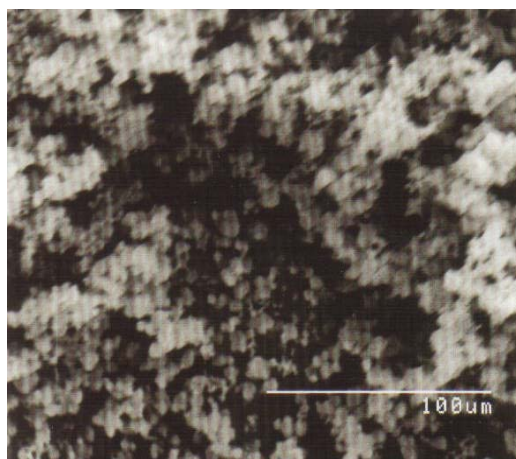
Fig. 16. SEM image of the FAU sample of a starting composition with n_{Si}/n_{Al} = 2.5 synthesized for 7 days after the modified synthesis of [39]. The maximum particle size is ~ 5 μm.
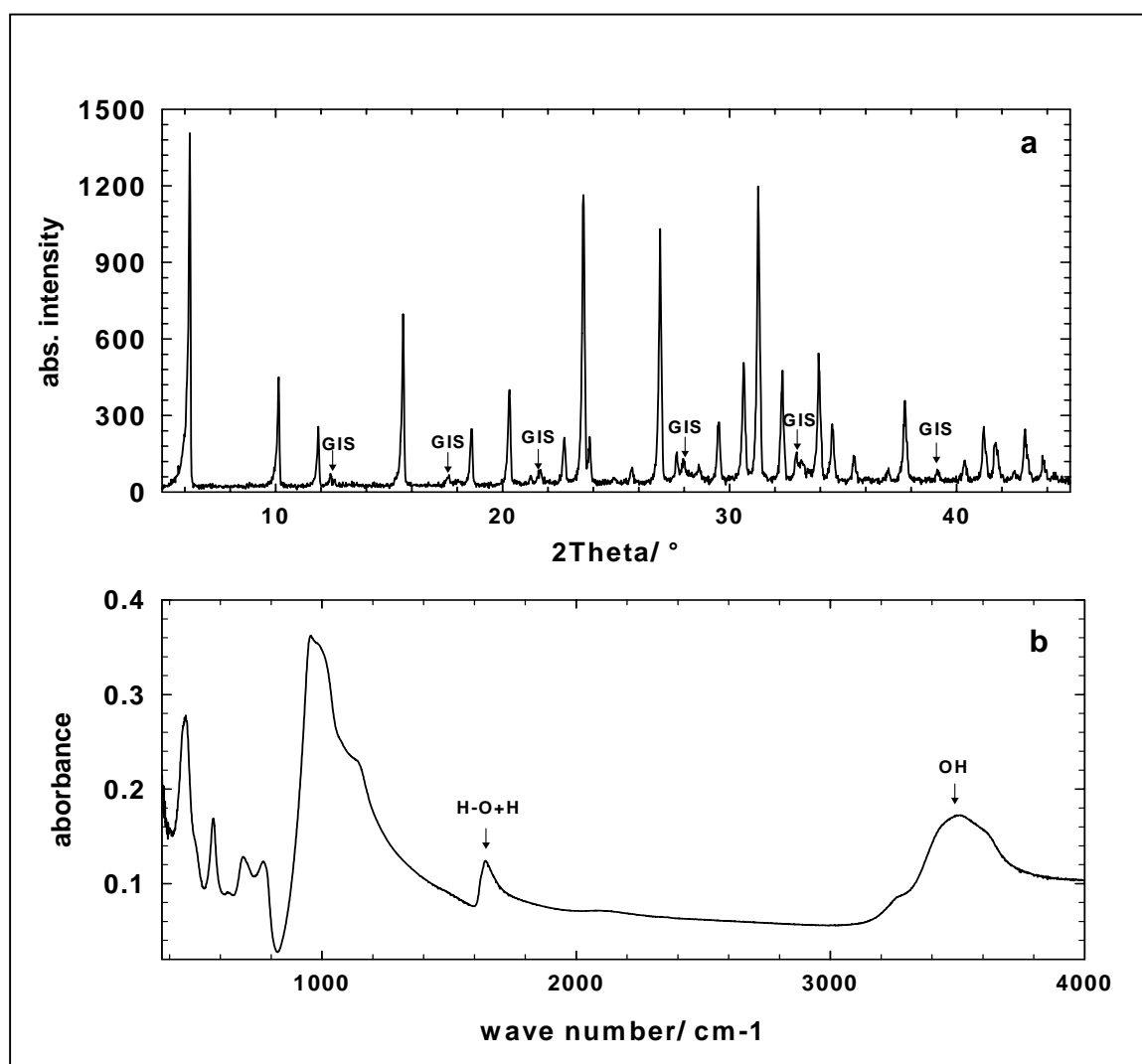
Fig. 17. X-ray diffraction pattern (a) and IR spectrum (b) of the FAU sample with a starting composition of n_{Si}/n_{Al} = 5 synthesized for 7 days after the modified synthesis of [39].
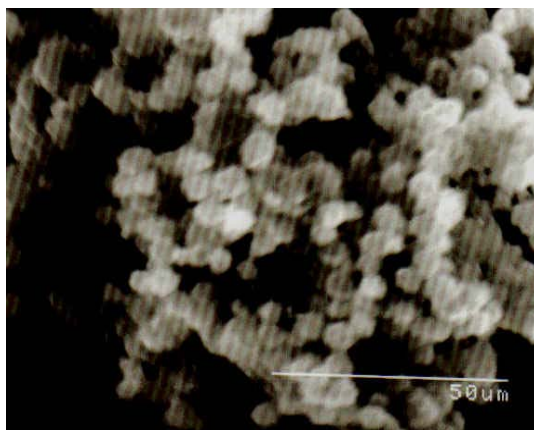
Fig. 18. SEM-image of the FAU sample with a starting composition of n_{Si}/n_{Al} = 5 synthesized for 7 days after the modified synthesis of [39]. The maximum particle size is ~ 5 μm.
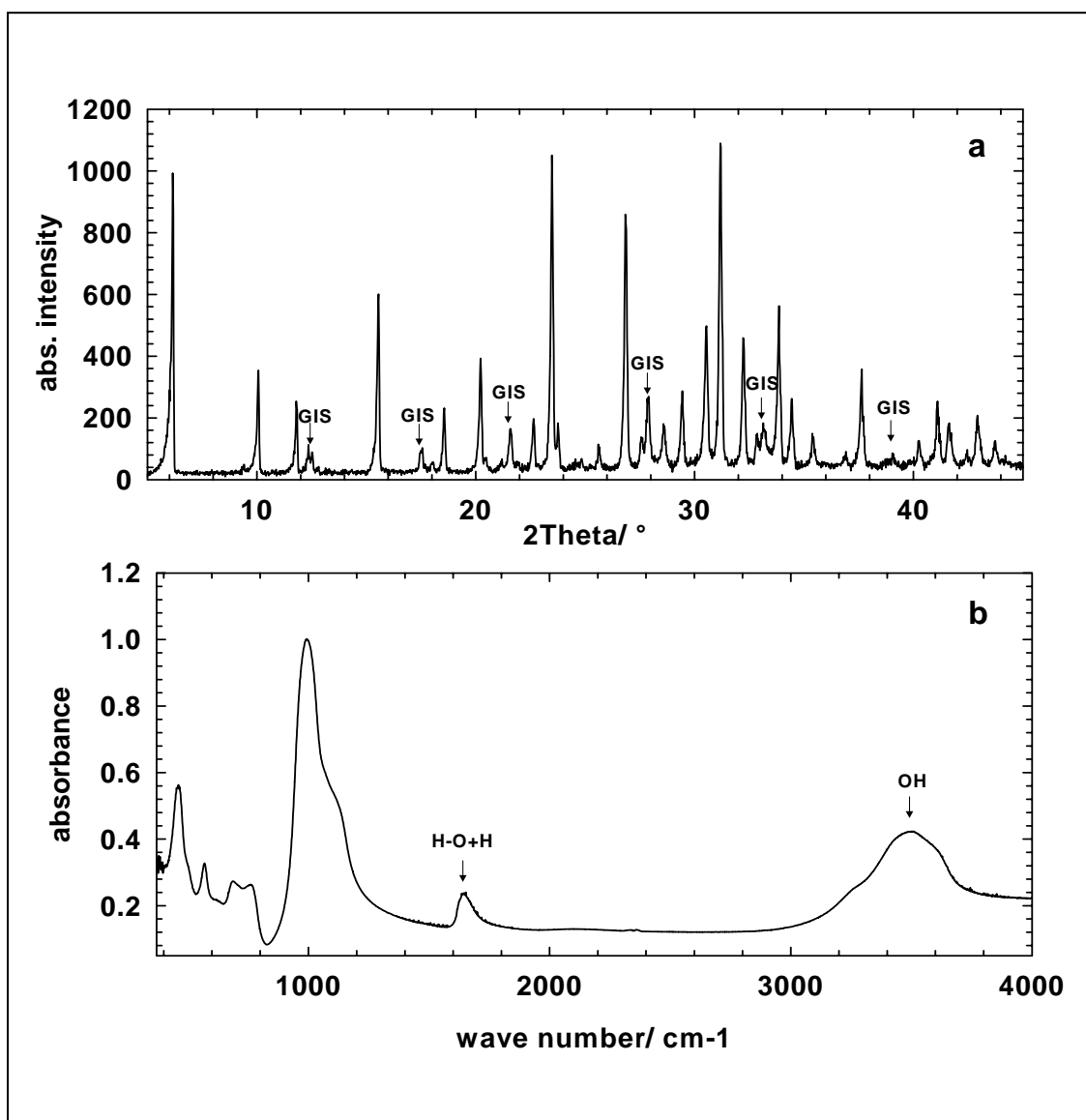
Fig. 19. X-ray diffraction pattern (a) and IR spectrum (b) of FAU and GIS phases with a starting composition of n_{Si}/n_{Al} = 5 synthesized for 14 days after the modified synthesis of [39].
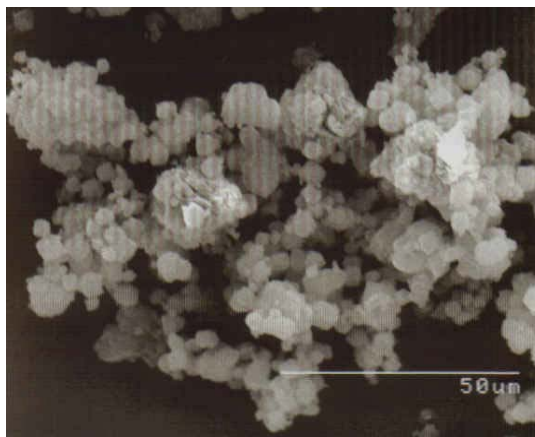
Fig. 20. SEM-image of FAU and GIS phases with a strating composition of n_{Si}/n_{Al} = 5 synthesized for 14 days after the modified synthesis of [39]. The maximum particle size is ~ 5 µm.

3.1.5. Characterization of the products prepared according to Ferchiche et al. [40] by XRD, FTIR and SEM

Ferchiche et al. [40] used the procedure described by Charnell [39] for the crystallization of large FAU crystals. They have modified this procedure by using TCl template together with the TEA. Filtration of the solutions was also carried out using the same filter type described in [39]. The final products contained mixtures of large FAU octahedral of ~ 175 -245 µm and polycrystalline spheres of GIS structure. The same procedure of [39] was repeated by Berger et al. [41] and faujasite crystals of crystal size between 10-100 µm were obtained with n_{Si}/n_{Al} < 1.8 and with formation of P zeolite as main product. Following the procedure described in [40] with respect to the mixing time of the starting gel at RT and the crystallization time FAU phase was crystallized within a multi-phase products. The maximum particle size obtained was ~ 32 µm. X-ray characterization of these samples reveal the formation of multi-phase products and shows the relation between average crystal size and crystallization time (Tab. 5). The average crystal size of FAU phase determined by XRD increases to 198(14) nm.

Table 5. X-ray data of samples synthesized according to Ferchiche et al. [40].

Synthesis[1]			*XRD data*				
Mixing time h	Time d	Product	Amount %	Maxim. particle size[2] µm	Avarage crystal size[3] nm	Cell parameter[4] a_0 Å	n_{Si}/n_{Al}[5]
5	14	FAU/ P1/ BSOD	70/ 17/13	07-16	62(12)	24.934(3)	1.29
5	18	FAU/ P1/ BSOD	34/ 43/ 24	13-30	198(14)	24.929(2)	1.30
24	14	FAU/ P1	38/ 62	30-32	75(6)	24.942(8)	1.27
24	18	FAU/ P1/ BSOD/ U[6]	10/5/ 42/43	10-12	152(21)	24.936(6)	1.28

[1] The samples were templated with TCl, [2,3,4, 5] determined for FAU phase, [6] U refers to the unknown phase.
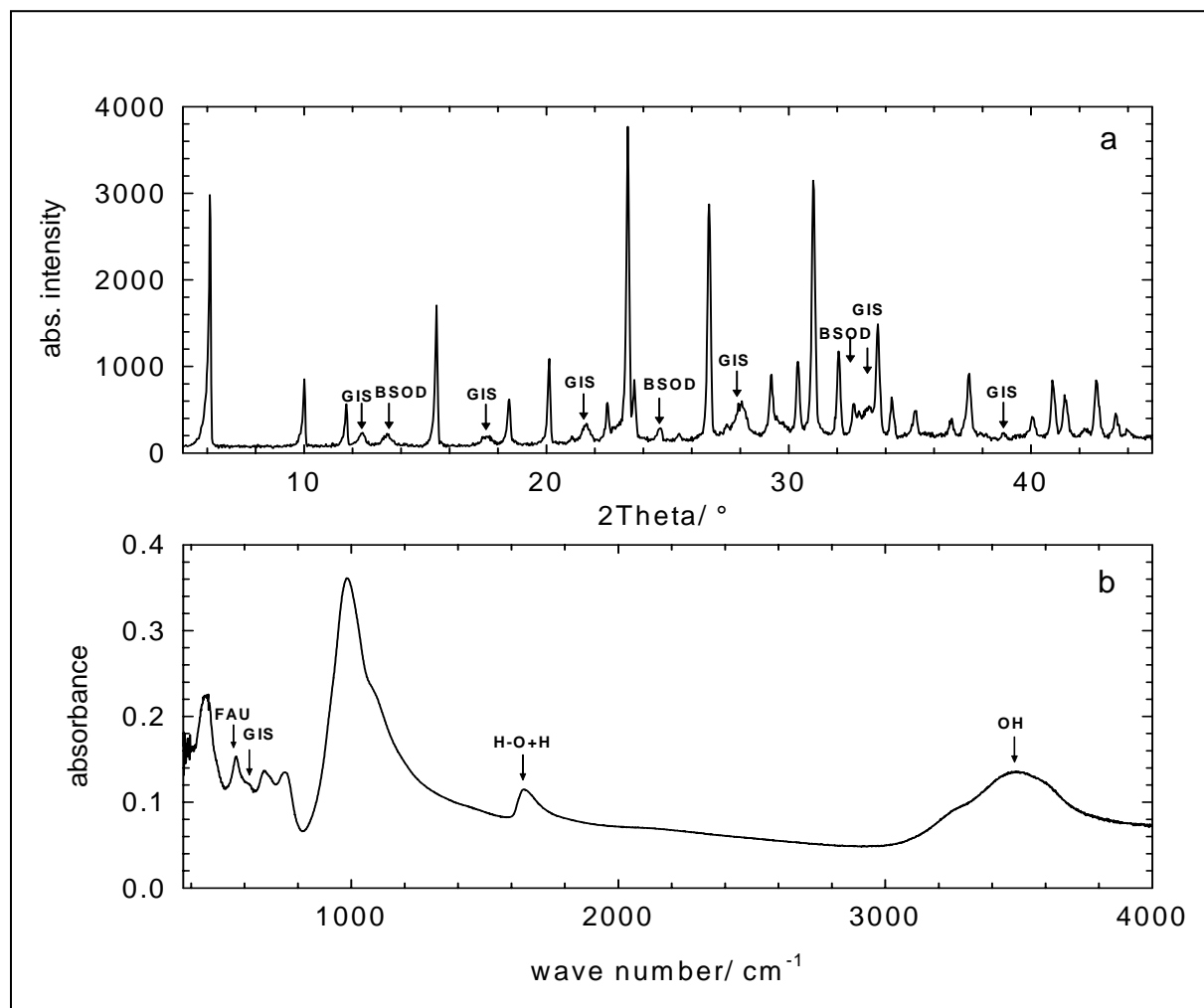
Fig. 21. XRD-pattern (a) and IR spectrum (b) of the sample prepared according to [40] with mixing time of 5h at RT and crystallization time of 14 days at 95°C.
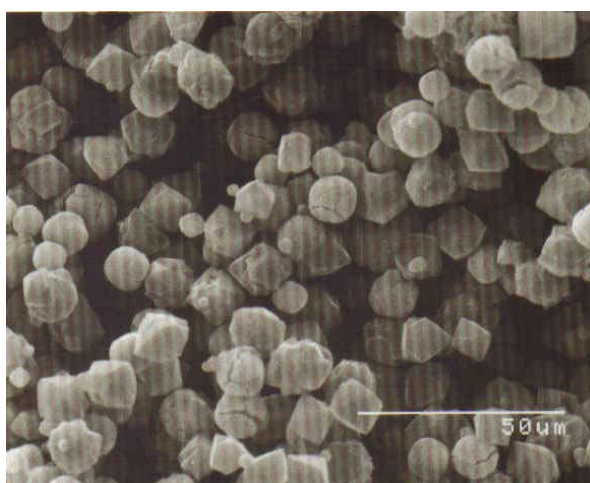
Fig. 22. SEM image of the sample with mixing time of 5h at RT and crystallization time of 14 days at 95°C prepared according to [40]. The well shaped octahedral crystals belong to FAU phase while the spherical particles belong to P1 and BSOD. The maximum particle size is 16 μm.
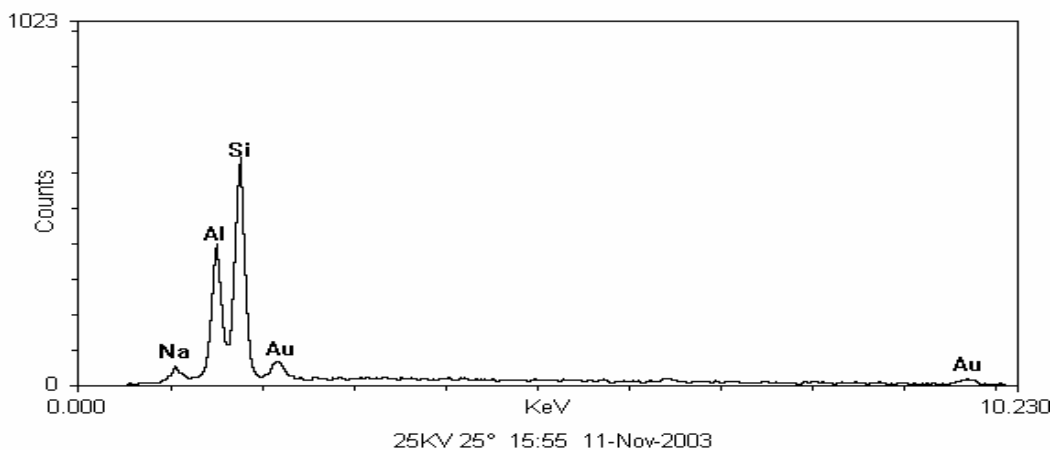
Fig. 23. EDX analysis of the octahedral crystal of the sample with 5 h mixing time and 14 days crystallization time.
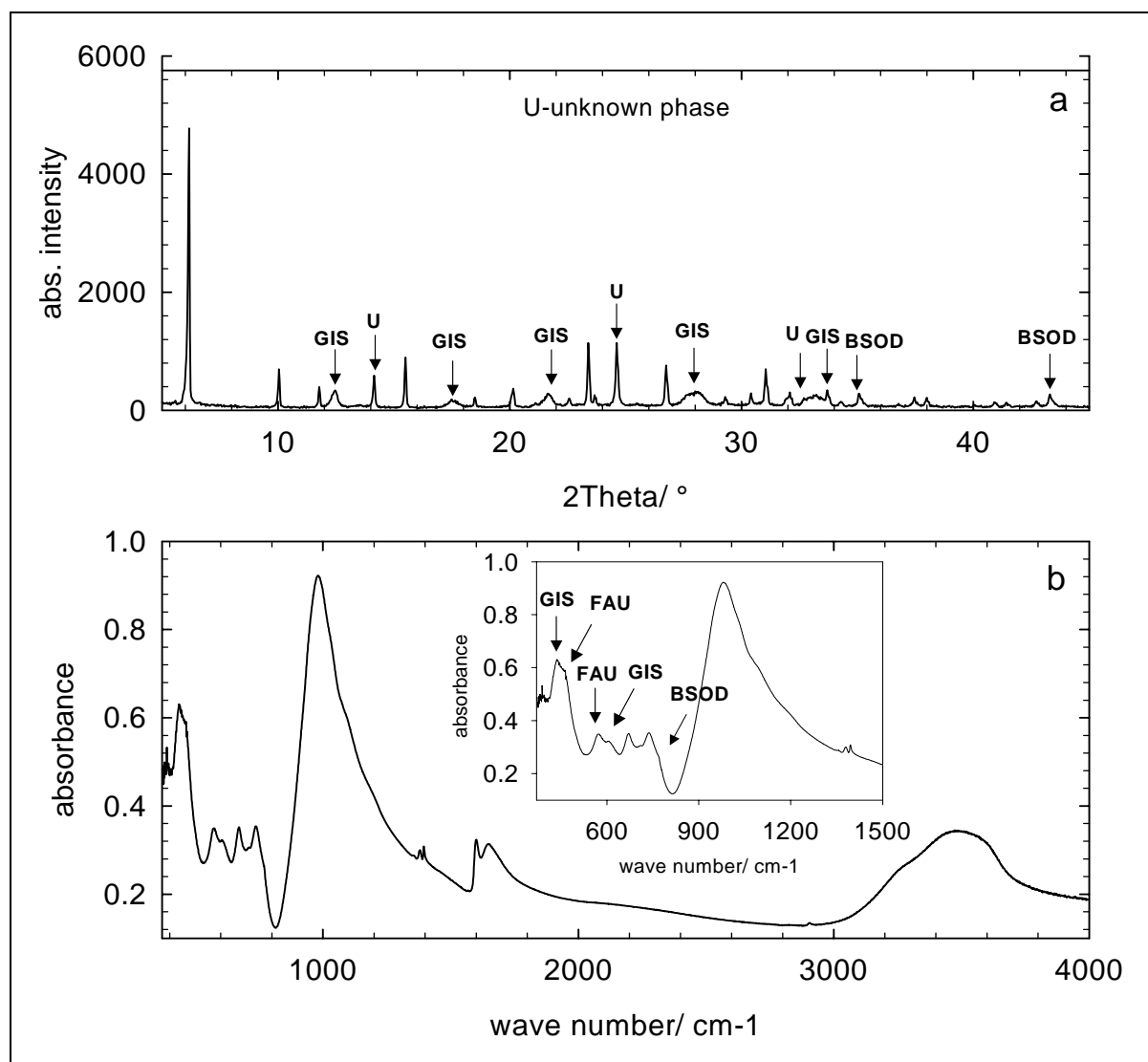
Fig. 24. XRD-pattern (a) and IR spectrum (b) of the sample prepared according to [40] with mixing time of 5 h and crystallization time of 18 days.
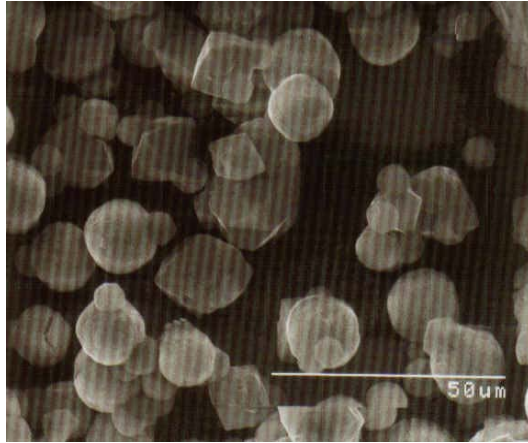
Fig. 25. SEM image of the sample with mixing time of 5 h at RT and crystallization time of 18 days at 95°C prepared according to [40]. The well shaped octahedral crstals belong to FAU phase while the spherical crystals belong to P1 and BSOD. The maximum particle size is 30 µm.
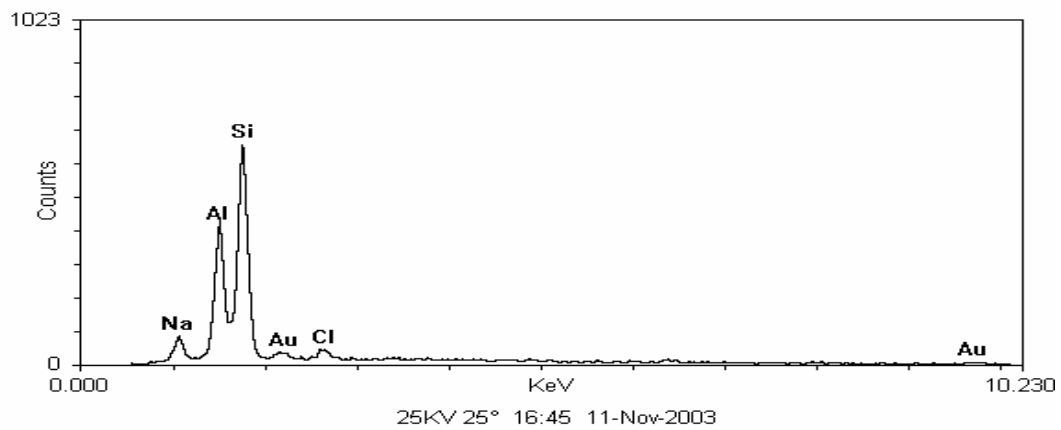
Fig. 26a. EDX analysis of the octahedral crystal of the sample with mixing time of 5 h and crystallization time of 18 days.
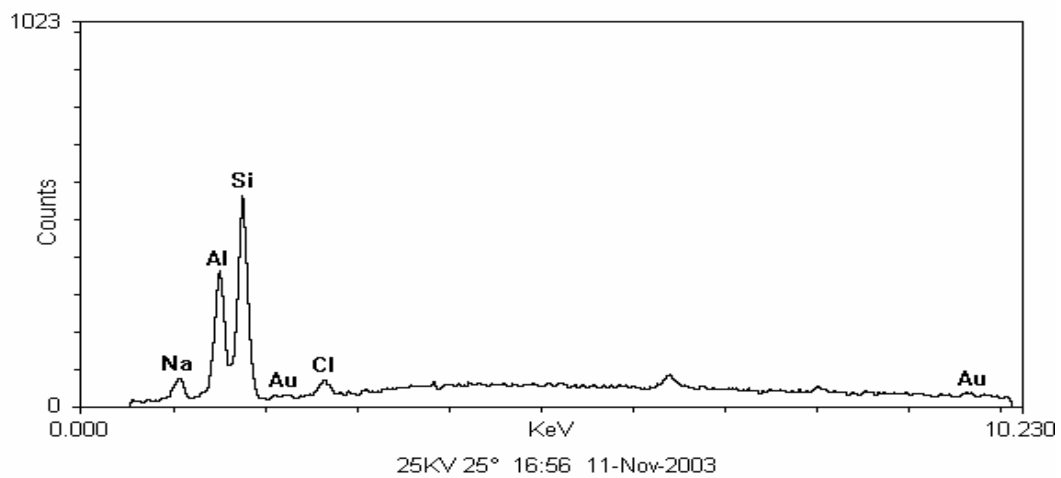
Fig. 26b. EDX analysis of the sphere of the sample with mixing time of 5 h and crystallization time of 18 days.

X-ray pattern of the sample synthesized for 14 days at 95°C of 5 h mixing time at room temperature shows FAU type as the main phase in the final product with an amount of ~ 70 % (Fig. 21a). P1 and basic sodalite (BSOD) types crystallize also as by-products. The average crystal size of FAU crystals determined by XRD is 62(12) nm. The IR spectrum shows a superimposition of FAU, P1 and BSOD phases in the frequency range between 550 cm^{-1} to 800 cm^{-1} (Fig. 21b). The maximum particle size is ca.10 μm (Fig. 22). The qualitative analysis of EDX refers the existence of Si, Al, Na elements in both octahedral and spherical crystals (Fig. 23). After 18 days synthesis time the amount of FAU decreases to about 34 % (Fig. 24a) with increasing the amounts of P1 and basic sodalite phases. IR spectrum reveals the superimposition of D6R mode of FAU with the S4R mode of P1 type zeolite (Fig. 24b). The maximum crystal size increases to ~ 22 μm (Fig. 25). EDX analysis detected Si, Al and Na elements in both octahedral and spherical crystals (26a, 26b).
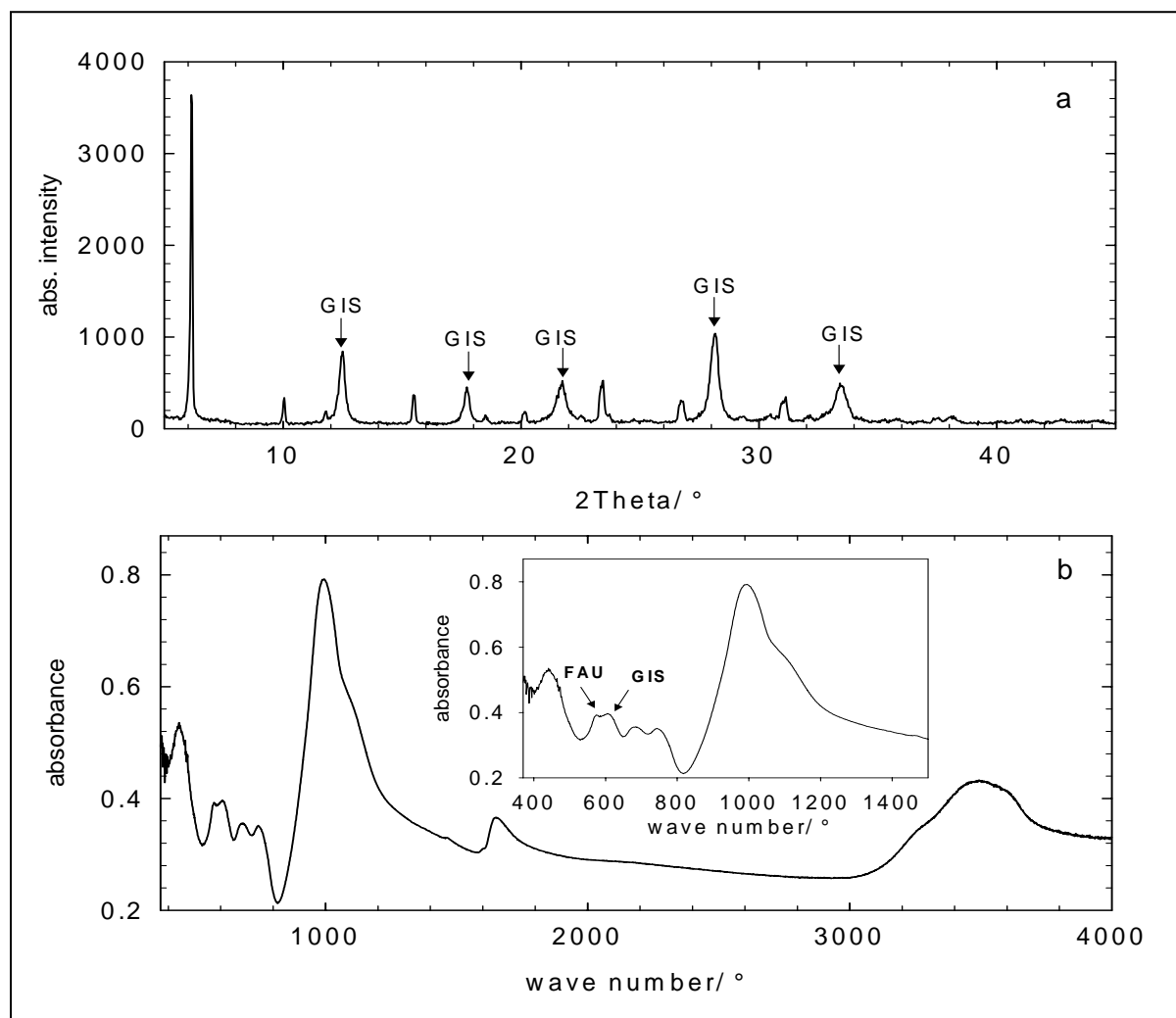
Fig. 27. XRD-pattern (a) and IR spectrum (b) of the sample prepared according to [40] with mixing time of 24 h at RT and crystallization time of 14 days at 95°C.
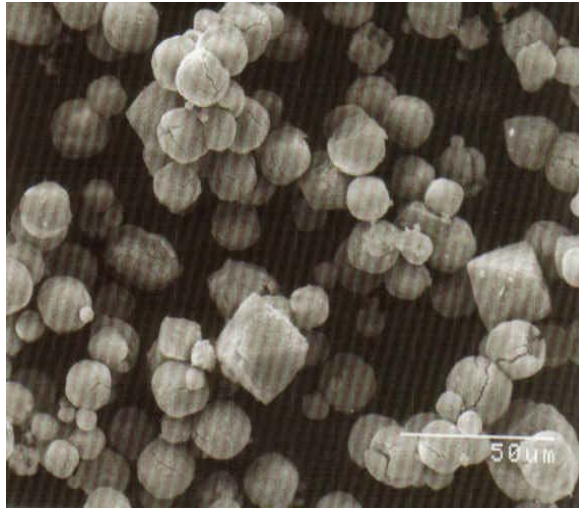
Fig. 28. SEM image of the sample with mixing time of 24 h at RT and crystallization time of 14 days at 95°C prepared according to [40]. The well shaped octahedral crystals belong to FAU phase while the spherical particles are of P1phase and BSOD. The maximum particle size is 32 μm.
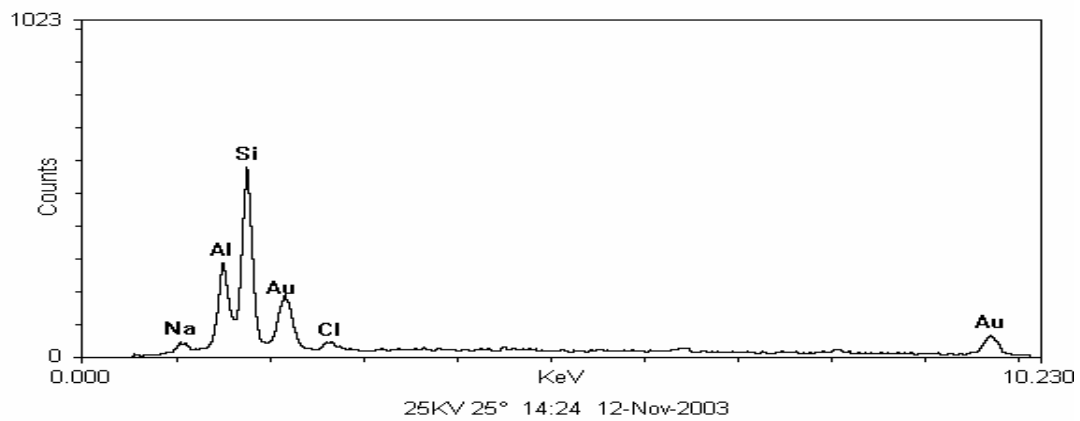
Fig. 29a. EDX analysis of the octahedral crystal of the sample with mixing time of 24 h and crystallization time of 14 days.
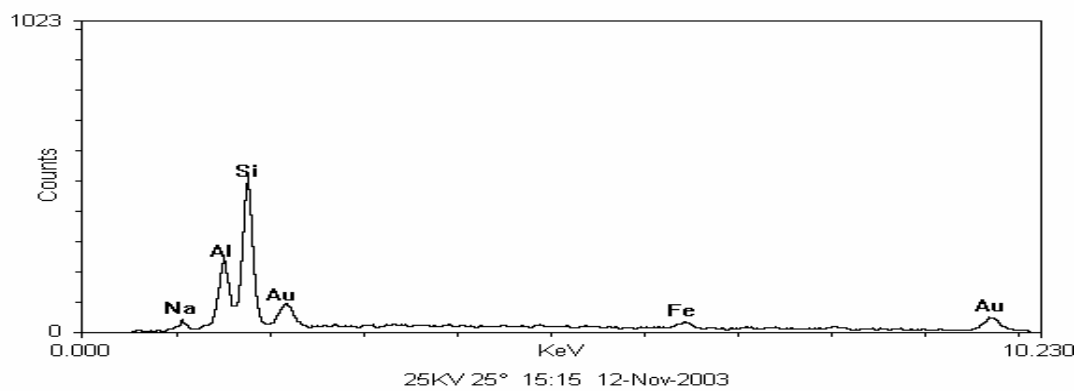
Fig. 29b. EDX analysis of a sphere in the sample with mixing time of 24 h and crystallization time of 14 days.

In contrast, in the sample of 24 h mixing time and 14 days synthesis time zeolite P grows as the main phase with 62 % (Fig. 27a). The average crystal size of FAU crystals determined by XRD is 75(6) nm. IR spectrum shows three superimposed phases in the range of bending mode, D6R vibration mode and symmetric streching mode (Fig. 27b). The maximum crystal size of the FAU is ~ 32 μm (Fig. 28). EDX analysis detected Si, Al and Na elements in both octahedral and spherical particles (29a, 29b).
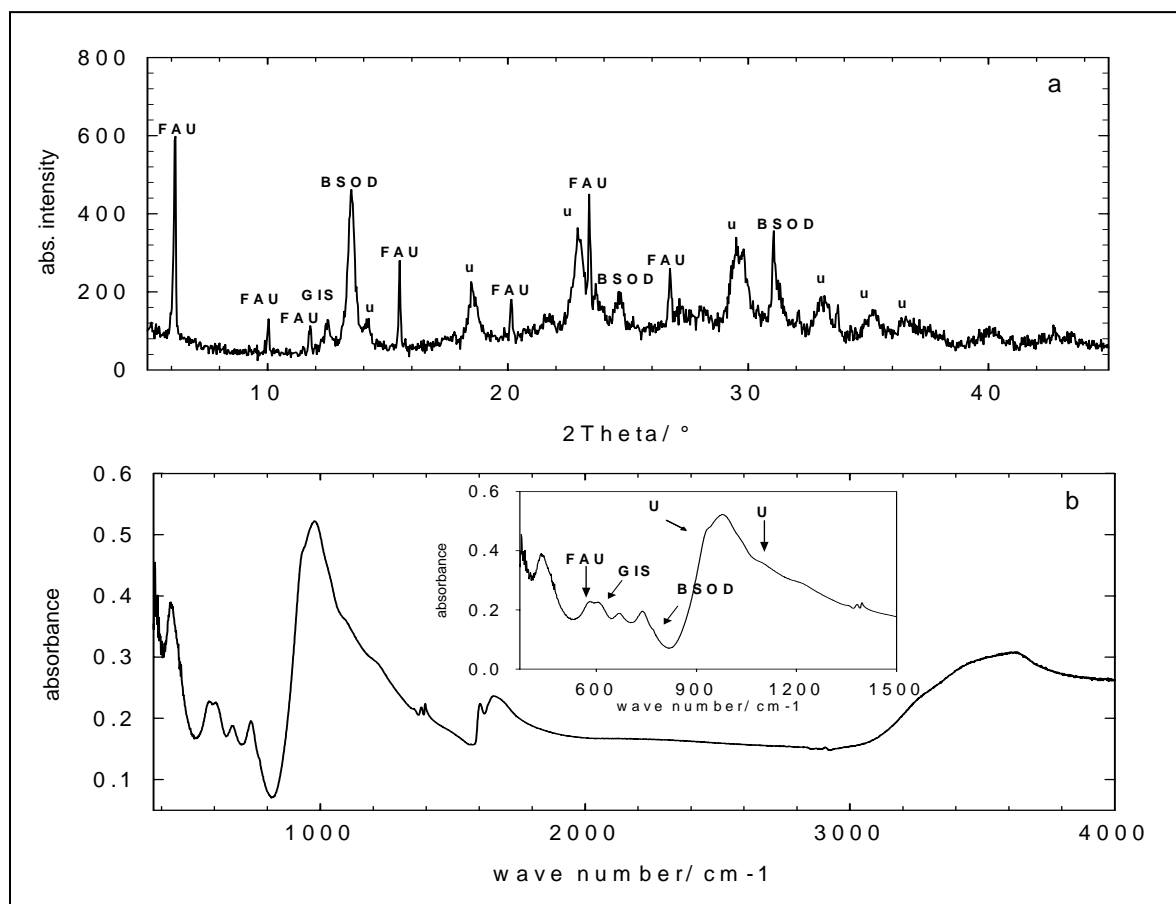
Fig. 30. XRD-pattern (a) and IR spectrum (b) of the sample prepared according to [40] with mixing time of 24 h at RTand crystallization time of 18 days at 95°C.

With increasing synthesis time to 18 days the amount of FAU phase decreases dramatically to 10 % and BSOD phase becomes significant in the sample with an amount of 42 % together with an unknown phase (characterized by XRD using Topas program) with an amount of 43 % while P1 phase decreases to 5 % (Fig. 30a). The average crystal size determined by XRD increases to 152(21) nm. IR spectrum reveals a superimposition of P1 and FAU phases resulting in a broadening of bending and D6R modes (Fig. 30b). The maximum particle size decreases to about 12 μm (Fig. 31). EDX analysis detected Si, Al and Na elements in both octahedral and spherical particles (32a, 32b).
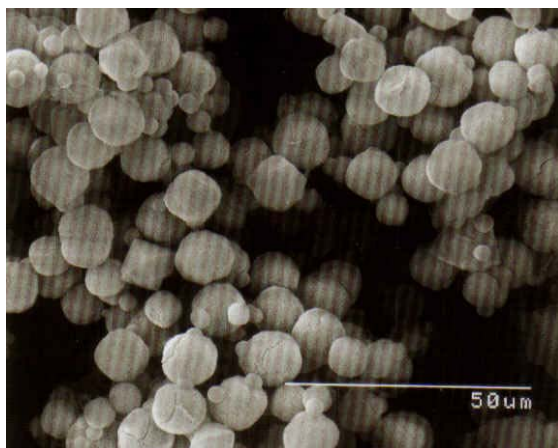
Fig. 31. SEM image of the sample with mixing time of 24 h at RT and crystallization time of 18 days at 95°C prepared according to [40]. The small and bigger spherical crystals belong to P1, BSOD and the unknown phase. The maximum crystal size of FAU particles is 12 μm.
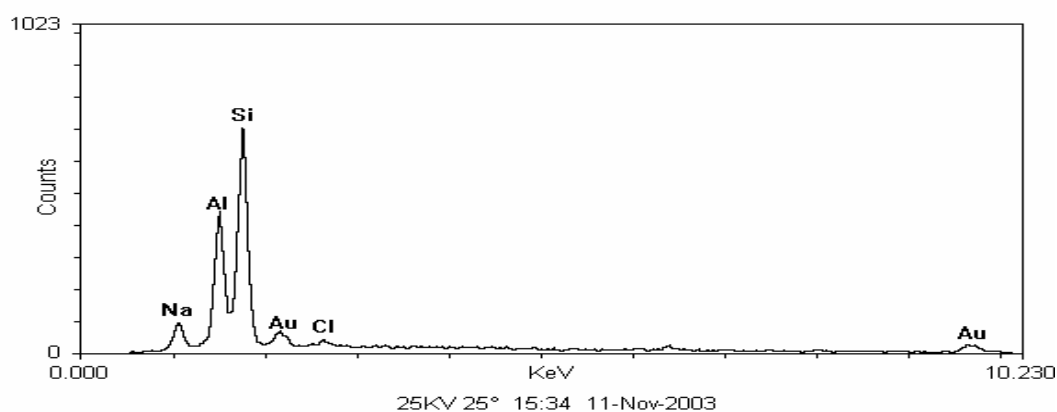
Fig. 32a. EDX analysis of the octahedral crystal of the sample with mixing time of 24 h and crystallization time of 18 days.
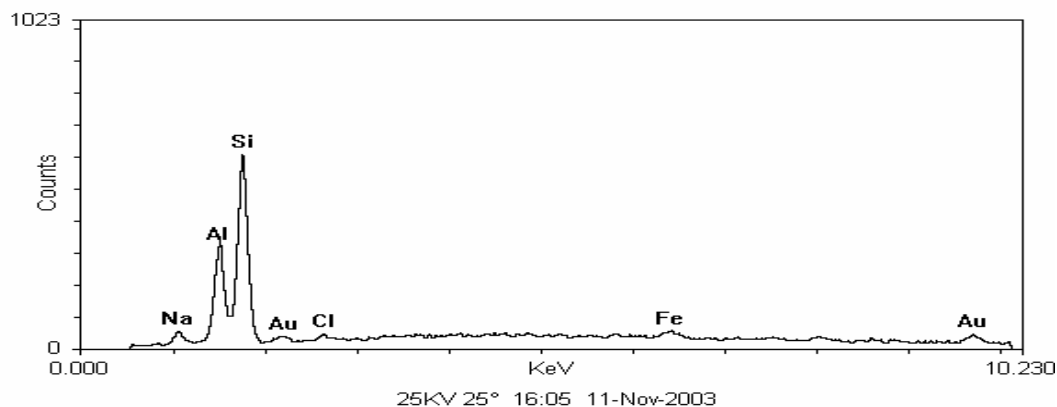
Fig. 32b. EDX analysis of the spheres of the sample with mixing time of 24 h and crystallization time of 18 days.

3.1.6. Characterization of the products of the modified procedure of Ferchiche et al. [40] by XRD, FTIR and SEM

The modification of this procedure was by adding nucleation solution to the initial batch in the presence of TEA and TCl and varying of crystallization time and temperature. Results of XRD characterizations of the samples synthesized after this modified procedure are given in table 6.

Table 6. X-ray data of samples after the modified synthesis of Ferchiche et al. [39].

Synthesis					XRD data			additive
Total time d	Product	Amount %	Average crystal size/ nm [1]	Crystallinitiy %	a_0 [2] Å	n_{Si}/n_{Al} [3]		
20	FAU	100	162(5)	99	24.766(1)	1.90		nucleation solution + TEA+ TCl
20	FAU/ GIS	65/ 35	217(11)	75	24.766(1)	1.88		TEA+ TCl

[1,2,3] determined for FAU phase
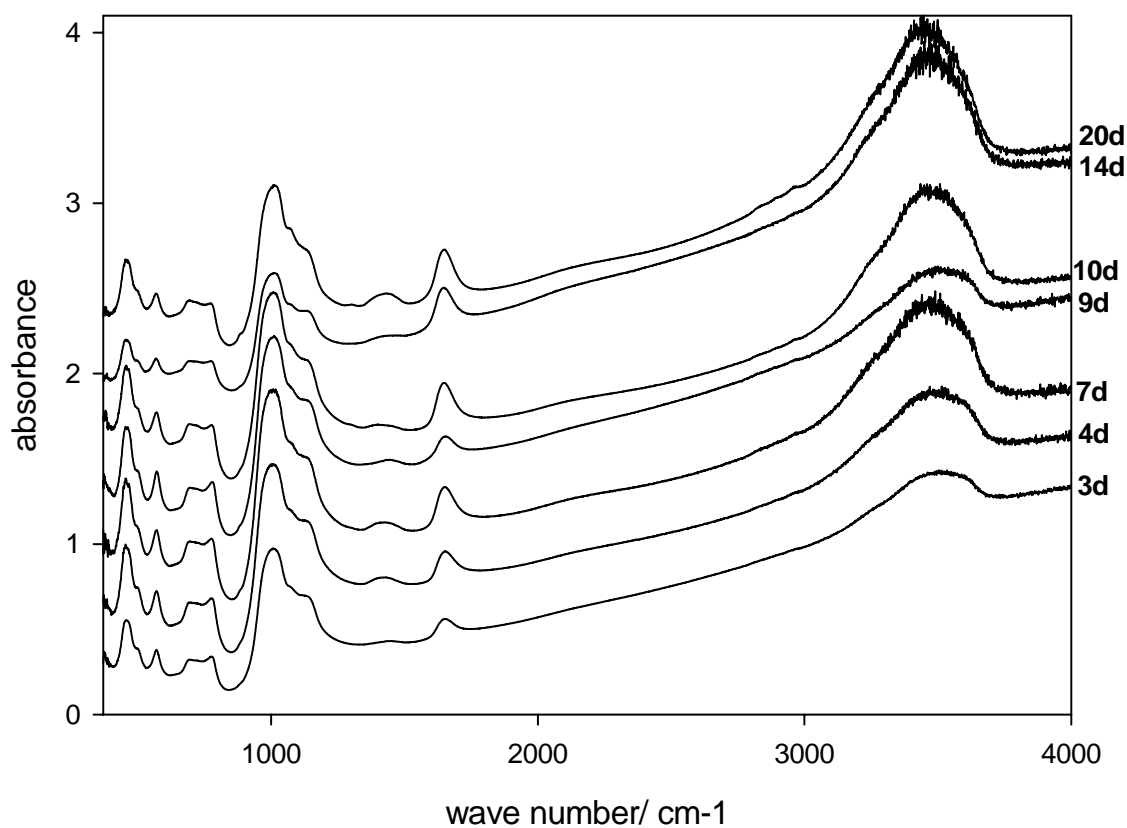
Fig. 33. IR spectra of kinetic measurement of samples prepared after the modified synthesis of [40] (templated) in the presence of nucleation solution.

IR spectra of this sample indicate a phase stability after 20 days (Fig. 33). However, the intensities of the D6R and ν_S T-O-T peaks decrease with increasing time and a general peak broadening is detected. Synthesis of a similar batch with the absence of the nucleation solution leads to crystallization of P zeolite at the late crystallization stage. X-ray pattern and IR spectra of these two batches with absence and presence of the nucleation solution are shown in figure 34. SEM-image of this sample shows a wide crystal size distribution with aggregates of nano-crystals (spherical shape) up to 15 μm (Fig. 35).
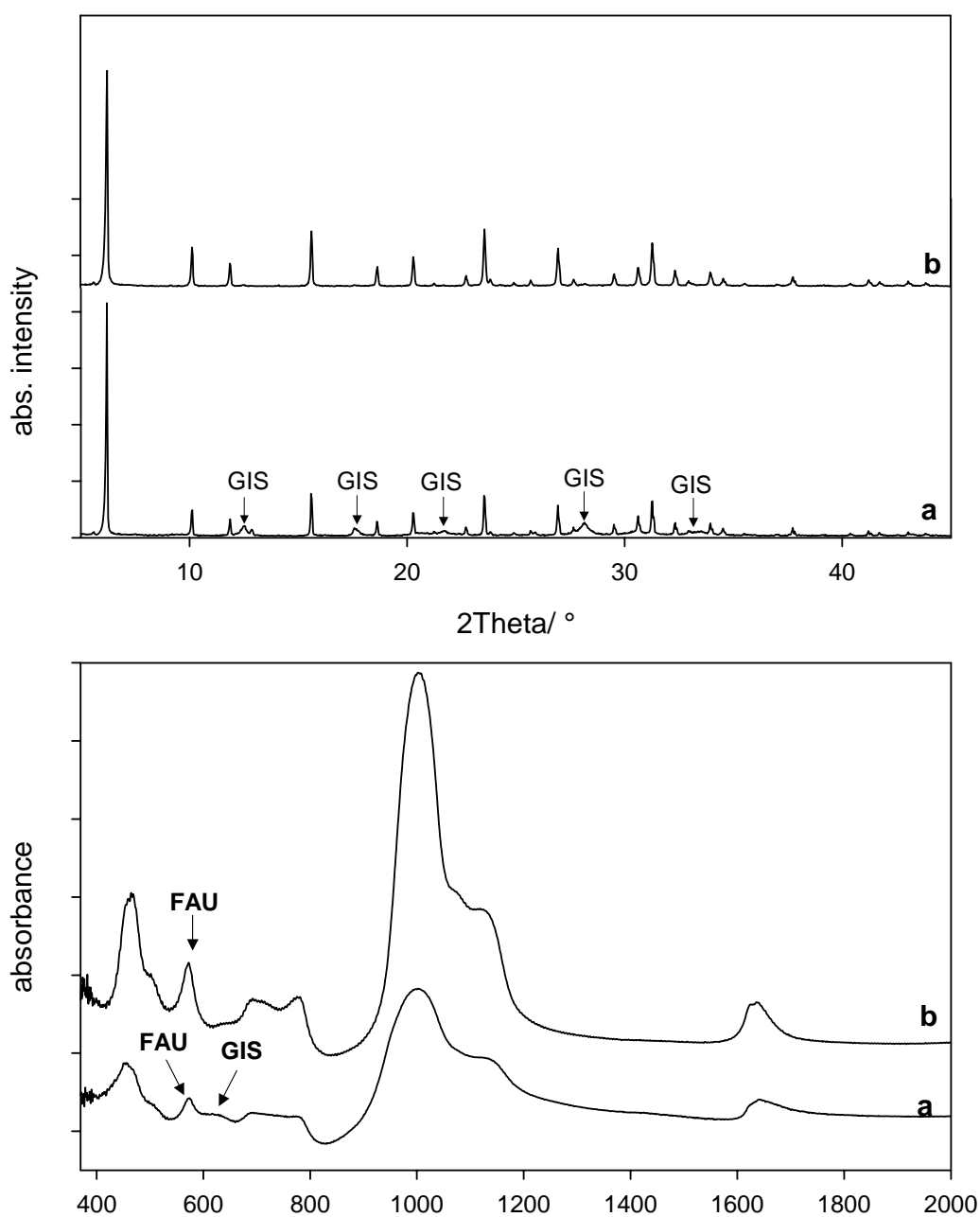
Fig. 34. X-ray diffraction patterns and IR spectra of samples crystallized with the absence of nucleation solution (a) and with its presence (b).
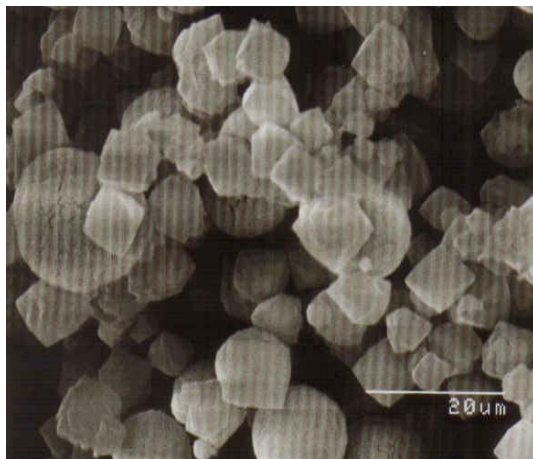
Fig. 35. SEM image of the sample prepared after the modified synthesis of [40], crystallized in the presence of a nucleation solution.

Another modification was performed concerning the incorporation of high silica content in the batch in order to obtain FAU crystals of higher n_{Si}/n_{Al}. Therefore, another trial was prepared with the same starting composition described by [40] and using same organic templates. The modification was done by adding "nucleation solution" and modifying the synthesis time and temperature (Tab. 7). X-ray pattern of the sample crystallized for 14 days is shown if figure 36a. Nearly a pure phase of FAU with only 1 % of P1 as an impurity phase was obtained. The degree of crystallinity of this sample is ~ 94 %. The cell parameter a_0 of FAU type is 24.726(2) Å (n_{Si}/n_{Al} of 2.07).

Table 7. X-ray data of samples of further modified synthesis after Ferchiche et al. [40].

Synthesis			XRD data				additive
Time d	Product	Amount %	Average crystal size[1] nm	Crystallinitiy %	a_0[2] nm	n_{Si}/n_{Al}[3]	
14	FAU/ P	99/ 1	92(2)	94	2.4726(2)	2.07	Nucleation solution + TEA+ TCl
28	FAU/P	95/ 5	142(4)	89	2.4773(2)	1.85	Nucleation solution + TEA+ TCl

[1,2,3] determined for FAU phase

The average crystal size estimated by XRD method is 92(2) nm. IR spectrum of this sample shows the typical FAU structure with a D6R peak of high intensity recorded at 579 cm^{-1} (Fig. 36b). The maximum particle size measured from SEM-image is 2 µm (Fig. 37).

After 28 days synthesis the sample shows a decrease in the crystallinity portion (89 %) with increasing of P1 phase amount up to 5 % (Fig. 38a).
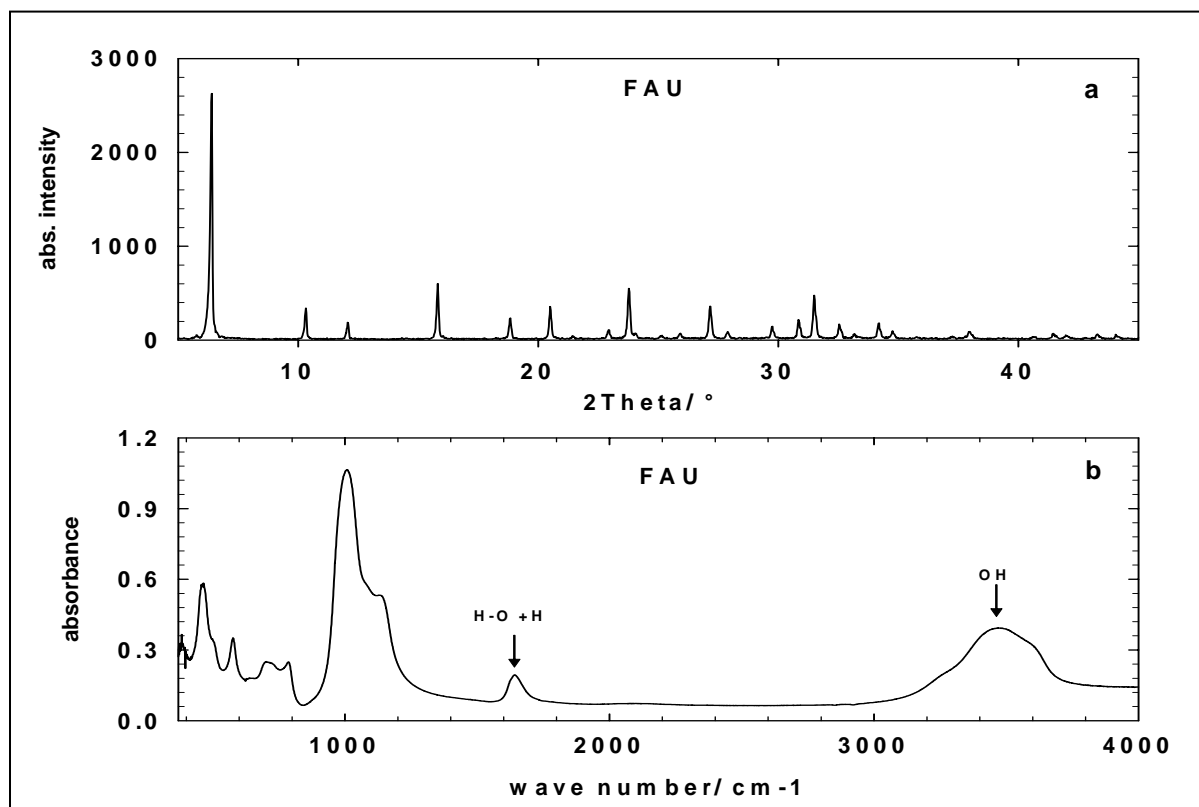
Fig. 36. X-ray diffraction pattern (a) and IR spectrum (b) of the sample prepared after the modified synthesis of [40] in the presence of the nucleation solution. Crystallization time is 14 days.
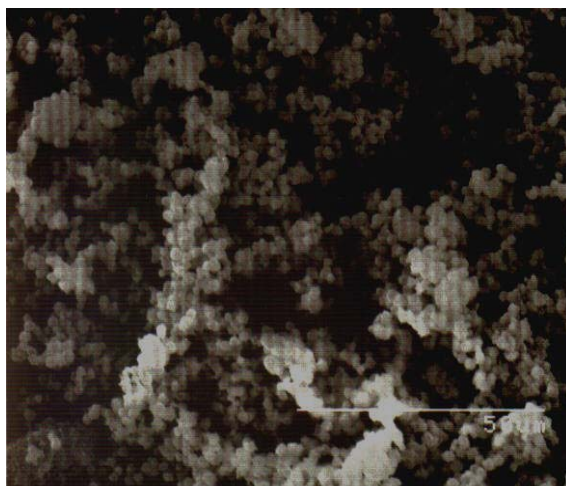
Fig. 37. SEM image for the modified sample prepared after the modified synthesis of [40] in the presence of nucleation soluton for 14 days crystallization time. The maximum particle size is ~ 2 μm.

The cell parameter a_0 of FAU increases to 24.773(2) Å and, consequently, the n_{Si}/n_{Al} value decreases (1.85) indicating an increase of the framework aluminium. The average crystal size estimated from XRD method increases to 142(4) nm. IR spectrum of the sample synthesized

for 28 d shows the D6R at 573 cm^{-1} and the ν_{as} T-O-T at 997 cm^{-1} (Fig. 38b). SEM image of this sample reveals a maximum crystal size of ca. 5 μm (Fig. 39).
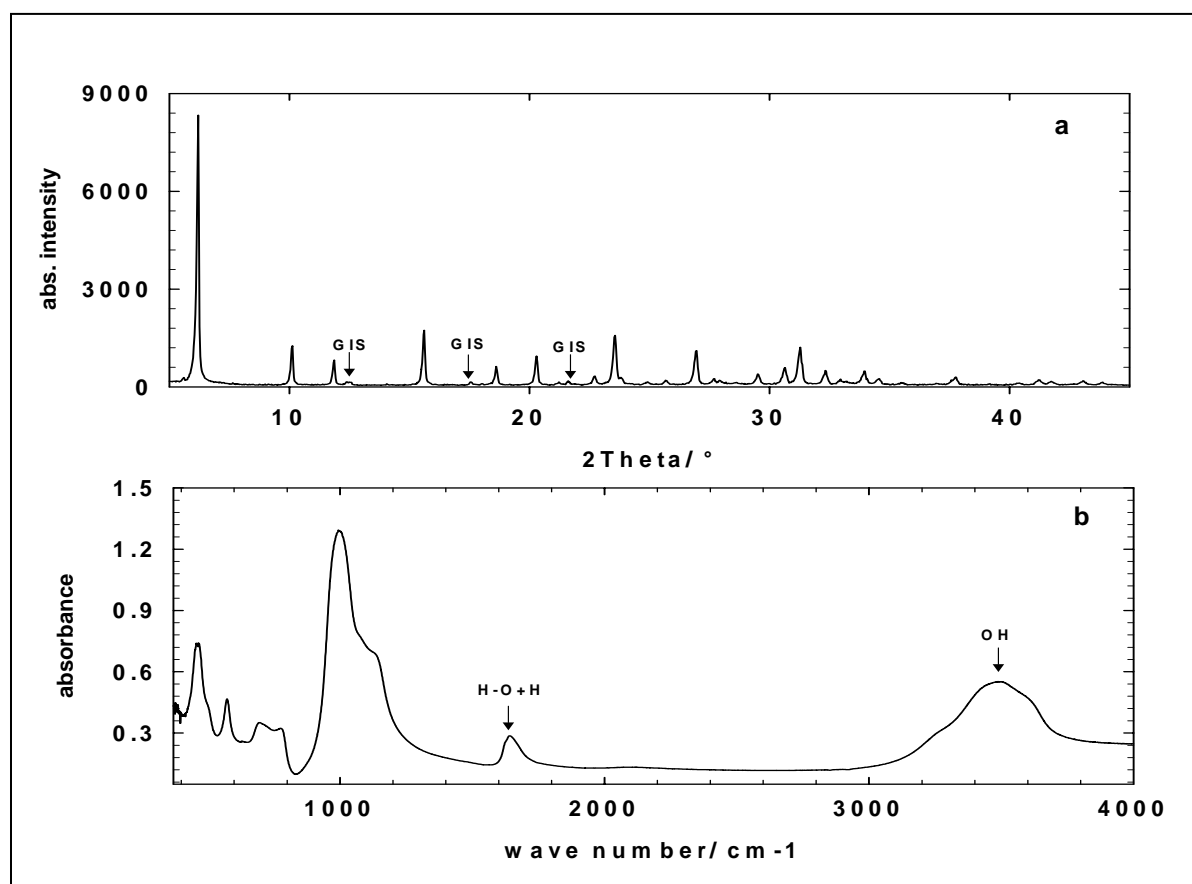
Fig. 38. X-ray diffraction pattern and IR spectrum of the modified sample prepared after the modified synthesis of [40] in the presence of the nucleation solution. Crystallization time is 28 days.
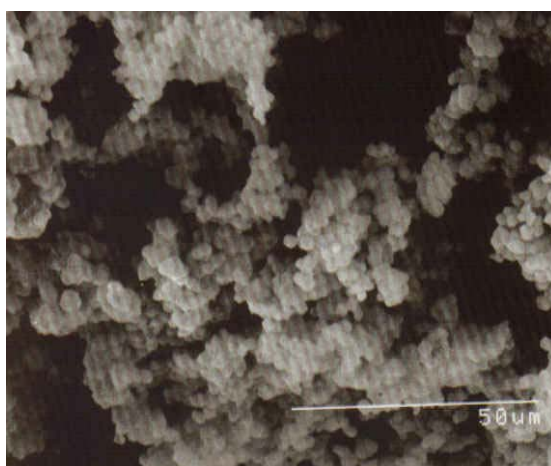
Fig. 39. SEM-image of the sample prepared after the modified synthesis of [40] in the presence of the nucleation solution for 28 days crystallization time. The maximum particle size is ~ 5 μm.

IR investigation within the mid infrared range has been employed to provide a kinetic view during crystallization. The studied aluminosilicate gel of X-type starting composition has been investigated in four cases; the absence of nucleation solution and template (Fig. 40), presence of nucleation solution and absence of template (Fig. 41), presence of templates and absence of nucleation solution (Fig. 42) and presence of both nucleation solution and templates (Fig. 43). These kinetic experiments were performed for observation of phase transition from the amorphous into the crystalline state affected by using additives as template (organic cations) or/and as directing agents of the crystallization process (nucleation solution). IR measurement of the gel was a suitable tool for such observation during synthesis at RT and at hydrothermal conditions (95°C and synthesis times between 0.5 h and 21 days for each sample). Important results have been estimated from this kinetic study pointed out in the following:
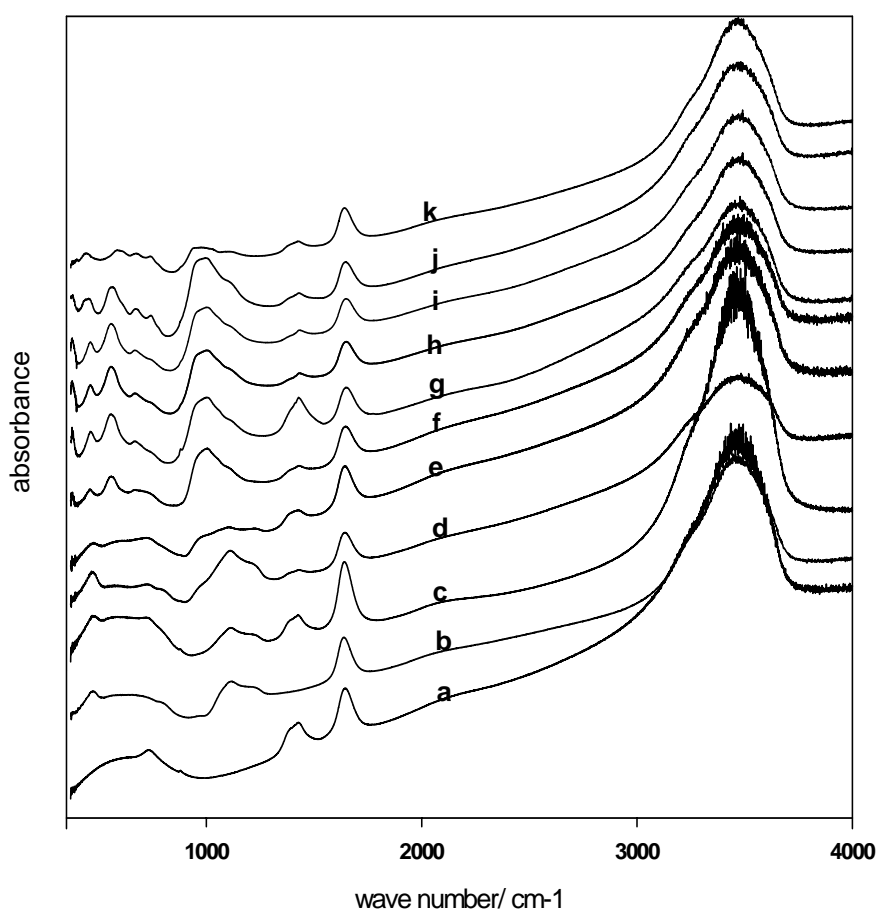
Fig. 40. IR spectra of kinetic measurements during crystallization of an aluminosilicate gel in the absence of nucleation solution and templates: a) aluminate solution at RT, b) silica slurry at RT, c) aluminosilicate gel at RT, d) at 90 ℃ after 30 min., e) at 90 ℃ after 2 h, f) at 90 ℃ after 5 h, g) at 90 ℃ after 1 d, h) at 90 ℃ after 2d, i) at 90 ℃ after 7 d, j) at 90 ℃ after 14 d, k) at 90 ℃ after 21 d.

- Synthesis of an aluminosilicate gel of a composition suitable for crystallization of A-, X- type zeolites without any additives leads to the formation of A type zeolite. this phase starts to appear after just 2 hours at 95°C and stays stable for long time (Fig. 40).
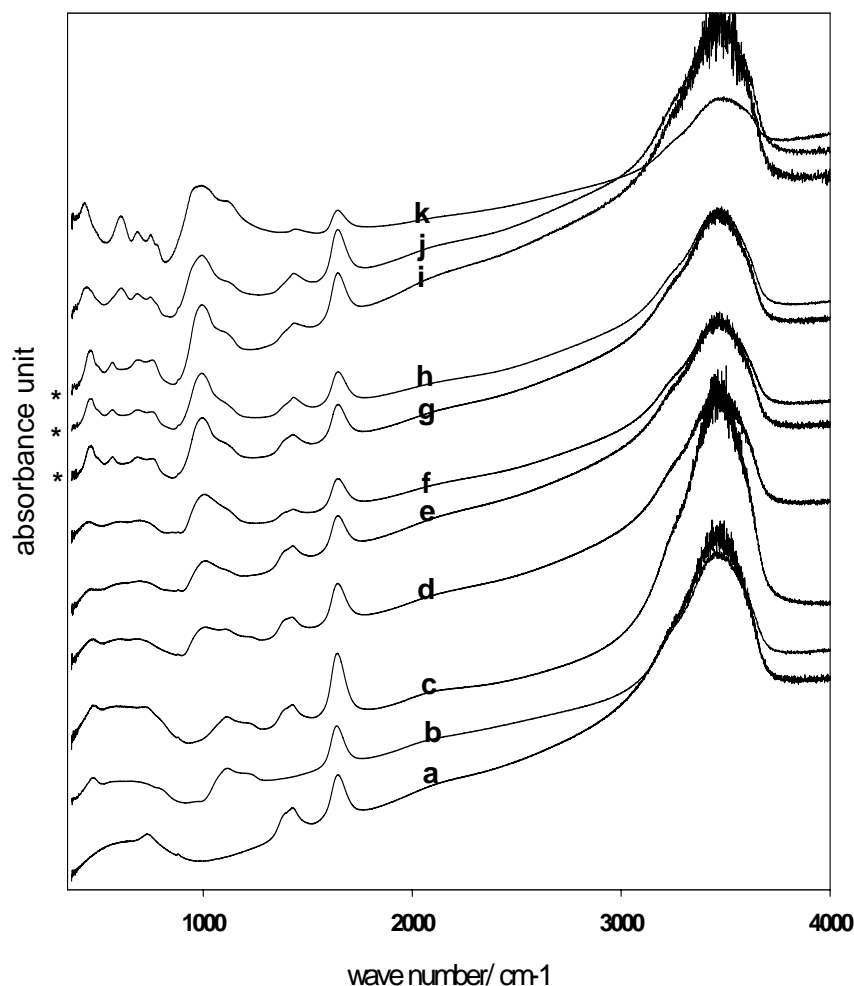
Fig. 41. IR spectra of kinetic measurements during crystallization of an aluminosilicate gel in the presence of nucleation solution and absence of templates: a) aluminate solution at RT, b) silica slurry at RT, c) aluminosilicate gel at RT, d) aluminosilicate gel + nucleation solution at RT, e) at 90 °C after 30 min., f) at 90 °C after 2 h, g) at 90 °C after 5 h, g) at 90 °C after 1 d, h) at 90 °C after 2 d, i) at 90 °C after 7 d, j) at 90 °C after 14 d, k) at 90 °C after 21 d.(* The crystallization of FAU as a pure phase).

- Synthesis of an aluminosilicate gel of a composition suitable for crystallization of A-, X- type zeolites, using a nucleation solution (mother liquor of a batch of Y starting composition) as a directing agent to the crystallization pathway leads to the crystallization of X-type after 1 day synthesis. After 3 days a re-crystallization of this phase into P1 type zeolite occurs (Fig. 41). The components in the added nucleation

solution causes the formation of FAU at the early stage. This phase is not stable and the already crystallized X type seeds dissolve again and recrystallize into P1 phase as a more stable phase. It is referred by [41] that P1 phase re-crystallizes from X and Y batches at the late synthesis period.
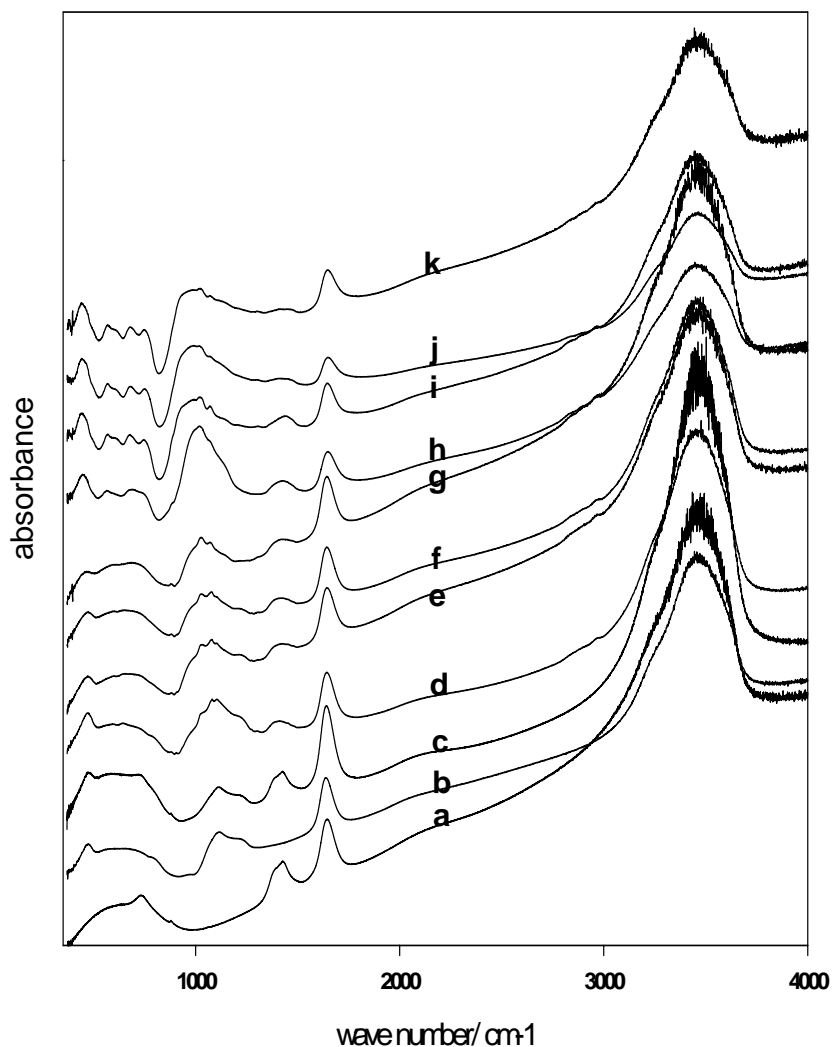
Fig. 42. IR spectra of kinetic measurements during crystallization of an aluminosilicate gel in the presence of templates and absence of nucleation solution: a) aluminate solution at RT, b) silica slurry at RT, c) aluminosilicate gel at RT, d) aluminosilicate gel + template at 90 ºC after 30 min., e) at 90 ºC after 2 h, f) at 90 ºC after 5 h, g) at 90 ºC after 2 d, h) at 90 ºC after 3 d, i) at 90 ºC after 7 d, j) at 90 ºC after 14 d, k) at 90 ºC after 21 d.

- Synthesis of an aluminosilicate gel of a composition suitable for crystallization of A-, X- type zeolites, using TEA as phase stabilizer and TCl as an organic template, leads to the formation of a multi-phase product. A simultaneous growth of X-, P- types

occurs. It seems that TEA, which stabilizes X zeolite during crystallization leads to crystallization of P zeolite as a second phase if the concentration of TEA is higher than Al concentration in the initial batch [41]. These two phases stays stable to the end of the crystallization course (Fig. 42).

- Synthesis of an aluminosilicate gel of a composition suitable for crystallization of A-, X type zeolites, using TEA as phase stabilizer and TCl as an organic template together with a nucleation solution leads to the formation of X-type as a single phase up to the end of the crystallization period (Fig. 43). The nucleation solution works together with TEA in formation and stabilizing of X phase. This result has been observed in all batches, in which TEA and nucleation solutions were used.
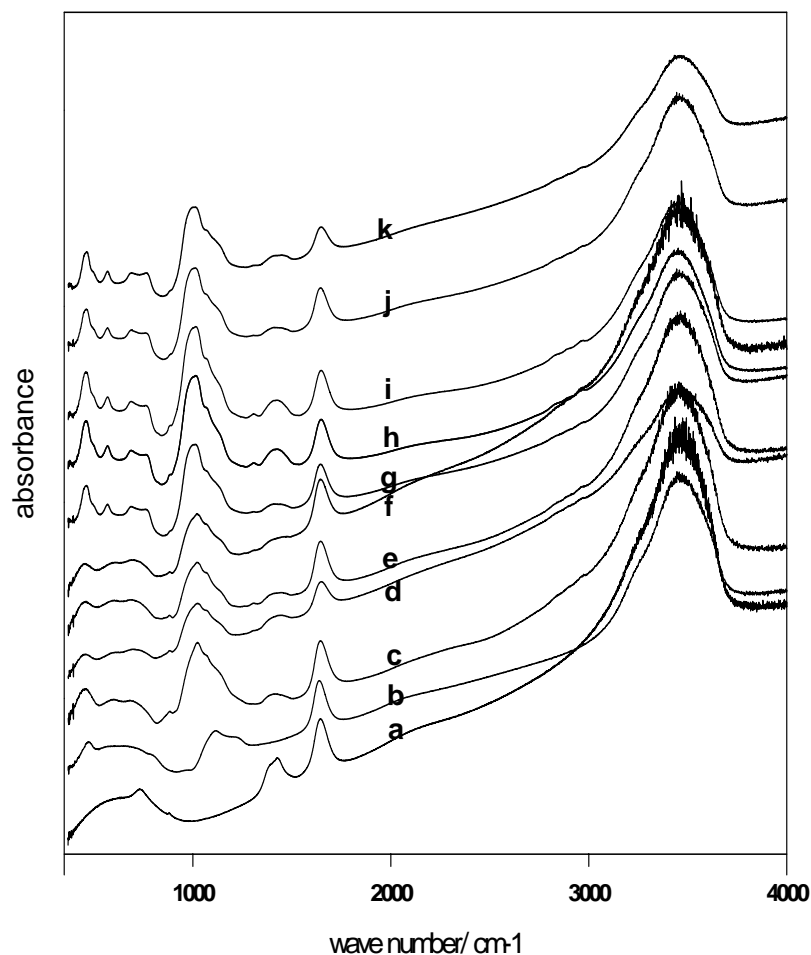
Fig. 43. IR spectra of kinetic measurements during crystallization of an aluminosilicate gel in the presence of nucleation solution and template: a) aluminate solution at RT, b) silica slurry at RT, c) aluminosilicate gel + template + nucleation solution at RT, d) at 90 °C after 30 min., e) at 90 °C after 2 h, f) at 90 °C after 5 h, g) at 90 °C after 2 d, h) at 90 °C after 3 d, i) at 90 °C after 7 d, j) at 90 °C after 14 d, k) at 90 °C after 21 d.

3.1.7. General discussion of all syntheses results

Synthesis of Y type zeolite as a pure phase of high crystallinity and large crystal size is a complicated task. It has been observed from literature and from samples prepared in this work, that P type zeolite of the gismondine (GIS) structure crystallizes very often as a second or main phase in zeolite Y or X batches although it has a different structure type. It seems that the synthesis conditions, at which zeolites of faujasite (FAU) type crystallize, are also suitable for the formation of GIS type. Consequently, many attempts were carried out to avoid crystallization of multi-phases from the batch employed for FAU zeolite synthesis. Lechert et al. [14] have used nucleation gels and seeds in the batches, from which zeolite Y should be crystallized, for increasing the crystallization rate. It was also discussed by Robson [43] that using of the liquid part of a nucleation gel aged at room temperature is active for the crystallization of Y zeolite and that the solid part is of less activity. However, P phase was present in the final product, too. Therefore, using of the nucleation solution was essential for the obtain of pure phases of FAU structure type zeolites.

The observation of the results estimated from the synthesis after Charnell [39] shows that a pure FAU phase with a particle size not bigger than ~ 12 μm could be crystallized. The comparison between our results and that described by [39] about synthesis of FAU particles up to 140 μm with crystallization of P zeolite as an impurity phase denotes a different growth behaviour. This indicates the very sensitive conditions, from which zeolite X and Y may crystallize. Since the general procedure is similar, details such as materials sources, type of filter used for the filtration of silicate and aluminate solutions and the thermal treatment condition applied seem to affect the FAU crystal growth and the phase purity as well. Triethanolamine is mentioned in literature as a stabilizing and complexing agent [39] and it, therefore, has been widely used in synthesis of large crystals of X-type zeolite. According to this, TEA was used again in the modified synthesis of [39] with applying another synthesis conditions. The gel composition chosen for crystallization of FAU type gives the desired result with $n_{Si}/n_{Al} = 1.44$ and a very small amount of zeolite P (3 %) as an impurity phase. Using a gel of a higher n_{Si}/n_{Al} leads to crystallization of FAU zeolite of higher n_{Si}/n_{Al} value than before (1.77) with a small amount of P phase (4 %). In the latter sample the amount of P zeolite increases to 21 % with increasing crystallization time. This means that TEA stabilizes the FAU structure for long crystallization time but it helps, on the other hande, in crystallization of P phase.

The second procedure followed in this chapter was the synthesis of FAU zeolite using a seed gel aged for 1 day at room temperature together with a gel composition of $n_{Si}/n_{Al} = 5$ as described by Ginter [7]. FAU crystals of size < 1 μm have been crystallized with, sometimes, competing of other phases such GIS, GME and CHA [7]. This procedure was repeated in this work and the result shows an X-ray amorphous pattern at the same synthesis time (7h). it is suggested that synthesis for 7 h at 100°C is not enough time for crystallization of Y under normal conditions. After 16 h, FAU phase was observed in the product together with P phase. After 24 h the intensity of P phase increases and it becomes the main phase in the product. This indicates either a re-crystallization of FAU zeolite into P zeolite or a simultaneous growth of both phases (Fig. 6, 7). Using of nucleation solution with the same initial batch used by [7], FAU zeolite of a high degree of crystallinity after only 7 h synthesis (Fig. 35) is obtained. The crystal size is < 1 μm (Fig. 9, 10, 44). According to this result it seems that the components in the nucleation solution control the crystallization process by nucleating FAU type crystals. However, after 24 h FAU phase disappears and GIS phase is formed as a single phase in the final product (Fig. 12d). This means that FAU crystals are formed temporary but they are not stable for longe time and they, therefore, dissolved and re-crystallized into another phase (normally GIS phase).
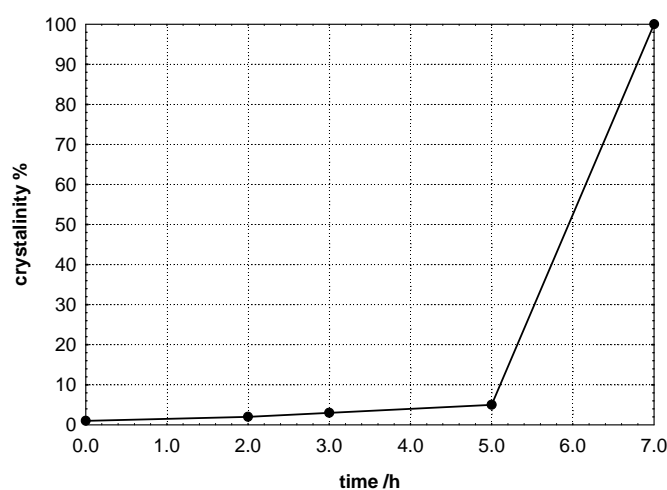
Fig. 44. The crystallinity of the sample synthesized for 7 h after [7] in presence of nucleation solution.

Using TEA together with an organic template for FAU zeolite crystallization with large crystal size as performed by Ferchiche [40] was the third procedure followed in this chapter. Large crystals described in this synthesis up to 245 μm in size could not be reproduced in this work. Crystals between 10 and 35 μm in size could be obtained in multi-phase products of P zeolite, hydroxy sodalite and, sometimes, an additional unknown phase (Fig. 21, 24, 27, 30).

A combination between the nucleation solution as a crystallization agent and TEA as a stabilizing agent together with the template used in [40] seems to be a suitable synthesis method for obtaining a pure FAU phase of relatively large particle diameter. Result of such application denotes the crystallization of a pure phase of FAU structure type after 3 weeks synthesis time at relatively low temperature value (65°C) with a maximum particle size of ~ 15 μm. A comparison between two samples, with and without nucleation solution, reveals the difference in crystallization rate and purity at the same crystallization time and temperature (Fig. 30). For the sample crystallized with the presence of nucleation solution together with TEA and TCl, FAU phase remains stable within the synthesis period from 3d to 21d, which indicates the distinct effect of such combination on the stability of FAU phase (Fig. 33).

The activity of the nucleation solution in crystallization of a pure phase of FAU structure has been proved by IR method. Aluminosilicate gels were prepared in the absence and the presence of nucleation solution (Fig. 40 and 41, respectively). The gel without nucleation solution crystallizes into A-type zeolite after 5 hours crystallization, while that with nucleation solution crystallizes into FAU structure after 1 day and it stays stable for 3 days and re-crystallize again into GIS which is more stable under the given conditions. using only TEA and TCl as stabilizer and template, respectively, both FAU and GIS phases grow simultaneously and remain stable up to the end of the applied crystallization course (20 days). If TEA and TCl are used together with the nucleation solution FAU phase crystallizes after 1 day and stays stable under the given conditions.This give another proof that the nucleation solution together with TEA and the template could keep a stable FAU phase during crystallization and no re-crystallization into another phase during synthesis time occurs.

Out of the previous observations it can be concluded that the size of FAU particles (crystals) is limited by the n_{Si}/n_{Al} of the final product. Therefore, large Y crystals of high n_{Si}/n_{Al} (> 2.5) could not crystallize by direct synthesis. This result shows together with other results collected and observed form different works (Tab. 8) that there is an inverse relation between the crystal size and the framework n_{Si}/n_{Al} of the synthesized FAU (Fig. 45). A reason therefore could be the change of gel composition during the crystallization process. The gel with low aluminate concentration and, therefore, also low alkalinity used for formation of FAU zeolite with high n_{Si}/n_{Al} undergoes a decrease of aluminate anions and sodium cations in the solution during crystallization and the reaction kinetics become lower and lower until all aluminate is totally incorporated into the zeolite framework. This causes the break down of

further crystallization before the total incorporation of silicate into the solid phase. This is because aluminate ions and the hydrated sodium ions are required for formation of the ß-cages as the main polyhedra of FAU-structure type [2].

Table. 8. Collected data from literature and own-synthesized samples reveal the maximum particle size with related n_{Si}/n_{Al}.

Maximum particle size/ μm	n_{Si}/n_{Al}	Ref.
0.3	2.16	This work
0.3	2.39	This work
0.5	~ 2.10	[7]
0.9	2.46	CKB[1]
1.0	2.66	Zeosorb[2]
1.4	2.80	[41]
1.5	2.00	This work
3.0	1.91	This work
3.0	4.20	[41]
5.0	3.80	[41]
5.0	1.77	This work
12	1.90	This work
32	1.3	This work
34	~ 1.4	[46]
50	1.75	[41]
140	1.36	[40]
150	1.70	[41]
227	1.71	[39]
245	1.70	[41]
250	1.087	[45]
340	1.40	[44]
500	~ 1.09	[45]

[1,2] Commercial Y type zeolites.
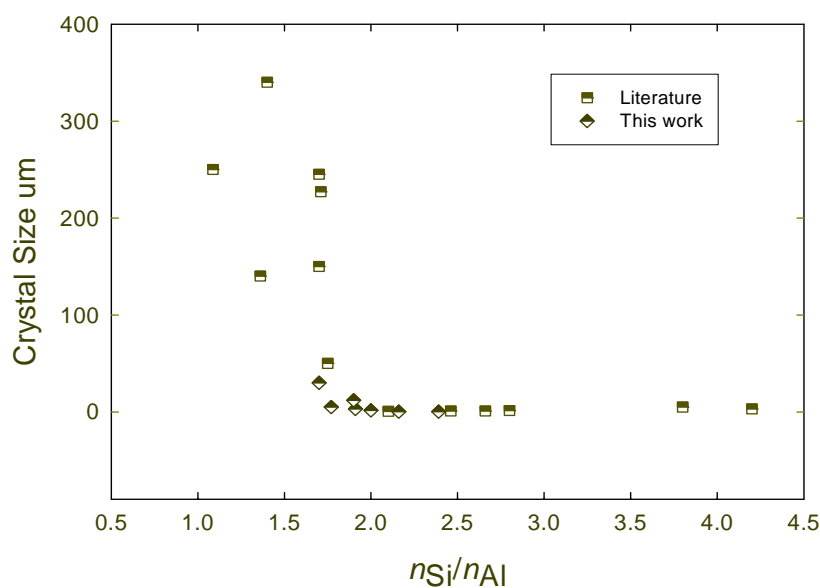
Fig. 45. The inverse relation between crystal size and the n_{Si}/n_{Al}.

The observed crystals with only low grain (particle) size are the result of this reaction pathway. According this discussion, the maximum crystal size as a function of n_{Si}/n_{Al} values of FAU zeolites reported in literature have been collected together with the data estimated from self-prepared samples after the procedures of [7], [39] and [40]. By comparing all samples, independently to the synthesis conditions, it is distinctly shown that all samples of n_{Si}/n_{Al} values between 2.10 and 4.2 have a crystal size between 0.5 μm and 5.0 μm. The other distinct range of n_{Si}/n_{Al} is between 1.1 and 1.75 by which large FAU crystals could be obtained of sizes between 32 μm and 500 μm.

3.2. Investigation on high silica Y-type formation mechanism

Results of the chemical analysis (ICP OES method) and the phase analysis of the samples synthesized after procedure I (see 2.1.9.1.) are summarized in tables 9 and 10, respectively. A view over the chemical analysis results of Y-batch and A-batch before liquid exchange provides important information about gel formation mechanism at room temperature. In case of A-batch (a batch prepared for A type zeolite crystallization) nearly all Si and Al are consumed into the gel which has the n_{Si}/n_{Al} of 1. This is supported by the ICP OES analysis result of the mother liquor of A-batch directly after aging at RT (Tab. 9, sample 2-14a).

Table. 9. Results of ICP OES analysis of mother liquors after aging at RT and at 80°C for 3 and 6 days (Procedure I, see 3.6.1.).

Probe	Al (g/l)	Si (g/l)	Na (g/l)
1-14a[1]	0.893	75.65	61.15
2-14a[2]	2.042	0.117	45.38
3-14b[3]	0.553	49.67	54.75
4-14b[4]	0.174	20.70	53.35
5-14b[5]	0.126	54.85	59.05
6-14b[6]	0.103	22.14	54.90

[1] mother liquor of Y batch after aging at room temperature for 1 day, [2] mother liquor of A batch after aging at room temperature for 1 day, [3] mother liquor of (Y gel + A mother liquor) batch after synthesis at 80°C for 3 days, [4] mother liquor of (A gel + Y mother liquor) batch after synthesis at 80°C for 3 days, [5] mother liquor of (Y gel + A mother liquor) batch after synthesis at 80°C for 6 days, [6] mother liquor of (A gel + Y mother liquor) batch after synthesis at 80°C for 6 days.

Out of this batch A type zeolite with perfect order of framework Si and Al tetrahedra should crystallize. X and Y type zeolite (of higher n_{Si}/n_{Al} than 1) also crystallize from gels of n_{Si}/n_{Al} =1. According the earlier studies of [2], [9] nuclei of lower n_{Si}/n_{Al} are formed on which X or Y zeolite of higher ratios crystallizes. The chemical analysis of the mother liquor of Y-batch

after aging at RT shows nearly no Al in the solution (0.893 g/l) but a high amount of Si (75.65 g/l) (Tab. 9, sample 1-14a). This refers the formation of a gel with n_{Si}/n_{Al} of 1 and the rest of Si has transferred into solution.

Effect of the upper solution components on the crystallization pathway has been detected by analysing the liquid phase of A-, Y-batches after the exchange of mother liquors and synthesis at hydrothermal conditions each for 3 and 6 days. Mixing of the gel of Y-batch with the solution of A-batch leads to the crystallization of NaP1 phase with a considerable portion of amorphous material characterized by X-ray method (Tab. 10, sample 3-14, Fig. 46).

The chemical analysis of mother liquor of this sample after synthesis shows an excess of Si in the solution but no Al. This sample has been formed from a gel with n_{Si}/n_{Al} of 1 (solid part of Y-batch at RT) and a solution with nearly no Si and Al but of a considerable amount of Na (liquid part of A-batch at room temperature).

Table 10. X-ray and IR data of samples of procedure I after crystallization at 80°C.

Sample[a]	Crystallization Time	Lattice Constant a_0	Si/Al Ratio	v_{DR}	T-O-T$_{AS}$	Final Product
	days	A°		cm-1	cm-1	
3-14	3	~10	-	-	-	P1
4-14	3	24.85	1.54	568	986	X
5-14	6	~10	-	-	-	P1
6-14	6	24.86	1.53	568	986	X
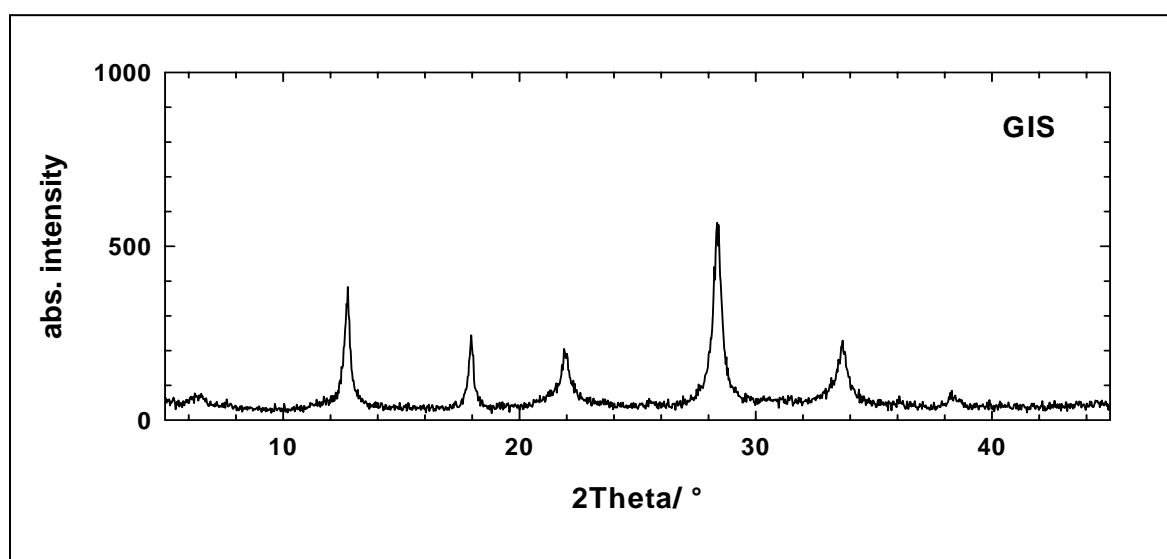
Fig. 46. X-ray diffraction pattern of NaP1 crystallized from a batch of Y gel and A upper solution after 3 days at 80°C.
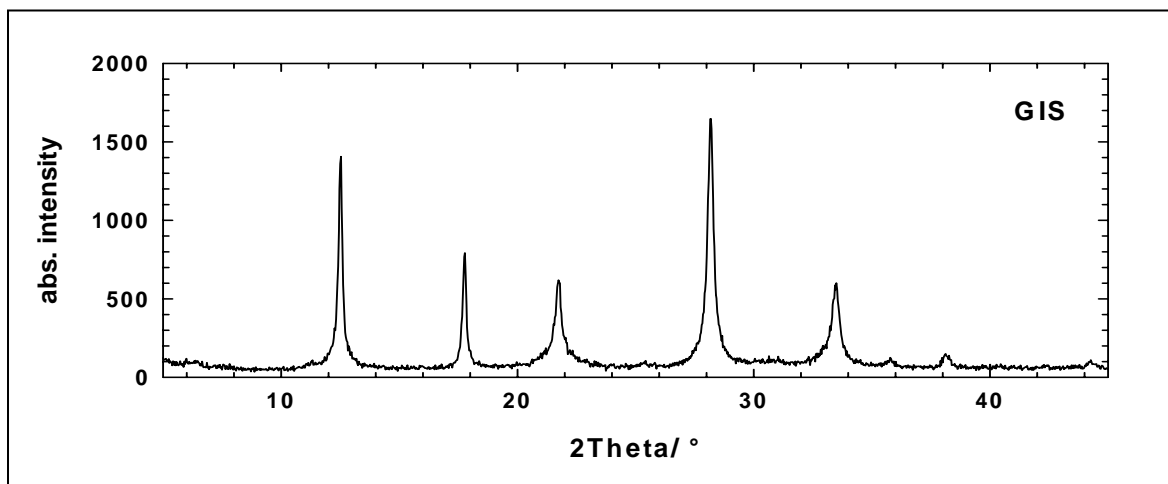
Fig. 47. X-ray diffraction pattern of NaP1 crystallized from a batch of Y gel and A upper solution after 6 days at 80°C.
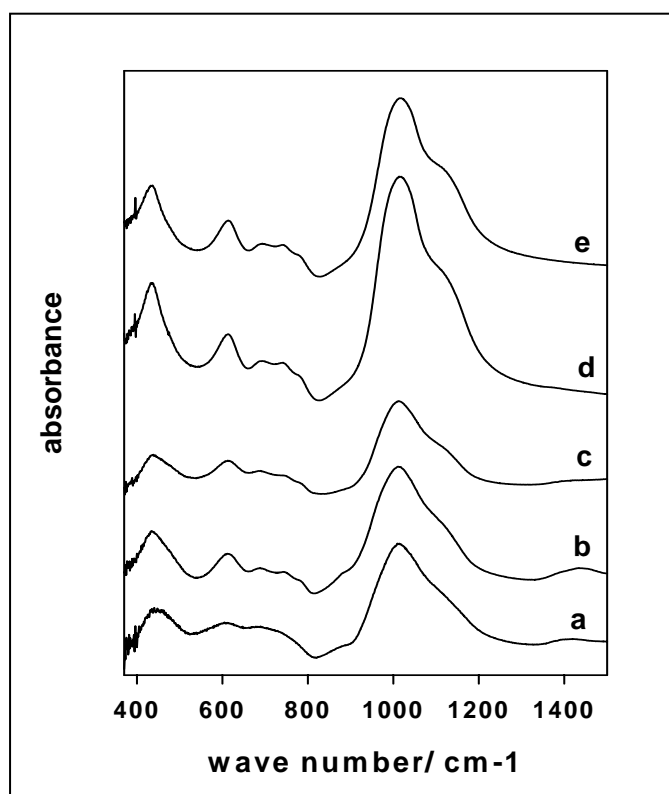
Fig. 48. IR spectra observed during gel transition into the crystalline state at 80°C after a) 24 hours b) 44 hours c) 65 hours d) 72 hours and c) 144 hours from a batch of Y gel and A upper solution.

Under hydrothermal conditions this mixture is not stable and the gel dissolves again in the presence of the alkaline solution. NaP1 zeolite of a cubic system and a cell parameter of ~ 10 Å seems to be the most stable phase in the given conditions. The amorphous phase also consumes Al and /or Al and Si species. This phase stays stable for longer time with a distinct increase of the degree of crystallinity (samples 5-14b, 5-14 in tables 9 and 10, respectively

(Fig. 47). IR investigation during the synthesis of this sample has been also performed (Fig. 48). Mixing of a gel of A-batch with the solution of Y-batch leads to crystallization of X-type zeolite (Fig. 49).
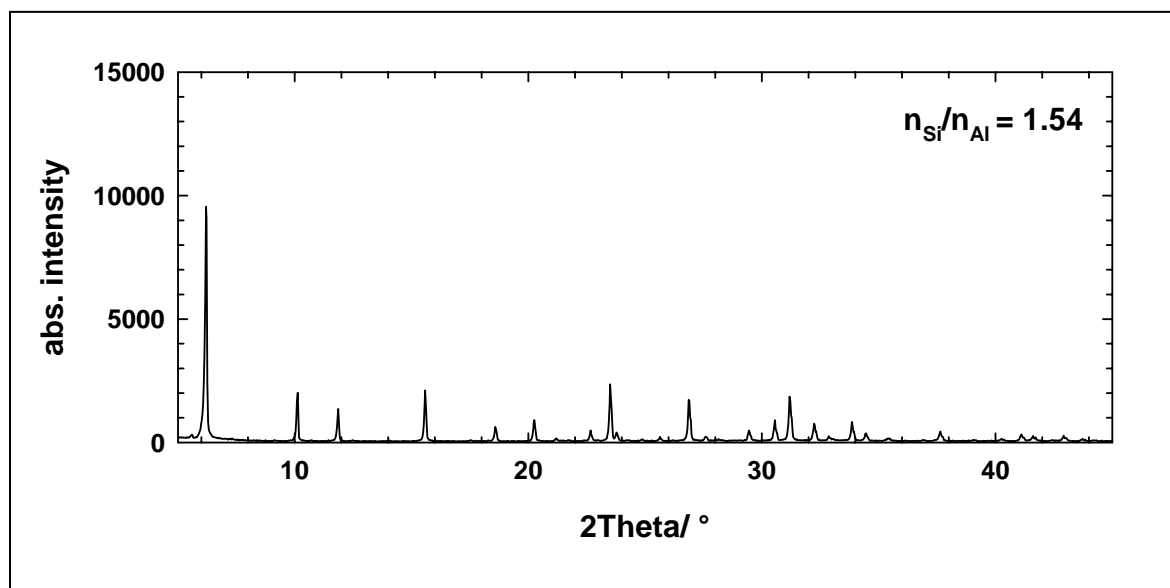
Fig. 49. X-ray diffraction pattern of NaP1 crystallized from a batch of A gel and Y upper solution after 3 days at 80°C.

X-ray diffraction pattern of this sample reveals a pure phase of high crystallinity with n_{Si}/n_{Al} of 1.54 (table 10, sample 4-14). The chemical analysis of the mother liquor shows nearly no Al but a rest of Si. Crystallization of X phase can be explained as a result of the interaction at hydrothermal conditions between the gel with n_{Si}/n_{Al} of 1 (solid part of A-batch at RT) and the solution with a high silicate concentration (liquid part of A-batch at RT).
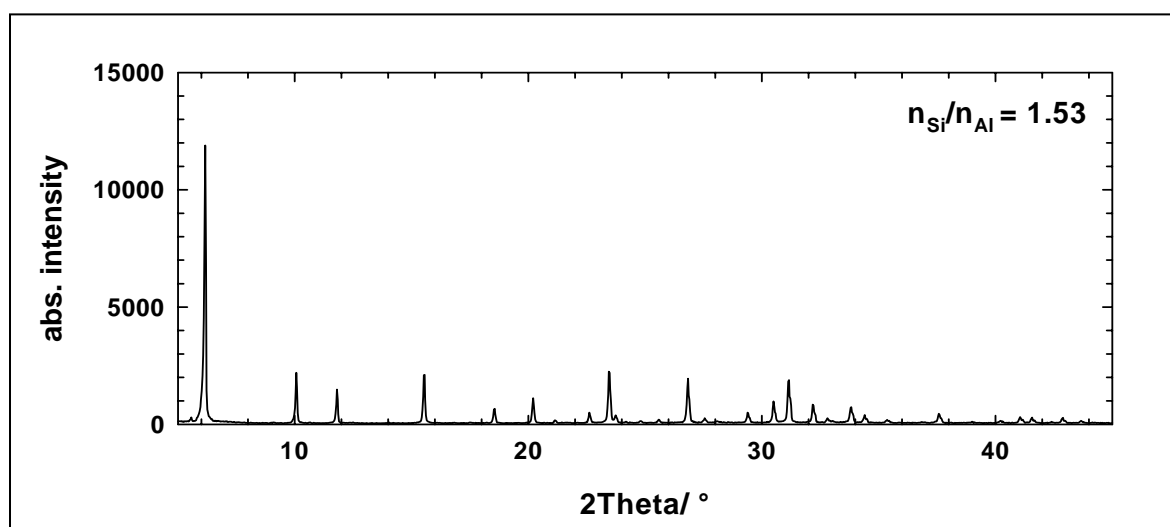
Fig. 50. X-ray diffraction pattern of NaP1 crystallized from a batch of A gel and Y upper solution after 6 days at 80°C.
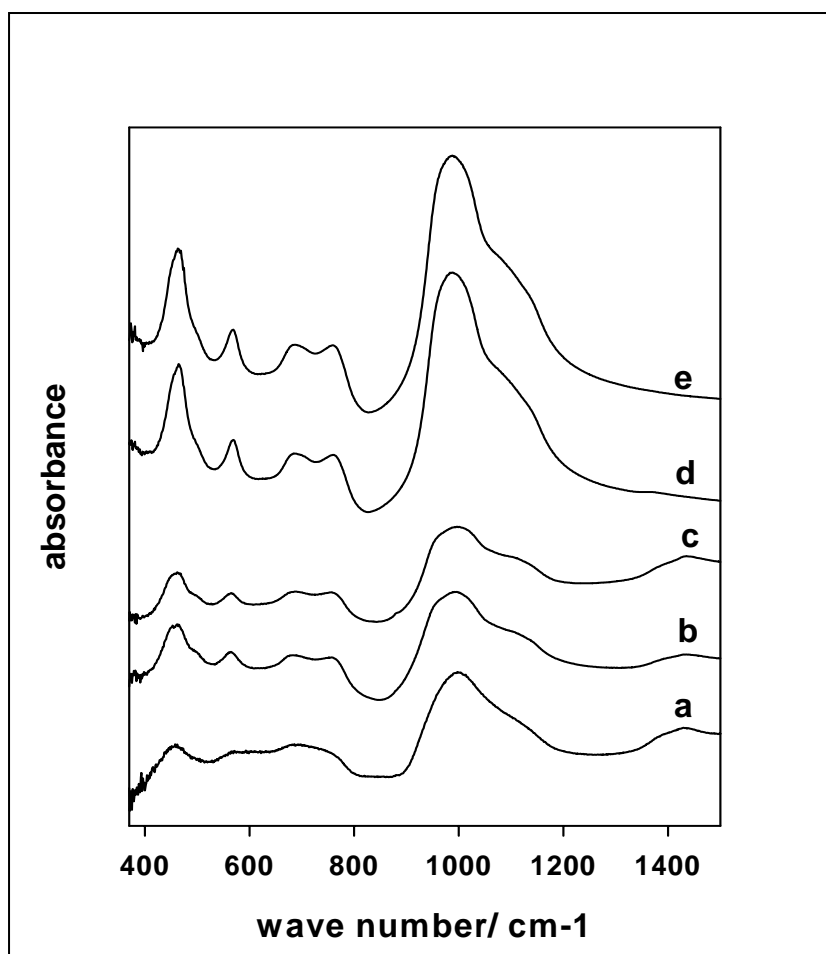
Fig. 51. IR spectra observed during gel transition into the crystalline state at 80°C after a) 24 hours b) 44 hours c) 65 hours d) 72 hours and c) 144 hours from a batch of A gel and Y upper solution.

The formed X zeolite stays stable for longer crystallization time with distinct increase in peak intensities (samples 6-14b, 6-14 in tables 9 and 10, respectively. Fig. 50). IR investigation during synthesis reveals, kinetically, the FAU phase formation (Fig. 51).

The previous discussion has declared that the components which drive the crystallization process exist in the liquid phase.

A modification of experiments by a directed influence on the composition of the mother liquor by its total exchange during the reaction is still lacking. Therefore, further study on the mother liquor through modifications on the alkaline concentration before or during crystallization has been discussed.

Results of the chemical analyses (ICP OES method) of the mother liquor after aging at room temperature or/ and after synthesis at hydrothermal conditions are included in table 11.

Results of the phase analysis of the studied samples are given in table 12. The chemical analysis of the mother liquor of a batch using silica sol as silica source and aged for 24 hours at room temperature indicates no Si in the liquid phase after aging. This is due to the net-like polymeric silicate corpus which has been directly formed after adding the sodium aluminate solution to the silica sol in the initial gel. During gel aging at RT most of the aluminate accumulate at the surface of the solid phase.

Table 11. Results of ICP OES analysis of mother liquors after aging at RT and at 80°C (Procedure II, see 3.6.2.).

Probe	Al (g/l)	Si (g/l)	Na (g/l)
1-15-1a[1]	19.71	0.88	66
1-15-1b[2]	0.10	63	55
1-16-3a[3]	0.54	73	48
1-16-4b[4]	0.08	62	49
1-16-5b[5]	0.53	83	81
1-16-6b[6]	0.07	47	43

[1] mother liquor directly after aging at RT, [2] mother liquor after aging at 90°C for 3 days, [3] mother liquor after 2 hours aging at 90°C, [4] mother liquor after substitution by sodium hydroxide solution and aging at 90°C for 3 days, [5] mother liquor after 3 days aging at 90°C with intermediate substitution by sodium hydroxide solution after 2days, [6] mother liquor after 3 days aging at 90°C with intermediate substitution by sodium hydroxide solution after 2 hours.

Table 12. X-ray and IR data of samples of procedure II after crystallization at 80°C.

Sample[a]	Lattice Constant a_0 A°	Si/Al Ratio	ν_{DR} cm^{-1}	T-O-T$_{AS}$ cm^{-1}	Final Product
1-15-1	24.69	2.25	578	1015	FAU
1-16-4	24.66	2.43	579	1017	FAU
1-16-5	24.71	2.15	574	1009	FAU
1-16-6	24.69	2.27	576	1014	FAU
1-16-8	24.74	2.00	574	1007	FAU

The chemical analysis after aging the batch at RT for 22 hours indicates a residual Al (ca. 20 %) in the solution. Aging at hydrothermal conditions (90°C) for 2 hours allows the Al rest to be incorporated into the gel (table 11, sample 1-16-3a). During this time the solution is rapidly enriched of silicon. This observation was early mentioned by [74]. The product after 3 days synthesis is a pure FAU phase of high crystallinity with n_{Si}/n_{Al} of 2.25 (table 12, sample 1-15-1).

Fig. 52. X-ray diffraction pattern of 1-15-1 sample crystallized at 90°C for 3 days.
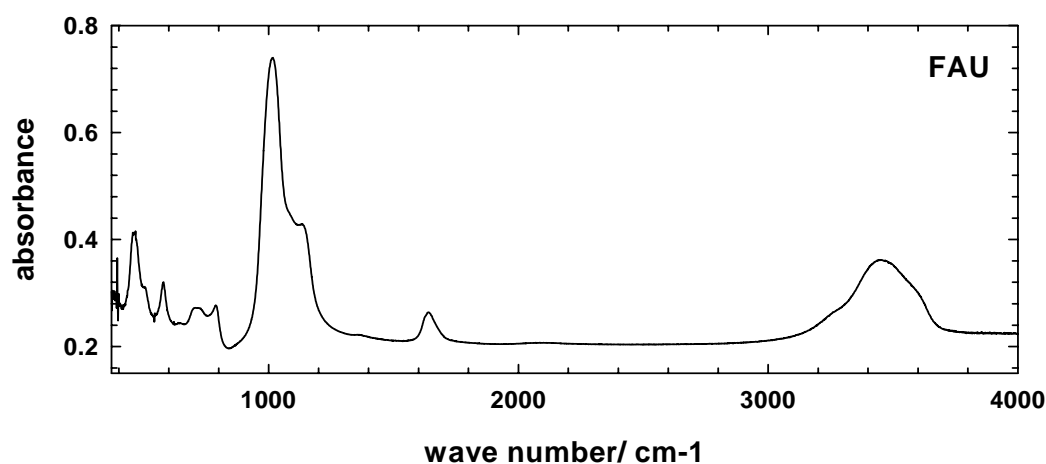
Fig. 53. IR-spectrum of 1-15-1 sample crystallized at 90°C for 3 days.

The IR spectrum of this sample shows the structural details of FAU with relatively high frequency value of the double six-ring vibration mode (v_{DR}) which has been detected at 578 cm^{-1} and v_{AS} T-O-T at 1015 cm^{-1} (Fig. 53). Observation of gel kinetics during crystallization of this batch has been provided using IR spectroscopy during aging at RT and synthesis at hydrothermal conditions for different times (Fig. 54). Phase transition of the gel into the crystalline phase can be clearly observed through the formation of the main features which characterize the FAU structure. The creation of the peak at around 1000 cm^{-1} and vanishing of the peak at nearly 1100 cm^{-1} may characterize the formation of Y zeolite framework.

A similar result has been obtained after substitution of the mother liquor of a similar batch by distilled water after 2 hours aging at 90°C. A FAU zeolite with n_{Si}/n_{Al} value of 2.27 is formed (tables 11 and 12, samples 1-16-6b and 1-16-6, respectively. Fig. 55, 56). The presence of

water, in this case, does not affect the crystallization pathway of the gel (compare samples 1-15-1 and 1-16-6). The effect differs if the mother liquor is substituted by sodium hydroxide solution instead of water. In such high alkaline medium the formation of a FAU structure zeolite of a lower n_{Si}/n_{Al} with 1.90 is preferrable (sample 1-17-2, Fig. 57, 58).
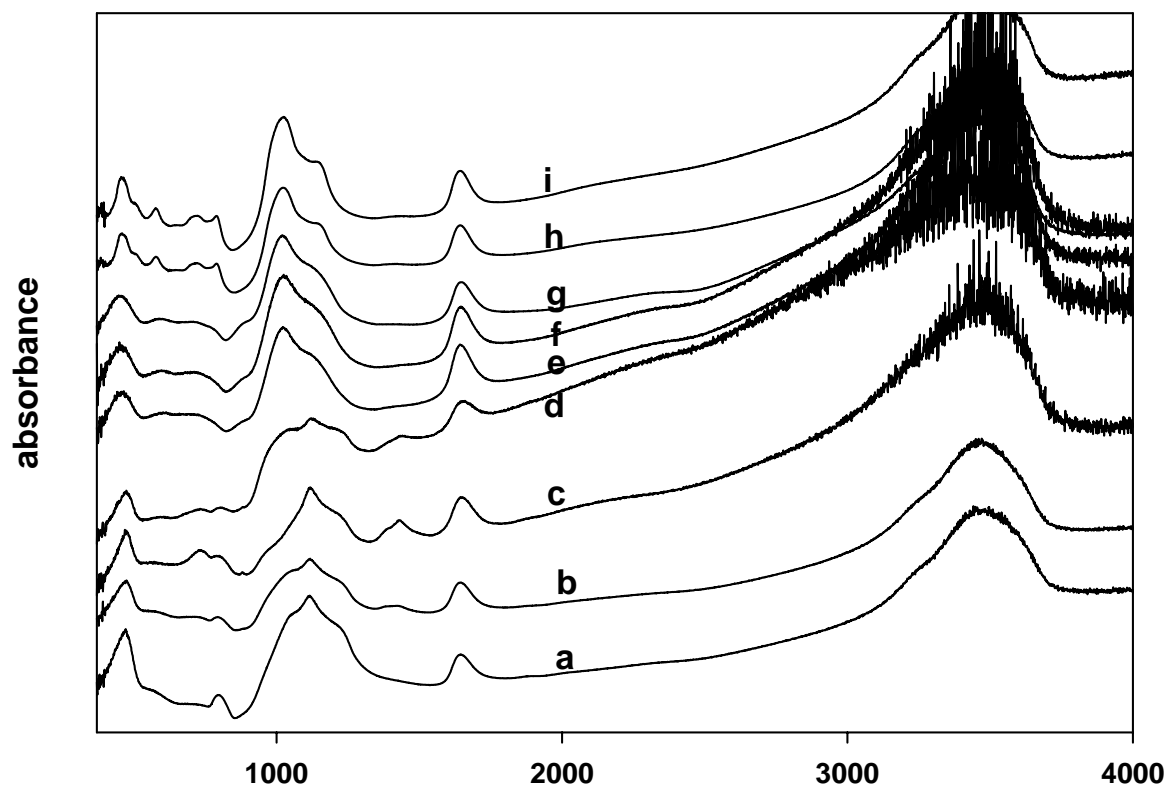
Fig. 54. IR-spectra of 1-15-1 during aging at RT for a) directly after aging b) 6 hours c) 23 hours, and during synthesis at hydrothermal conditions for d) 1 hour e) 2.5 hours f) 5 hours g) 24 hours h) 50 hours i) 72 hours.

A higher n_{Si}/n_{Al} value with 2.43 has been obtained by substitution of the mother liquor after aging at RT by sodium hydroxide solution (table 12, sample 1-16-4, Fig. 59, 60). In this case the total amount of Al is reduced because of the absence of the residual Al in solution while the whole amount of silicate is still accumulated in the silicate corpus and protected by an aluminum cover. On the other hand, the excess of alkalinity creats a new condition during heating in which the gel is not more stable and dissolution-recrystallization process may occur. The chemical analysis of this sample is shown in table 11 (sample 1-16-4b). A general shift of the IR peaks towards higher values (ν_{DR} at 579 cm^{-1}, ν_{S} T-O-T at 789 cm^{-1} and ν_{AS} T-O-T at 1017 cm^{-1}) refers the decrease of the framework Al. If the mother liquor is substituted

by sodium hydroxide solution after 2 days aging at hydrothermal conditions a reduction in the total silicate content happens. This is because a considerable amount of silicate has existed in the solution during these two days synthesis which has been excluded after substitution. The increase of alkalinity concentration changes, in turn, the stabilization condition and a dissolution-recrystallization process of the gel with consuming less Si into the crystalline phase may occur leading to the formation of FAU structure zeolite of lower n_{Si}/n_{Al} value of 2.15 (table 12, sample 1-16-5, Fig. 61, 62). The IR spectrum indicates a total peaks shift towards lower frequency values (v_{DR} at 574 cm^{-1}, v_S T-O-T at 782 cm^{-1} and v_{AS} T-O-T at 1009 cm^{-1}). Result of the chemical analysis of the liquid at the end of the synthesis period is shown in table 11 (sample 1-16-5b).
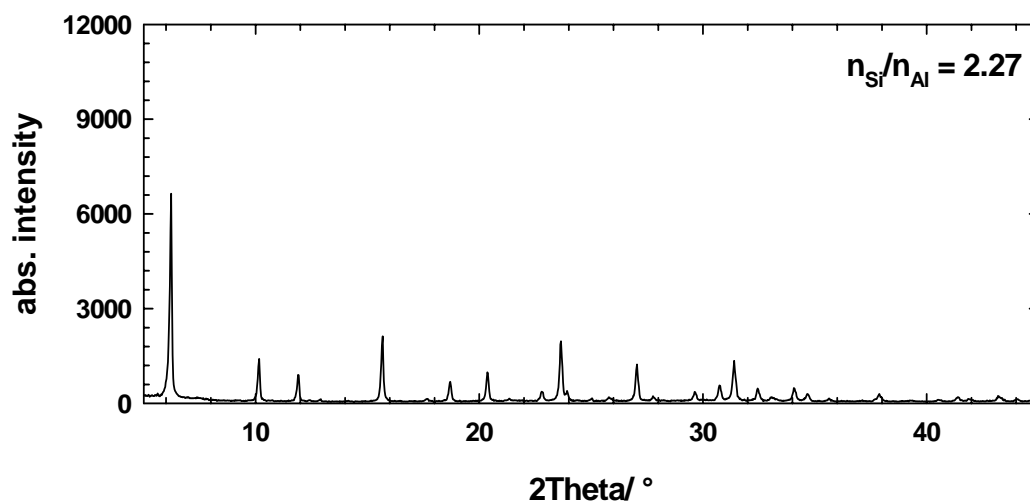
Fig. 55. XRD-pattern of 1-16-6 sample crystallized at 90°C for 3 days.
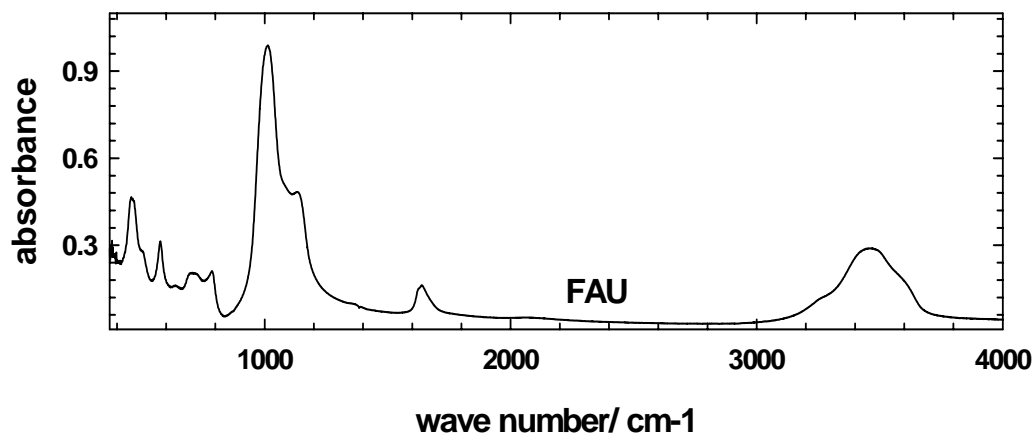
Fig. 56. IR-spectrum of 1-16-6 sample crystallized at 90°C for 3 days.
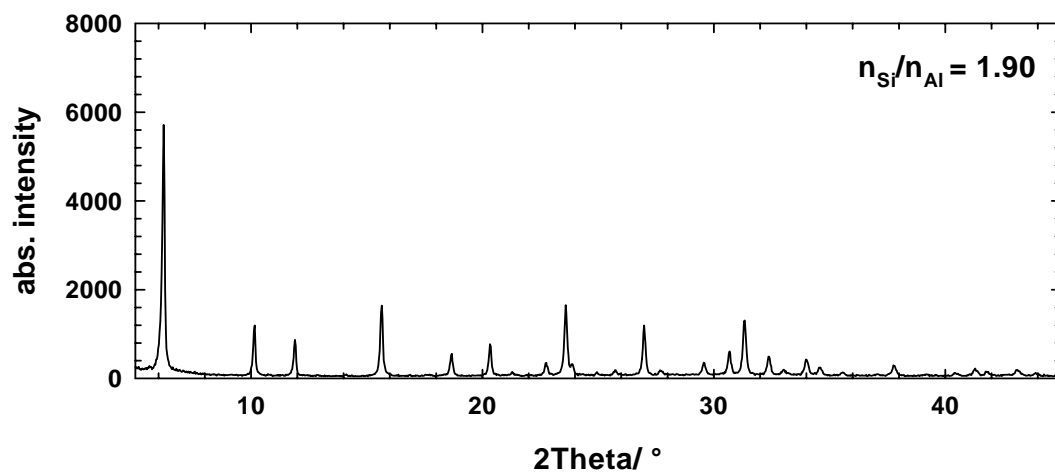
Fig. 57. XRD-pattern of 1-17-2 sample crystallized at 90°C for 3 days.

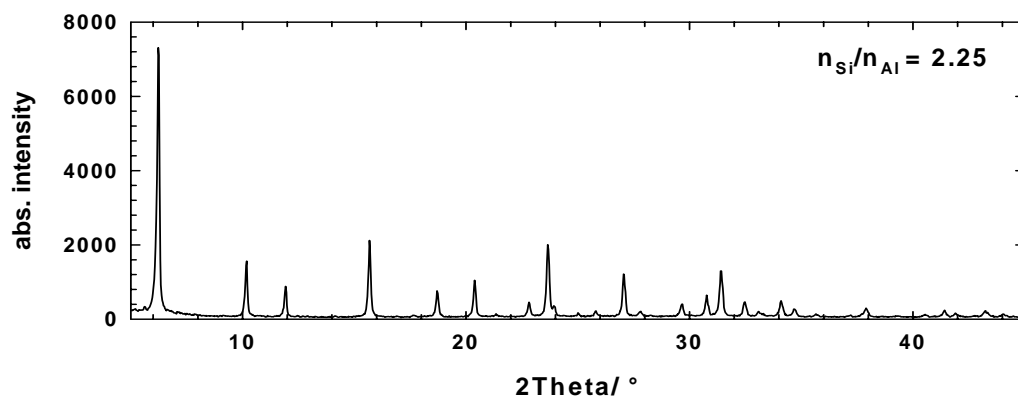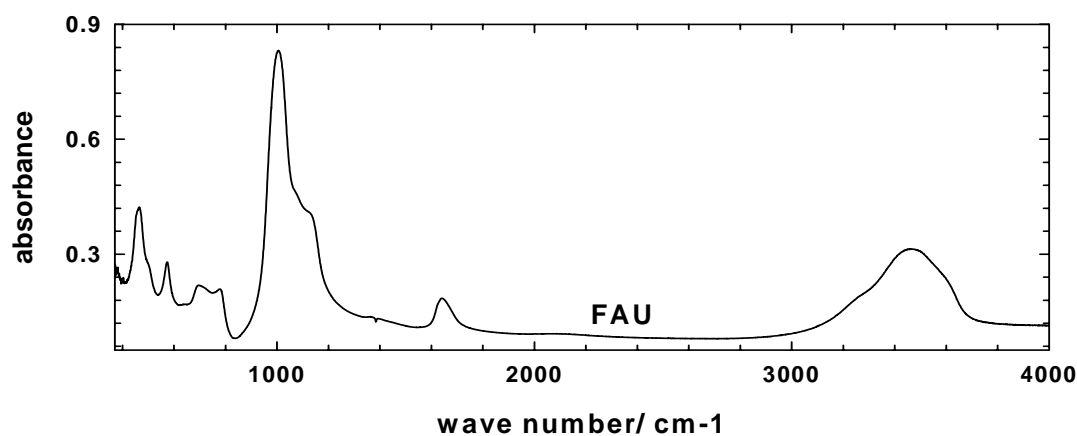Fig. 58. IR-spectrum of 1-17-2 sample crystallized at 90°C for 3 days.
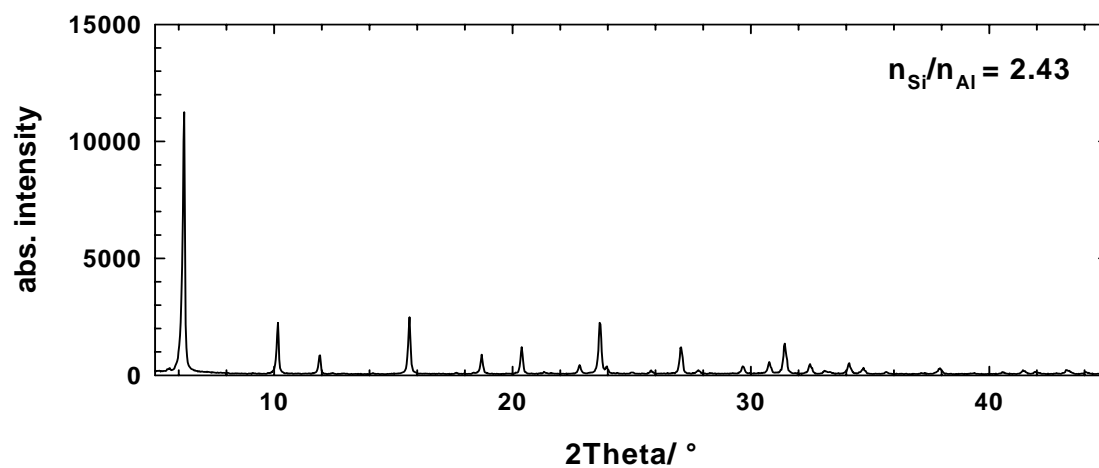
Fig. 59. X-ray diffraction pattern of 1-16-4 sample crystallized at 90°C for 3 days.
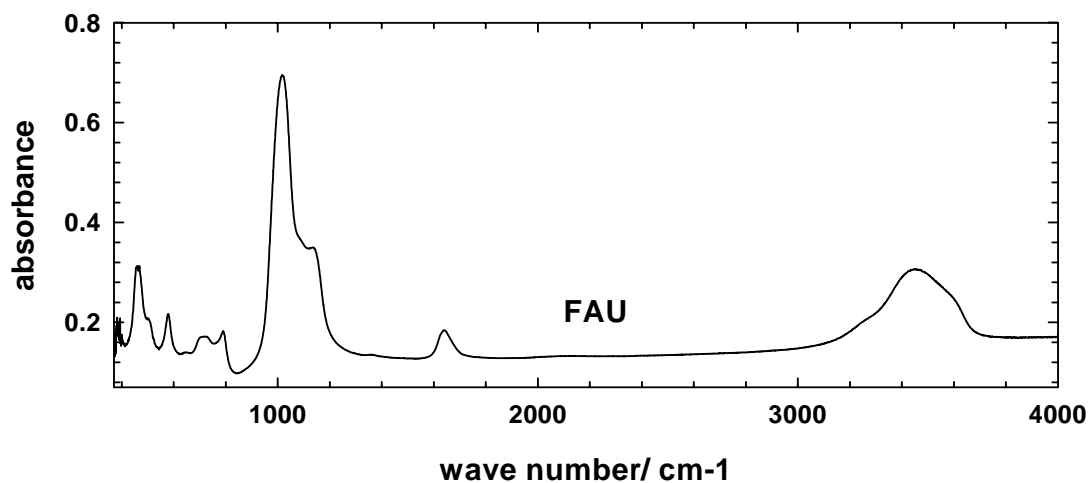
Fig. 60. IR-spectrum of 1-16-4 sample crystallized at 90°C for 3 days.
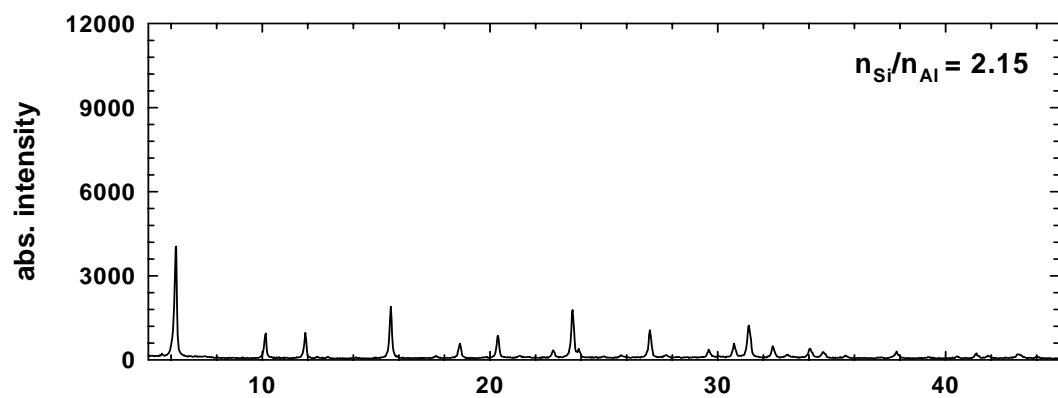
Fig. 61. X-ray diffraction pattern of 1-16-5 sample crystallized at 90°C for 3 days.
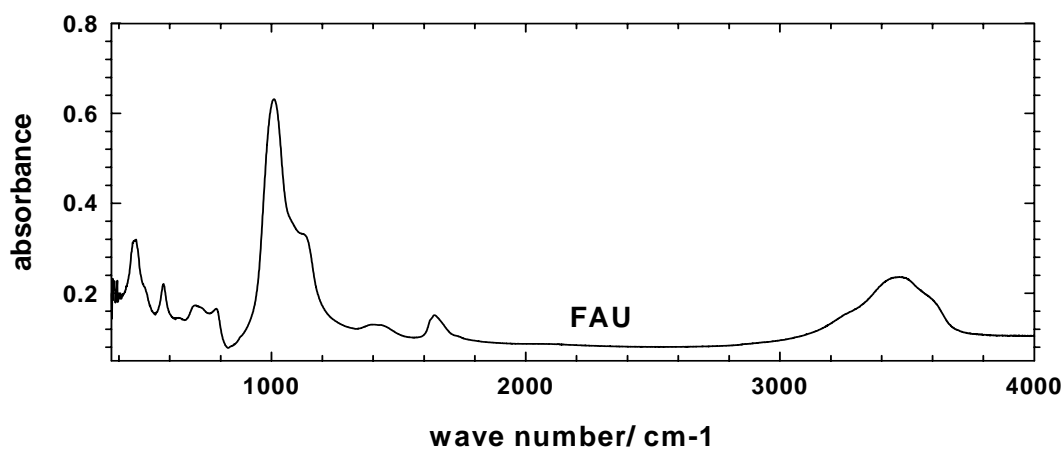
Fig. 62. IR-spectrum of 1-16-5 sample crystallized at 90°C for 3 days.

3.3. Effect of the chemical and thermal treatment of Y zeolite on the degree of ion-exchange

The maximum degree of $Na^+ : NH_4^+$ exchange of Y zeolite given in literature was 78 % shown by Engelhardt et al**.** [58]. The BET analysis data of our NH_4Y (with $n_{Si}/n_{Al} = 2.66$ of its parent zeolite) after $Na^+ : NH_4^+$ using NH_4Cl salt solution 0.1M, were worked out and the degree of ion-exchange in the zeolite were calculated. The result denotes a maximum exchange degree of about 69 % (Tab. 13) and nearly a constant value with time is shown (Fig. 63). The residual Na^+ which could not be exchanged with NH_4^+ are located inside the β-cage at SI` position from where they can not be removed because NH_4 ions are not able to enter the β-cage due to their big molecular diameter [76]. Therefore, a complete substitution of Na^+ by NH_4^+ is not possible under the given conditions.

Table 13. The calculated data of BET analysis of NH_4Y sample in 9 steps ion-exchange measurement for 18 h gives the maximum degree of ion-exchange (in %).

Step	Time/h	Result of $Na^+: NH_4^+$ exchange (%)
4	3	60.6
5	6	65.0
6	9	67.5
9	18	69.2
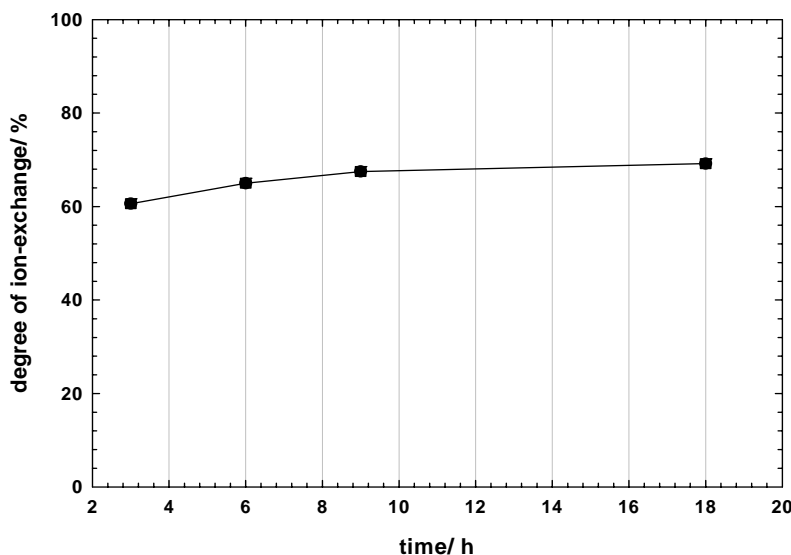
Fig. 63. Maximum degree of $Na^+ : NH_4^+$ exchange (~ 60 %) is reached after 3 h and remains nearly stable with time (~ 69 % after 18 h).

* Parts of this chapter are already published. See ref.. [76] and [77].

Analysis of the solution after the ion-exchange by ICP OES method, after the Na^+ : NH_4^+ exchange using $(NH_4)SO_4$ salt solution of same Y zeolite, shows (after calculation) a higher exchange value up to 80 % (Tab. 14). This means a higher degree of exchange is shown but a residual of Na^+ still exists. In order to obtain a higher exchange value the NH_4Y sample was hydrothermally treated at 775 K, 5 h and 1 bar water pressure and ion-exchanged again. The ICP OES result shows that the degree of exchange has reached additionally about 15 % which means a total ion-exchange degree of 95 % (Tab. 15). This is because the small sized H^+ allows the exchange of more Na^+ [76].

Table 14. ICP OES analysis of the ion-exchanged solution of Y before steaming using $(NH_4)_2SO_4$ salt solution.

Sample	Al (mg/l)	Si (mg/l)	Na (mg/l)
0.1M $(NH_4)SO_4$ – 1h/1. step	6.45	1.97	134.3
0.1M $(NH_4)SO_4$ – 2h/2. step	2.56	1.03	12.54
0.1M $(NH_4)SO_4$ – 3h/3. step	1.69	0.77	4.15

Table 15. ICP OES analysis of the ion-exchanged solution of Y after steaming. using $(NH_4)_2SO_4$ salt solution.

Sample	Al (mg/l)	Si (mg/l)	Na (mg/l)
0.1M $(NH_4)_2SO_4$ – 1h/1. step	0.131	0.236	7.788
0.1M $(NH_4)_2SO_4$ – 2h/2. step	0.072	0.176	3.139
0.1M $(NH_4)_2SO_4$ – 3h/3. step	0.070	0.202	1.993

However, there is a slight difference in the degree of ion-exchange at RT between $(NH_4)SO_4$ and NH_4NO_3 of 0.1M (Tab. 16).

Table 16. ICP OES analysis of the ion-exchanged solution of Y using different salt solutions.

Type of salt solution	Treatment	Al (mg/l)	Si (mg/l)	Na (mg/l)
$(NH_4)SO_4$	1h/1. step	6.45	1.97	134.3
$(NH_4)SO_4$	2h/2. step	2.56	1.03	12.54
$(NH_4)SO_4$	3h/3. step	1.69	0.77	4.15
NH_4NO_3	1h/1. step	1.05	2.00	138.5
NH_4NO_3	1h/1. step	0.69	1.15	14,30
NH_4NO_3	1h/1. step	0.58	0,93	4,67

3.4. The behavior of FAU zeolites with high or low n_{Si}/n_{Al} during steaming: a suitable tool to reveal structural differences resulting from the nature of the gel during crystallization *

3.4.1. Relation between hydrothermal behavior and structure of FAU zeolite with different n_{Si}/n_{Al} values

Faujasite zeolites with n_{Si}/n_{Al} values between 1.2 and 2.7 were hdrothermally treated and studied. Before treatment the proton form of the samples was obtained by heating the ammonium form (see 2.2.2.). Two separated groups of steaming experiments were performed. One series demonstrates the steaming behavior of the sample of the NH_4Y modification. The other series denotes the effect of intermediate treatment (ion exchange- steaming- calcination- ion exchange) between two steaming stages on the degree of dealumination, amorphization and n_{Si}/n_{Al} values of the treated zeolites. Summary of the X-ray and IR characterizations of the as-synthesized and the steamed samples is included in table 17.

Table 17. XRD and IR data of as-synthesized and steamed FAU type samples.

As-prepared	a_0 Å	X^*	n_{Si}/n_{Al}	w_{DR} cm^{-1}	Steamed 773K, 5h, 1bar H2O	a_0 Å	x	n_{Si}/n_{Al}	w_{DR} cm^{-1}
FAU1	24.63	0.2716	2.66	580	STFAU1	24.52	0.2139	3.60	588
FAU2	24.70	0.3080	2.23	576	STFAU2	24.58	0.2497	2.93	582
FAU3	24.71	0.3149	2.16	576	STFAU3	24.62	0.2700	2.72	578
FAU4	24.74	0.3329	2.00	575	STFAU4	24.62	0.2666	2.75	581
FAU5	24.76	0.3422	1.91	573	STFAU5	24.64	0.2791	2.58	578
FAU6	24.79	0.3598	1.77	570	STFAU6	24.68	0.2850	2.43	576
FAU7	24.82	0.3764	1.65	569	STFAU7	amorph.	-	-	no peak
FAU8	24.87	0.4026	1.47	566	STFAU8	amorph.	-	-	no peak
FAU9	24.88	0.4080	1.44	566	STFAU9	amorph.	-	-	no peak
FAU10	24.98	0.4604	1.16	564	STFAU10	amorph.	-	-	no peak

* *x* represents the Al molar fraction.

X-ray diffraction patterns of the samples with different n_{Si}/n_{Al} values steamed at 773K for 5h and 1bar water pressure are shown in figure 64. The peak intensities decrease systematically with the decrease of n_{Si}/n_{Al} of the parent zeolite and the backgrounds increase which refers an increase in amorphization portion. Shifting of peak positions to higher 2θ values indicates the higher number of framework silica after steaming which denotes, in turn, the degree of dealumination. This shift is higher for the samples with higher n_{Si}/n_{Al} of the parent zeolite. Figure 65 represents the change of amorphization degree as a function of n_{Si}/n_{Al} for the mentioned samples. IR investigation of the same group of samples assures the results of X-ray

diffraction (Fig. 66). The increase of dealumination degree with increasing the n_{Si}/n_{Al} of the parent zeolite can be seen in three main domains in the spectrum; The double six-ring vibration mode ν_{DR} which is considered as external linkage according to Flanigen et al. [52]. This building unit is sensitive to the change of framework silica content (Fig. 67). This mode shows a higher frequency value with higher dealumination, i.e. higher n_{Si}/n_{Al} (see table 17). The symmetric stretching mode ν_S T-O-T reveals higher values also with increasing dealumination degree.
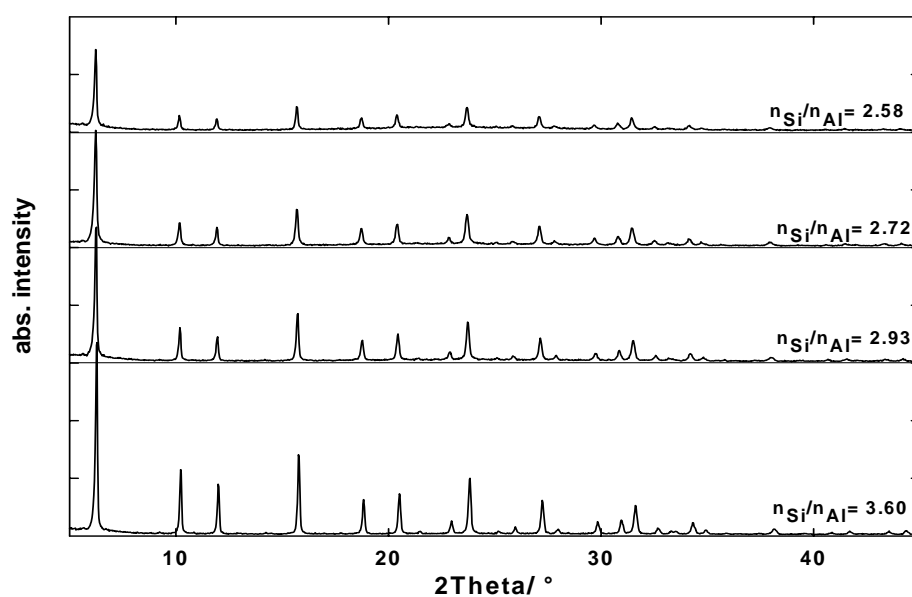
Fig. 64. XRD- patterns of the steamed samples at 773 K, 5 h and 1 bar H_2O pressure. The n_{Si}/n_{Al} values belong to the steamed samples (Tab. 17).
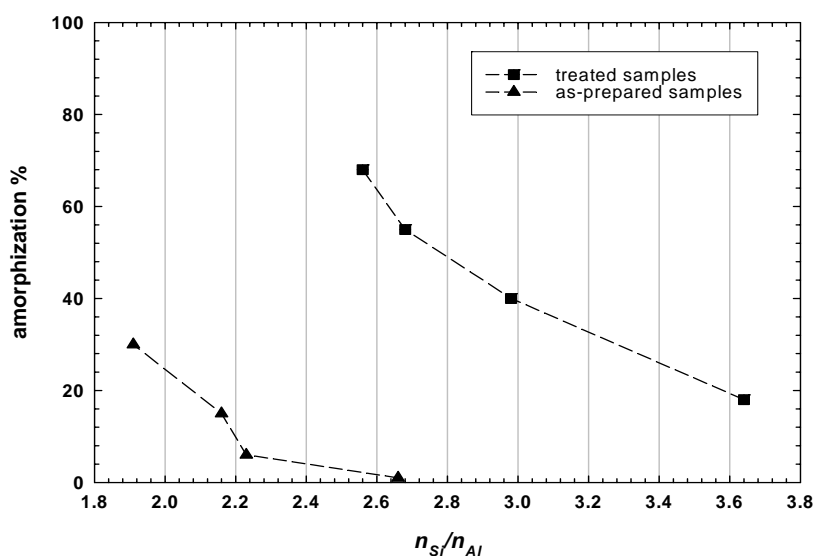
Fig. 65. Relation between n_{Si}/n_{Al} and the amorphization portion of parent and steamed samples.

The asymmetric stretching mode v_{AS} T-O-T shows also higher values with increasing the total silicate concentration (framework and non-framework silica) of the steamed samples (Fig. 68). A total amorphization can be also recognized from the slight shape over the whole spectra resulting in lower intensities of each vibration mode with the decrease of n_{Si}/n_{Al} of the parent zeolite. Results of water adsorption of the parent zeolites and the steamed ones are revealed in tables 18, 19.

Fig. 66. IR-spectra of the steamed samples at 773K, 5h and 1bar H_2O. The n_{Si}/n_{Al} belong to the steamed samples (Tab. 17).
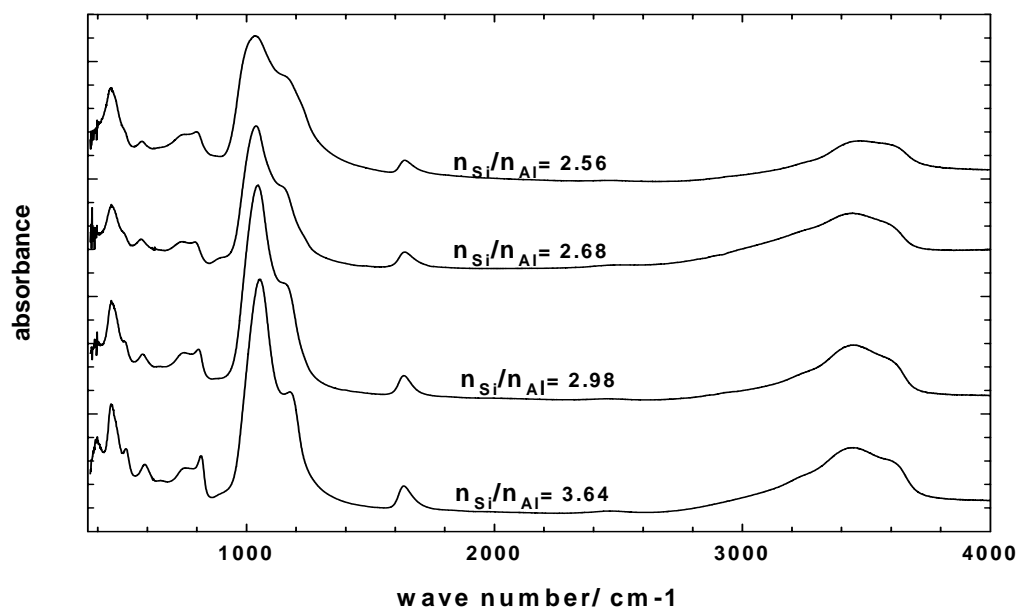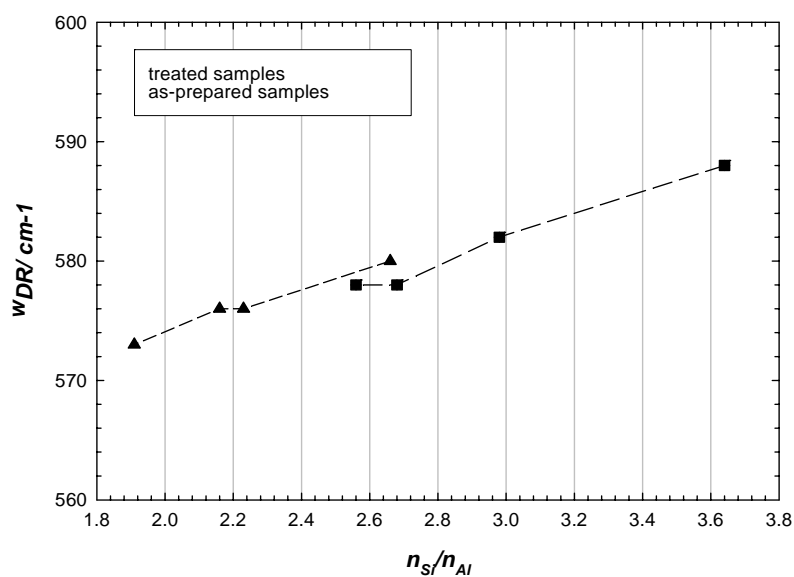

Fig. 67. The increase of v_{DR} with increasing the framework and non-framework silica of the parent zeolites and related steamed samples.

Table 18. Water adsorption capacity values of the parent NaFAU samples with variant n_{Si}/n_{Al}.

n_{Si}/n_{Al}	Glass weight + lid	Glass weight + lid + zeolite	Zeolite weight	Adsorption weight 1	Adsorption 1[1]	Adsorption weight 2	Adsorption 2[2]
	mg	mg	g	mg	mg/g	mg	mg
2.00	16.2756	16.5435	0.2679	16.6350	349	16.6370	349
1.91	16.2007	16.3523	0.1516	16.4020	336	16.4033	336
2.23	15.1777	15.4122	0.2345	15.4806	295	15.4814	295
2.16	16.8770	17.1008	0.2238	17.1591	263	17.1596	263
1.65	16.6489	16.7665	0.1176	16.7987	270	16.7983	270
1.44	18.4778	18.4848	0.007	18.4870	314	18.4865	243
1.77	15.1777	15.1986	0.0209	15.2051	311	15.2044	277
1.00*	16.1283	16.4461	0.3178	16.5309	267	16.5315	269

* Standard A zeolite of an adsorption value of 267 mg/g, [1] water adsorption capacity (in mg/g) after the first measurement, [2] water adsorption capacity (in mg/g) after the second measurement.

Table 19. Water adsorption capacity of the steamed ST-FAU samples at 773 K, 5 h and 1bar H_2O pressure with variant n_{Si}/n_{Al}.

n_{Si}/n_{Al}	Glass weight + lid	Glass weight + lid + zeolite	Zeolite weight	Adsorption weight 1	Adsorption 1[1]	Adsorption weight 2	Adsorption 2[2]
	mg	mg	g	mg	mg/g	mg	mg
2.75	16.3961	16.6385	0.2424	16.7117	301	16.7116	301
2.58	17.5166	17.6088	0.0922	17.6255	185	17.6259	185
2.93	15.2222	15.3928	0.1706	15.4375	264	15.4379	264
2.72	17.3920	17.5707	0.1787	17.6203	276	17.6201	276
amorph.	14.1383	14.3885	0.2502	14.4102	87	14.4102	87
amorph.	16.8091	16.9340	0.1249	16.9508	134	16.9510	136
2.43	15.2222	15.2779	0.0557	15.2908	231	15.2904	224

[1] water adsorption capacity (in mg/g) after the first measurement, [2] water adsorption capacity (in mg/g) after the second measurement.
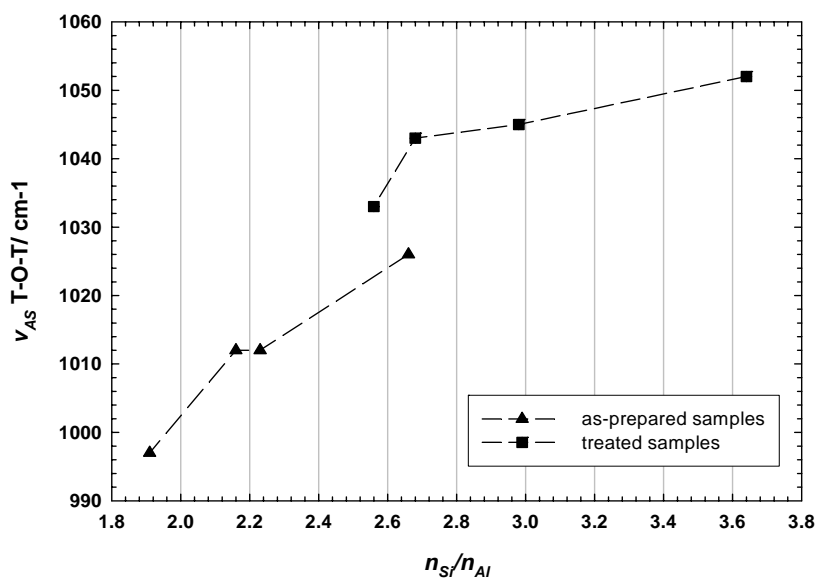

Fig. 68. The increase of v_{AS} T-O-T with increasing the framework and non-framework silica of the parent zeolites and related steamed samples.

The reduce in the water adsorption values of the steamed samples is distinctly seen. Three samples show relatively high adsorption values after steaming, which are: 301 mg/g, 264 mg/g and 276 mg/g (Tab. 19). This may due to the high degree of homogeneity of the parent samples. Figure 69 reveals the adsorption of parent and steamed samples as a function of the amorphization portion.
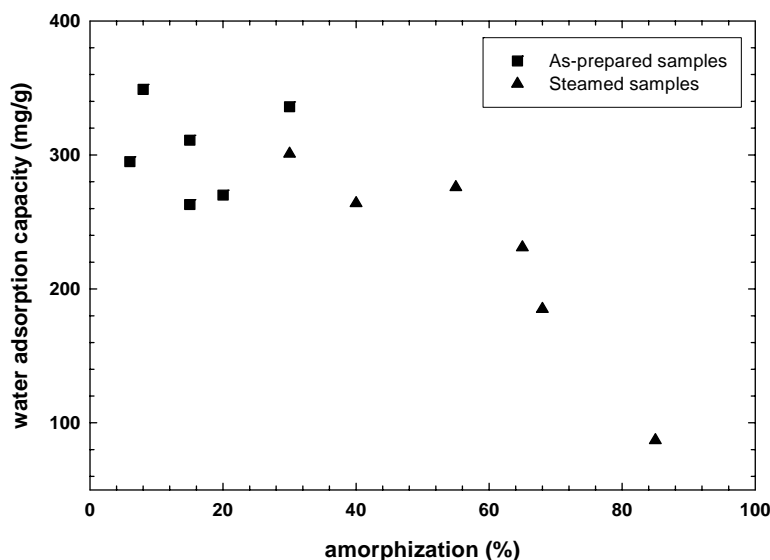
Fig. 69. Water adsorption as a function of amorphization of parent and steamed samples.

It has already been shown that the hydrothermal treatment of Y zeolite (in steam) causes a framework dealumination with increasing the n_{Si}/n_{Al}. If the dealuminated zeolite is treated in an ammounium salt solution a further ion-exchange [76] and, therefore, a further dealumination of the framework occurs. In this part a further chemical and hydrothermal treatment on dealuminated Y zeolite is discussed. Such hydrothermal treatment is consisting in: ion exchange- steaming- calcination- ion exchange of the already dealuminated Y. After applying these processes Y sample is steamed again in order to achieve the highest degree of dealumination of the framework. Taking into concideration the effect of the n_{Si}/n_{Al} of the parent zeolite on the dealumination degree two Y zeolite samples with $n_{Si}/n_{Al} = 2.66$ (> 2.5) and $n_{Si}/n_{Al} = 2.23$ (< 2.5) were used. Figur 70 reveals the X-ray patterns of Y sample with $n_{Si}/n_{Al} > 2.5$ after the first steaming (a) and second steaming with intermediate treatment (b). For this sample the intermediate treatment causes higher intensity of all diffraction peaks and lower broadening in their width. This clearly indicates a higher dealumination after the second steam. There is also a slight shift of the peaks towards higher 2θ values which refers higher n_{Si}/n_{Al} framework value. The increase of the framework silicate after the second steam with

intermediate treatment is shown in figure 71. All vibration modes become sharper in shape indicating the enrichment of framework silica. The systematic shift of the whole peaks towards higher frequency values denominates the increase of the framework silicate, i.e. the n_{Si}/n_{Al} increase. The effect of the intermediate steaming on a self-prepared sample with n_{Si}/n_{Al} < 2.5 (n_{Si}/n_{Al} =2.23) is also discussed (Fig. 72, 73).
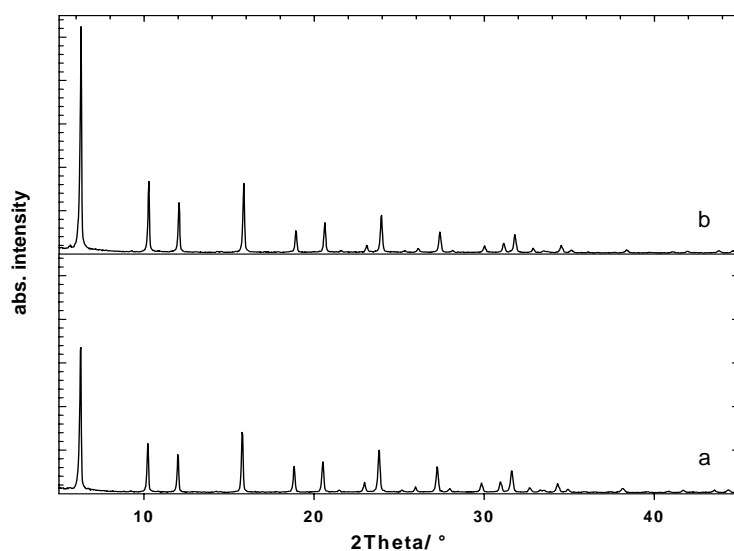
Fig. 70. X-ray patterns of commercial Y sample of n_{Si}/n_{Al} > 2.5 a) after first steam b) after second steam with intermediate treatment (ion exchange- steaming- calcination- ion exchange).
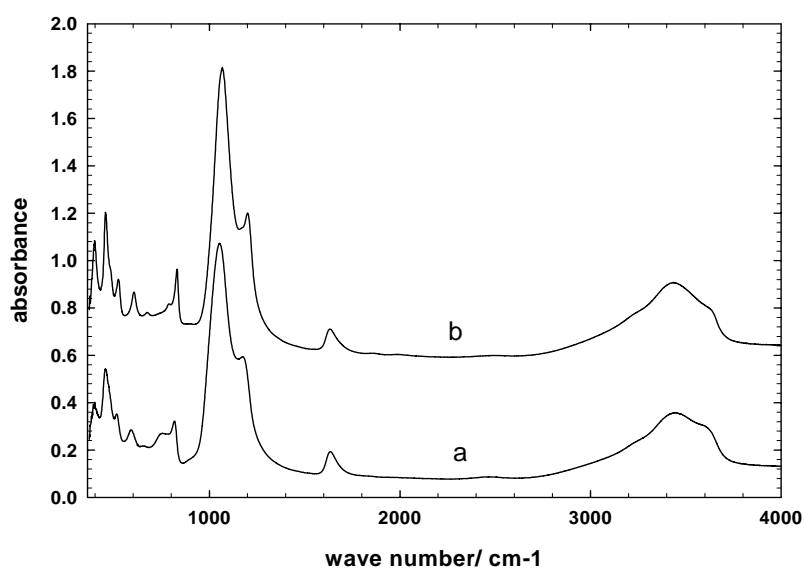
Fig. 71. IR-spectra of commercial Y sample of n_{Si}/n_{Al} > 2.5 a) after first steam b) after second steam with intermediate treatment (ion exchange- steaming- calcination- ion exchange).
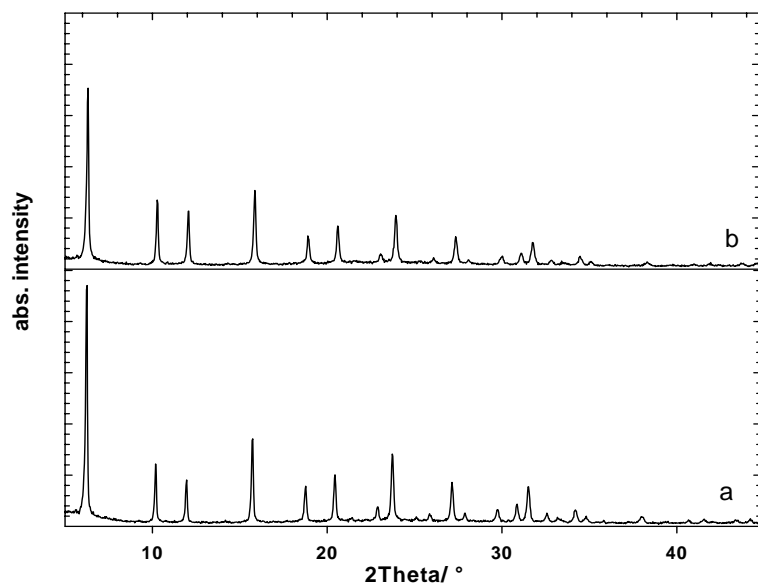
Fig. 72. X-ray patterns of Y sample of $n_{Si}/n_{Al} < 2.5$ a) after first steam b) after second steam with intermediate treatment (ion exchange- steaming- calcination- ion exchange).
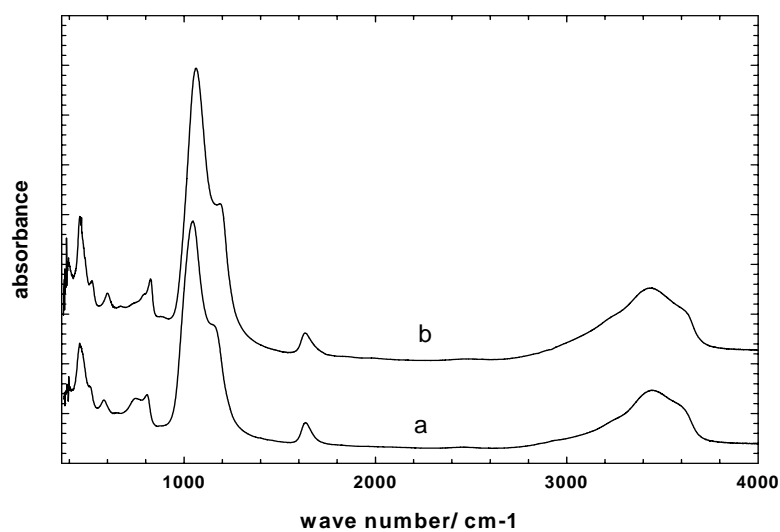
Fig. 73. IR-spectra of Y sample of $n_{Si}/n_{Al} < 2.5$ a) after first steam b) after second steam with intermediate treatment (ion exchange- steaming- calcination- ion exchange).

This sample was further dealuminated, but more amorphization also occurred, i.e. there was no healing of the defected domains. In order to explain the simultaneous occurrence of dealumination and amorphization the inhomogeniety of the silica and alumina tetrahedra distribution in the framework may be considered. In other words, there are Si-rich domains

which are able to be dealuminated and Al-rich domains destruct after steaming in the same crystal or within the aggregates.

To define the limit of silicon rich and aluminum rich sections further investigation on the definition of X- and Y-type zeolites has been performed. X and Y zeolites are related structurally to the mineral faujasite (FAU). According to Breck [4], X type is defined with $n_{Si}/n_{Al} \leq 1.5$ and Y type with $n_{Si}/n_{Al} > 1.5$. Structure behavior of these two types after steaming denotes the existence of intermediate composition within the approximate range of $1.7 \leq n_{Si}/n_{Al} \leq 2.2$. This observation has been estimated for the steamed samples of self-prepared parent zeolites. The n_{Si}/n_{Al} values have been calculated according the following empirical relation given by Rüscher et al. [63] (Fig. 74): $x = 5.348a_0 - 12.898$, where x is the Al molar fraction ($n_{Si}/n_{Al} = (1 - x)/x$) and a_0 is the lattice parameter (given in nm) estimated from X-ray powder diffraction method. These data are compared with earlier work [64] following a linear relation in the range $0.1 < x < 0.5$ which is of a good agreement with Breck's [4] description of relation between cell parameter and Al atoms per unit cell within the range of non-steamed samples ($\sim 48 < $ Al atoms $ < \sim 87$). Table 15 reveals the X-ray and IR data of synthesized and steamed samples. The steamed samples of $n_{Si}/n_{Al} \leq 1.5$ each shows an X-ray amorphous phase and no IR feature.
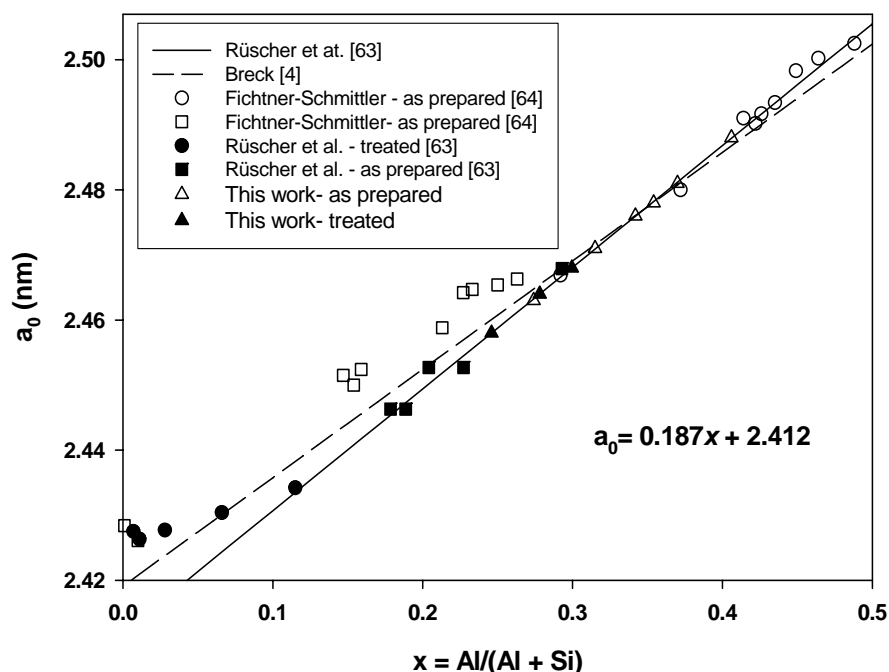

Fig. 74. Relation between Al molar fraction x and lattice parameter a_0.

With respect to their composition a strong hydrolysis of the framework may occur because of the sensitive Si-O-Al bonds in the presence of steam under which a framework hydrolysis occurs and no healing of the defected parts resulting from Al vacancies is possible because the short silicate chains inside X zeolie cannot hold the framework together. A well dealuminated FAU structure after steaming has been detected for the samples of $n_{Si}/n_{Al} > 2.5$ ($n_{Si}/n_{Al} = 2.66$) with a minimum structure destruction. ^{29}Si MAS NMR investigation of this sample detected two non-framework species after steaming; an amorphous aluminosilicate and silica gel [65]. These species denominate the heterogeneous nature of the parent Y zeolite crystals. Principally, Y zeolite crystallizes from aluminosilicate gels of a high silicate concentration. In such gels, and normally after aging at room temperature, the aluminate is totally consumed and a gel of $n_{Si}/n_{Al} = 1$ is formed with the most stable form under the given conditions. In this sense, Y zeolite may consist of a homogeneous core of a systematic Si and Al distribution which becomes gradually richer in Si in the outer sections. Consequently, the inner section of the crystal hydrolyses during steaming followed by a partial to total healing by the silicic acid supported from the rich Si parts. In the intermediate field of compositions ($1.7 \leq n_{Si}/n_{Al} \leq 2.2$) a sever to slight destruction occurs during steaming according the n_{Si}/n_{Al}. Crystals of a composition within this range are inhomogeneous and have Si-rich domains, exist already in the parent Y zeolite and they become more by dealumination, and Al-rich domains become amorphous after steaming. Such crystals may be considered as X/Y phase admixtures (Fig. 75, 76).

These results are supported theoretically and experimentally by ^{29}Si MAS NMR investigation done by Engelhardt et al. [57-58]. These authors have studied the variation of Si and Al tetrahedra as a function of silicon/aluminum ratio. For n_{Si}/n_{Al} around 1.5 the Si(3Al) group shows a maximum intensity. For $n_{Si}/n_{Al} \geq 2$ the group Si(0Al) appears significantly and Si(2Al) shows a maximum, while the group Si(4Al) shows a rapid decrease. Si(1Al) increases gradually for $n_{Si}/n_{Al} \geq 3$. In sense of this discussion and taking into consideration the n_{Si}/n_{Al} as the main factor, silicon bridges (Si-O-Si) over the whole framework should occur up n_{Si}/n_{Al} value of 2.

A practical model of FAU framework has been built up for deeper insight of the n_{Si}/n_{Al} between 2 and 3 (Fig. 77). T atoms has been consumed in two colors represent either Si or Al. The framework skeleton is first built with $n_{Si}/n_{Al} = 1$. Then Al atoms are substituted with Si atoms in selected ratios (1.40, 1.66, 2.00, 2.2, 2.43). up to $n_{Si}/n_{Al} = 2.2$ no long connected Si-

O-Si chains occur. The β-cage consists of 8 single six-ring units and each of them has 4Si : 2Al if the n_{Si}/n_{Al} of the framework is 2.
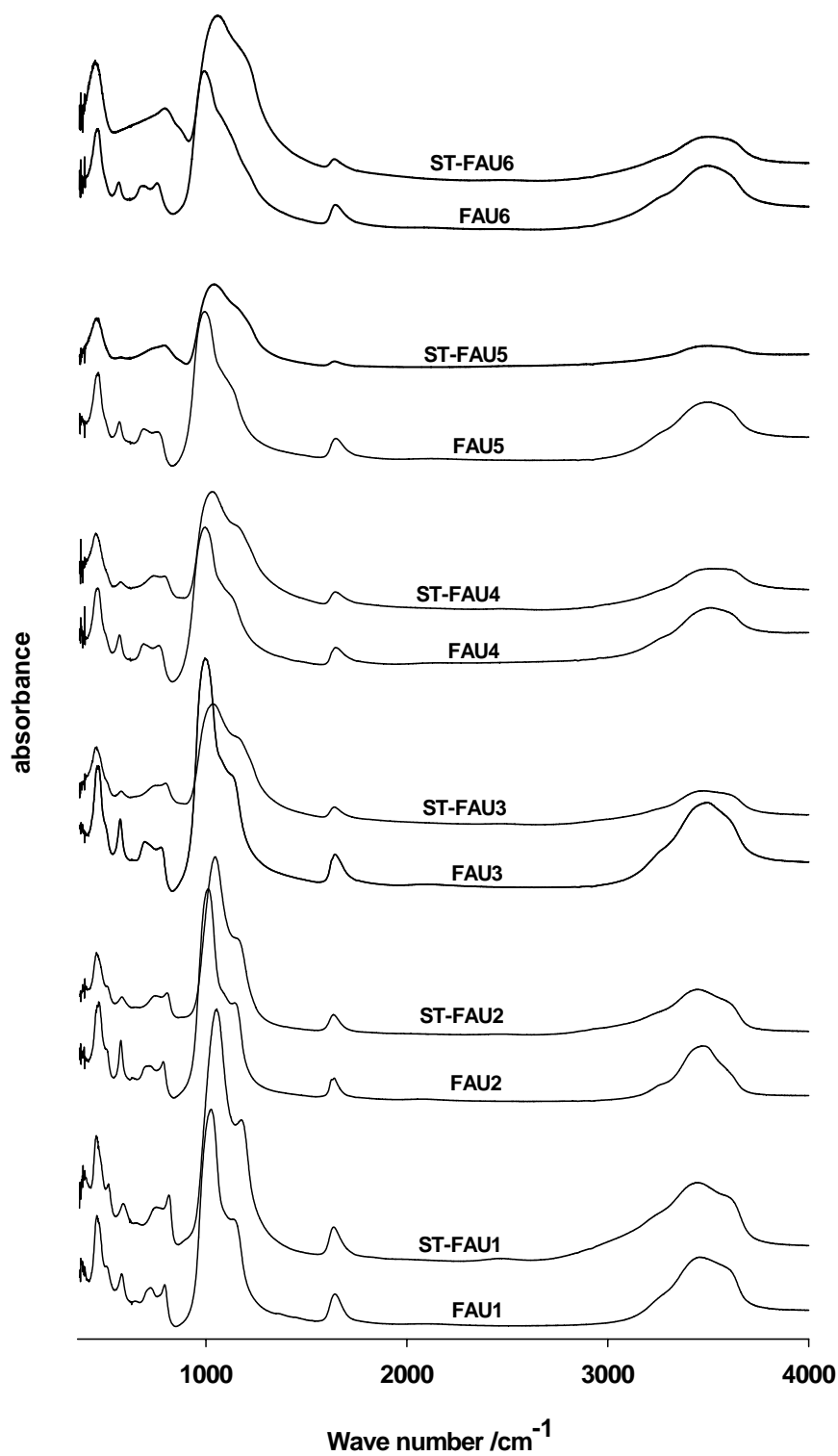

Fig. 75. IR-spectra of as-prepared and steamed samples at 773 K, 5 h, 1 bar H_2O with different n_{Si}/n_{Al} values. Related n_{Si}/n_{Al} values are given in table 17.
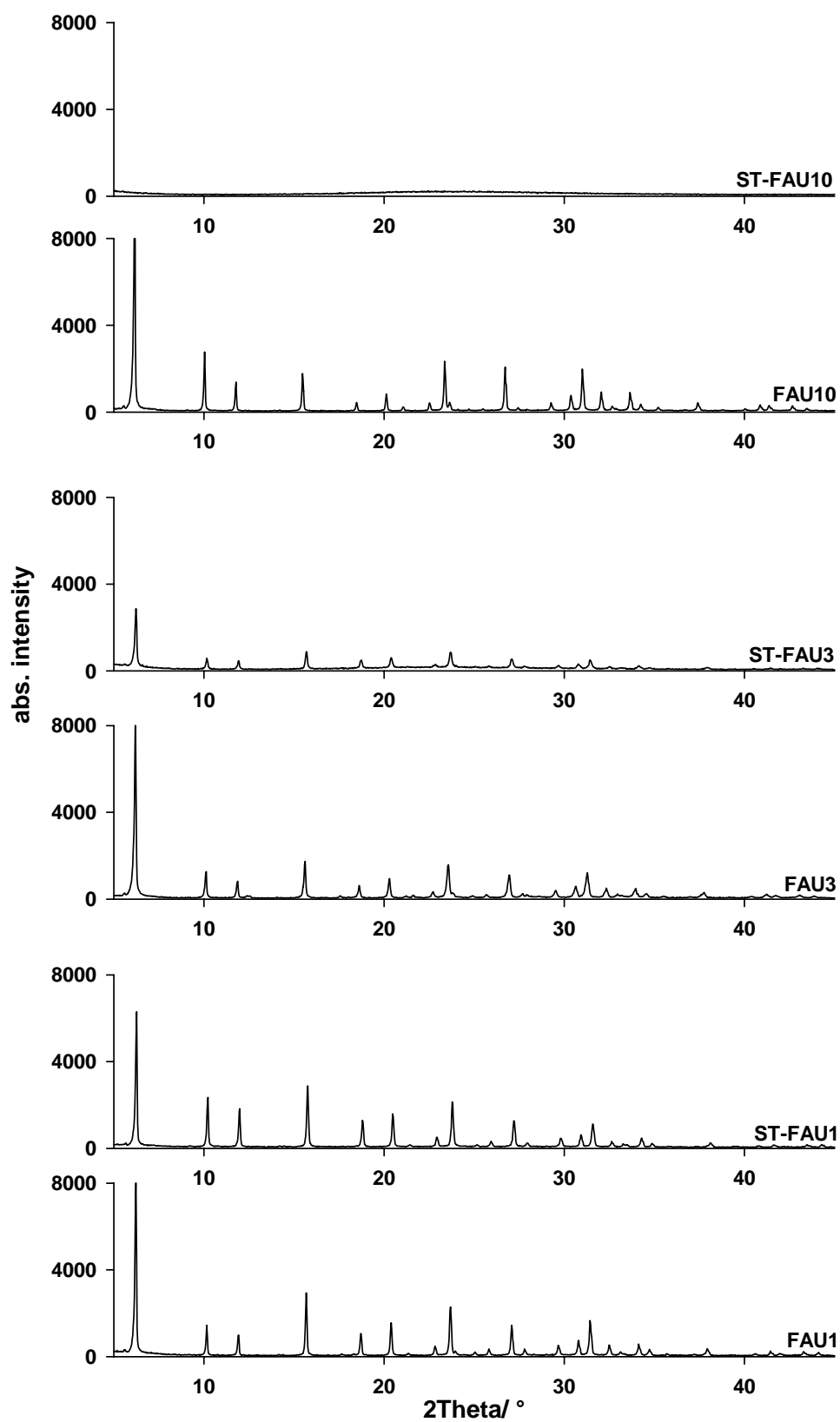
Fig. 76. XRD-patterns of as-prepared and steamed samples at 773K, 5h, 1bar H_2O with different n_{Si}/n_{Al} values. Related n_{Si}/n_{Al} values are given in table 17.
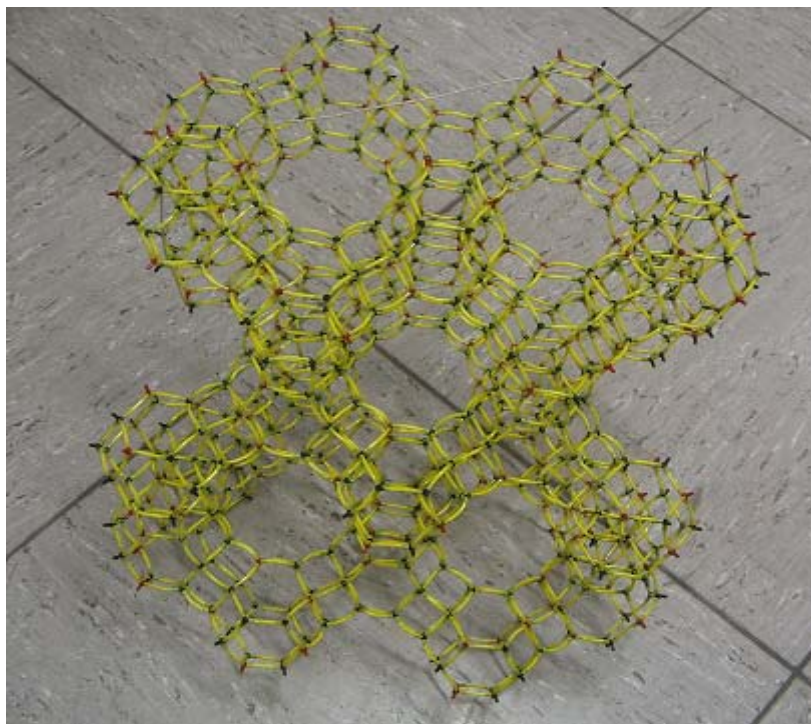
Fig. 77. Demonstration of a practical model of FAU framework.

Table 20. FAU structure types according the new definition of X and Y zeolites with respect to related n_{Si}/n_{Al} values.

Maximum partcle size/ µm	n_{Si}/n_{Al}	Ref.	Zeolite type according this work and [77]
0.3	2.16	This work	X/Y
0.3	2.39	This work	Y
0.5	2.10	[7]	X/Y
0.9	2.46	CKB[1]	Y
1.0	2.66	Zeosorb[2]	Y
1.4	2.80	[41]	Y
1.5	2.00	This work	X/Y
3.0	1.91	This work	X/Y
3.0	4.20	[41]	Y
5.0	3.80	[41]	Y
5.0	1.77	This work	X/Y
12	1.90	This work	X/Y
32	1.3	This work	X
34	~ 1.4	[46]	X
50	1.75	[41]	X/Y
140	1.36	[40]	X
150	1.70	[41]	X/Y
227	1.71	[39]	X/Y
245	1.70	[41]	X
250	1.087	[45]	X
340	1.40	[44]	X
500	~ 1.09	[45]	X

[1,2] Commercial Y zeolites

Theoretically, for the value $n_{Si}/n_{Al} = 2.428$ (17Si : 7Al in every β-cage) just one single six-ring in each β-cage will have the ratio 5Si : 1Al and a connected Si-O-Si pathway through this six ring crosses over the next β-cages defining an infinite silicon chain over the whole skeleton which stabilizes the framework during hydrothermal treatment. According to this, there is a critical n_{Si}/n_{Al} value ($n_{Si}/n_{Al} = 2.428$) above which infinite silicon bridges exist and this is the reason why Y type is most more stable than X type under steam conditions because Y type cannot collapses by the removal of Al atoms if infinite long Si-O-Si chains are present.

From all previous results presented in this study concerning the growth behaviour of X-, Y-types zeolites and the inverse relation between their crystal size and n_{Si}/n_{Al} on one hand, and the steaming behaviour of these two types on the other hand with respect to the new estimated definition of X ($n_{Si}/n_{Al} \leq 1.5$), X/Y ($1.5 < n_{Si}/n_{Al} < 2.428$) and Y ($n_{Si}/n_{Al} \geq 2.428$) types discussed here it can be concluded that Y type crystals can not grow to more than a few micrometers in size (maximum crystal size reported in literature of Y type zeolite is 5 μm with n_{Si}/n_{Al} between 3.8 and 4.2) and all large crystals (up to ca. 250 μm) reported in literature as Y type zeolite according Breck's definition (Y type is of $n_{Si}/n_{Al} > 1.5$) [4] are, indeed, X/Y mixtures. The exact type of some FAU zeolites taken from literature and this work with respect to the related n_{Si}/n_{Al} values and according the new definition of Y-type discussed here and in [77] are shown in table 20.

3.4.2. Effect of hydrothermal treatment on Y type zeolite of $n_{Si}/n_{Al} = 2.66$ as a function of temperature and time

Temperature and time effects on Y type zeolite with n_{Si}/n_{Al} of 2.66 during steaming has been investigated.

3.4.2.1. Temperature effect

X-ray diffraction patterns and IR absorption spectra (Fig. 78 and 79, respectively) reveal the dealuminated Y series of 3h steaming time and different temperatures (473 K – 1073 K). Three significant behaviors during steaming within the applied temperature ranges have been observed: Steaming at 473 K causes an amorphization of the framework Taking into consideration the inner Al-rich parts and the outer Si-rich parts of the parent zeolite. The amorphization can be explained as a partial decomposition of both parts under the influence

of water which exists as a high density steam phase at such temperature. Al-rich parts are unstable and dissolve into non-framework Al species. This effect is denoted by a significant lower peak intensity of the XRD pattern as well as the general broadening and low intensity peaks of IR spectrum. Si-rich zeolite is also soluble under saturated steam [78] and together with the residual Na^+ the high siliceous parts form a non-framework silica in form of silica gel which is denoted by a slight decrease of n_{Si}/n_{Al} indicating a loss in the framework silica. In addition to the in situ decomposition there is a slight amorphization effect of the ex situ treatment of the steamed sample at 573 K for 1 h during the transformation of NH_4Y modification into the proton form (HY). This effect is referred by the increase of v_{AS} T-O-T towards higher value whereas the w_{DR} mode does not change. At such temperature no dealumination occurs. For higher temperature step at 573 K the framework is slightly healed up because of lower water concentration with increasing temperature referred by higher intensity of the X-ray pattern. Comparing with the starting sample there is no significant change. A considerable amount of amorphous material is still denotes in this phase. At the temperature range between 673 K and 973 K a significant dealumination behavior occurs denoted by the gradual increase of peak intensities of XRD patterns and the shift towards higher 2θ values which, in turn, indicates higher framework silicate.
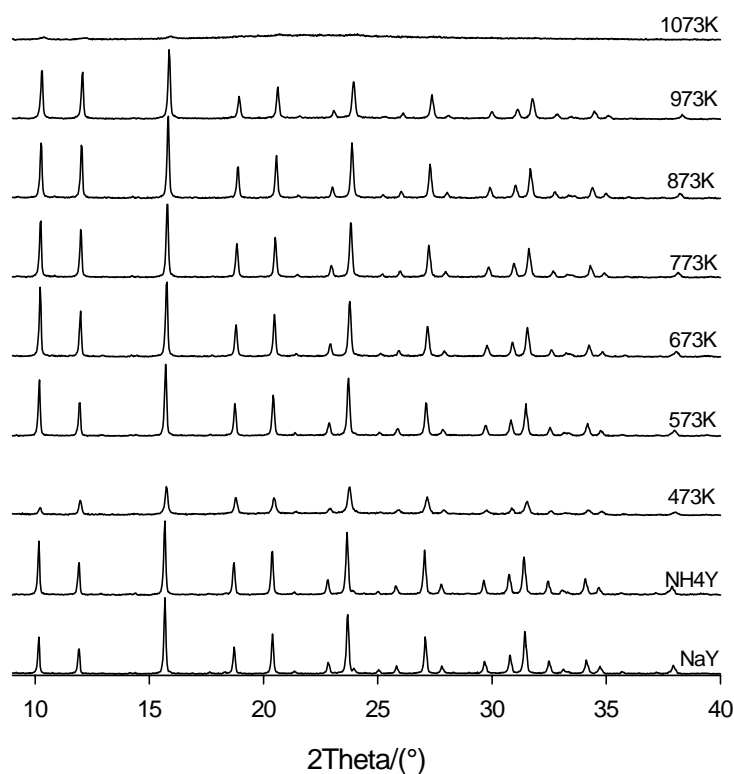

Fig. 78. Selected XRD- patterns of DAY zeolites steamed for 3 h as a function of temperature.

IR spectra also show a systematic shift of w_{DR} and v_S T-O-T modes to higher values whereas v_{AS} T-O-T shows no significant changes. The shoulder at about 518 cm^{-1} as a characteristic peak of Y type according to Flanigen et al. [52] becomes more significant dominates the increase of the framework silica. The comparison between X-ray patterns at 873 K and 973 K shows that the peak intensities of the sample at 973 K is distinctly lower than that of 873 K indicating the exist of an amorphization portion results from a partial thermal framework decomposition.
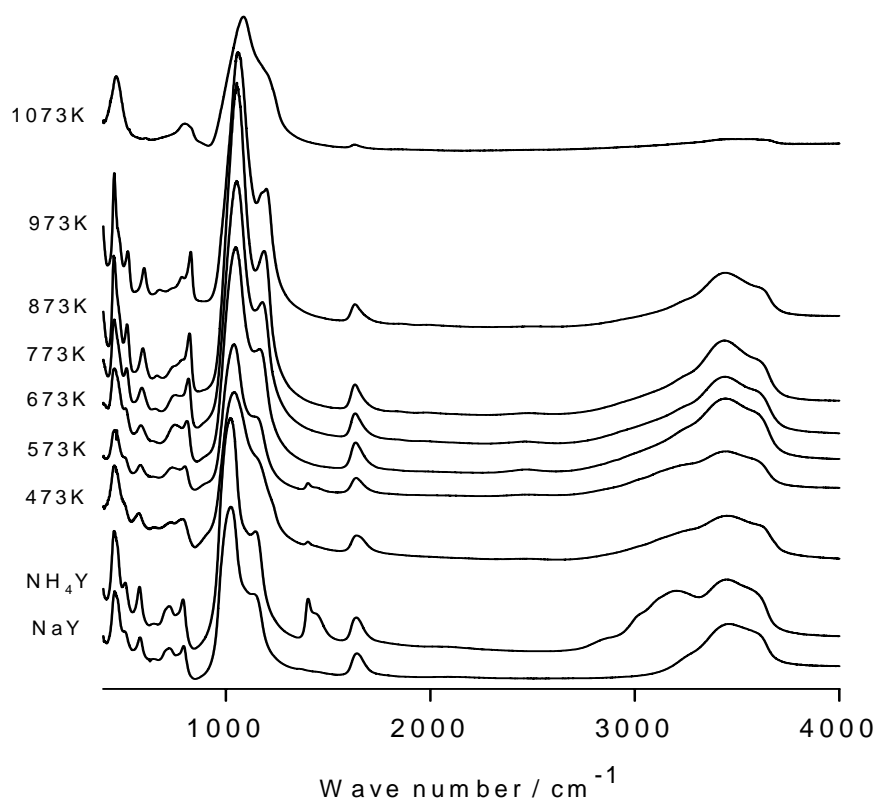

Fig. 79. Selected IR spectra of DAY zeolites steamed for 3 h as a function of temperature.

Although the IR spectrum of the 973 K sample shows a uniform Si enriched framework with highest n_{Si}/n_{Al} of 7, the 873 K sample shows the highest peak intensities (lowest amorphization portion) in the whole series. According to this, 873 K seams to be the optimal temperature range for dealumination of Y zeolite. On the other hand, it can be suggested that the whole spectra are superimposed by amorphous aluminosilicate and silica gel phases [65]. This can be referred by increasing of v_{AS} T-O-T of the whole spectra towards higher frequencies. At higher temperature step of 1073 K a sudden total framework collapse occurs denoted by an X-ray amorphous pattern without any significant peak and no IR features. This behavior is explained by an extreme loss of water vapor, which may play the role of

transportation medium of silicic acid needed for healing of the framework Thus the amorphization of the sample represents the most stable phase at such elevated temperature. The general shape of the IR spectrum of this phase is an amorphous aluminosilicate material. This is supported by earlier results revealed by [65], [79]. A systematical increase in n_{Si}/n_{Al} is observed with temperature increase (Fig. 80). However, a saturation effect in n_{Si}/n_{Al} occurs during dealumination at all applied stages. This could be due to the different stabilities of certain distributions in the Si-O-Al configurations [80].
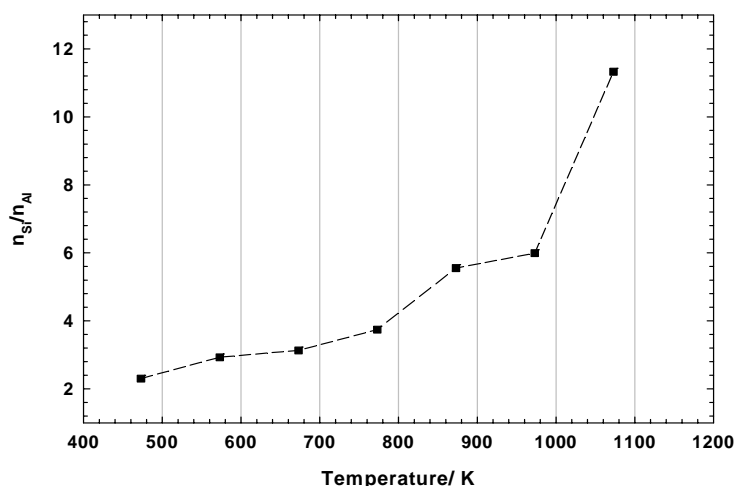
Fig. 80. Increasing n_{Si}/n_{Al} values with the increase of steaming temperature. Steaming time is 3 h.
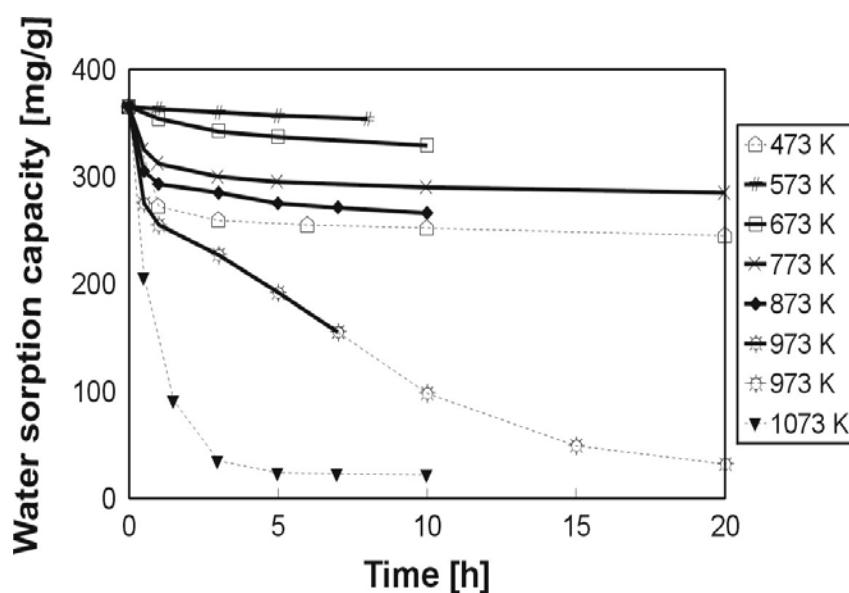
Fig. 81. Water sorption capacity of DAY zeolites as a function of temperature and time (dashed lines: range of partial up to total zeolite amorphization).

Adsorption measurement has been also performed on this series (Fig. 81). The adsorption curves of the steamed samples show a decrease towards lower values because of decrease in the total micropore volume (and formation of mesopore) and raising of hydrophobic character as a direct consequence of dealumination. A stronger decrease in adsorption values occurs at higher temperature region because of formation of amorphous non-porous materials.

3.4.2.2. Time effect

Effect of steaming time on the degree of dealumination/amorphization of HY sample at selected temperature has been also discussed. XRD patterns of the series of steamed Y samples at 473 K and different times (1, 3, 6, 10 and 20 hours) are revealed in figure 82. The decomposition at 473 K can be observed as a function of steaming time. This appears in the reduced peak intensities. A sharp decrease is caused, however, during the formation of HY modification at 573 K for 1h in air. Very slight decrease in peak intensities is shown with increasing time.

IR spectra of the same series is shown in figure 83. A similar decomposed spectra-shape over the whole spectra at different times indicates a saturation in amorphization degree directly at the beginning of treatment. The w_{DR} has the same value of 574 cm^{-1}. Also the v_{AS} T-O-T stretching mode shows slight changes in the frequency value after 1h (1039 cm^{-1}) and 20h (1043 cm^{-1}).

X-ray diffraction patterns of a series of steamed samples taken from the middle temperature range at 773 K is also presented as an example for time-variation effect at fixed temperature value (Fig. 84). A significant healing of HY framework occurs directly after 1h steaming indicating dealumination of the framework. A saturation of the dealumination portion is then achieved at this temperature with increasing time and no change in peak intensities is observed between 1h and 20h steaming time. X-ray result is supported by IR investigation on the same series (Fig. 85). A notable dealumination behavior over the whole spectra is observed starting from 1h. Low intensity and broadening of w_{DR} mode already caused during formation of HY appears in all samples which denominates the partial amorphization. A significant shift of this mode towards higher values (585 cm^{-1} after 0.5 h to 591 cm^{-1} after 5 h) is also observed at the first 5h steaming time which is explained by the framework dealumination.

On the other hand, a gradual shift of v_{AS} T-O-T mode to higher values indicates the enrichment of framework and non-framework silica. Generally, sharper peaks are obtained as a result of the dealumination effect and, consequently, higher n_{Si}/n_{Al} values.
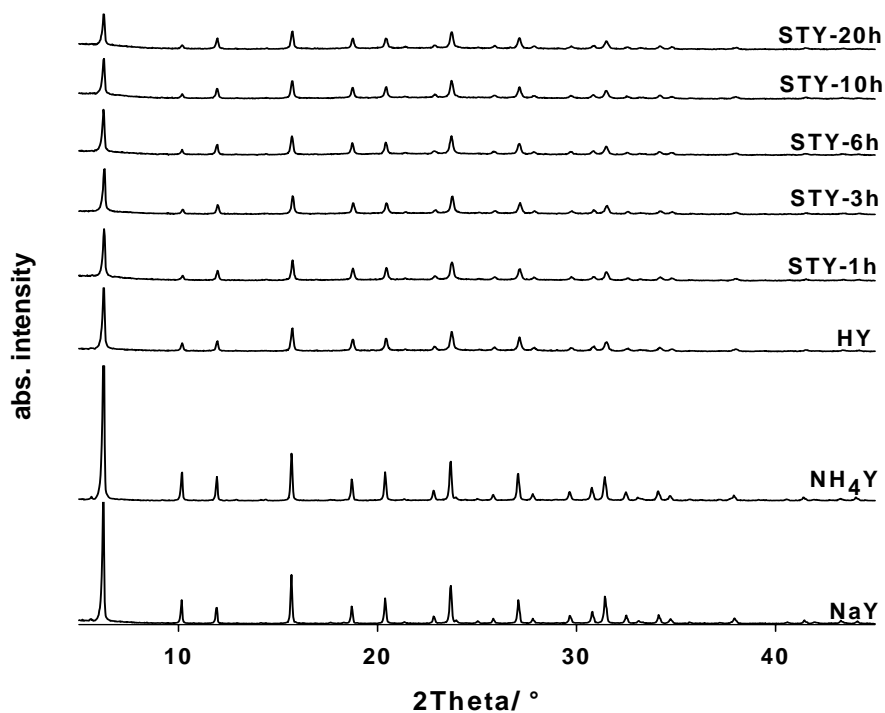

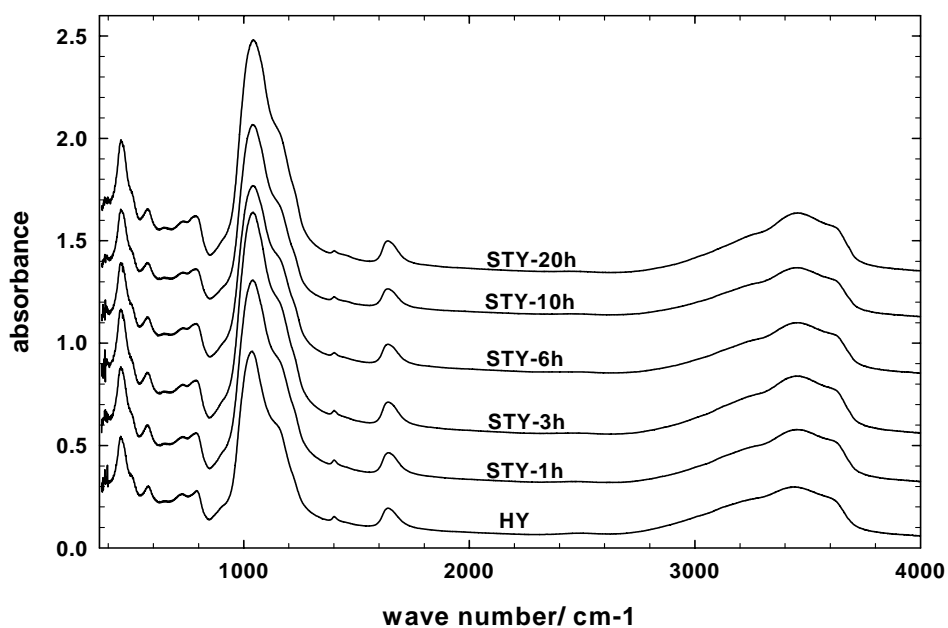Fig. 82. XRD-patterns of steamed samples for different times at 473 K.

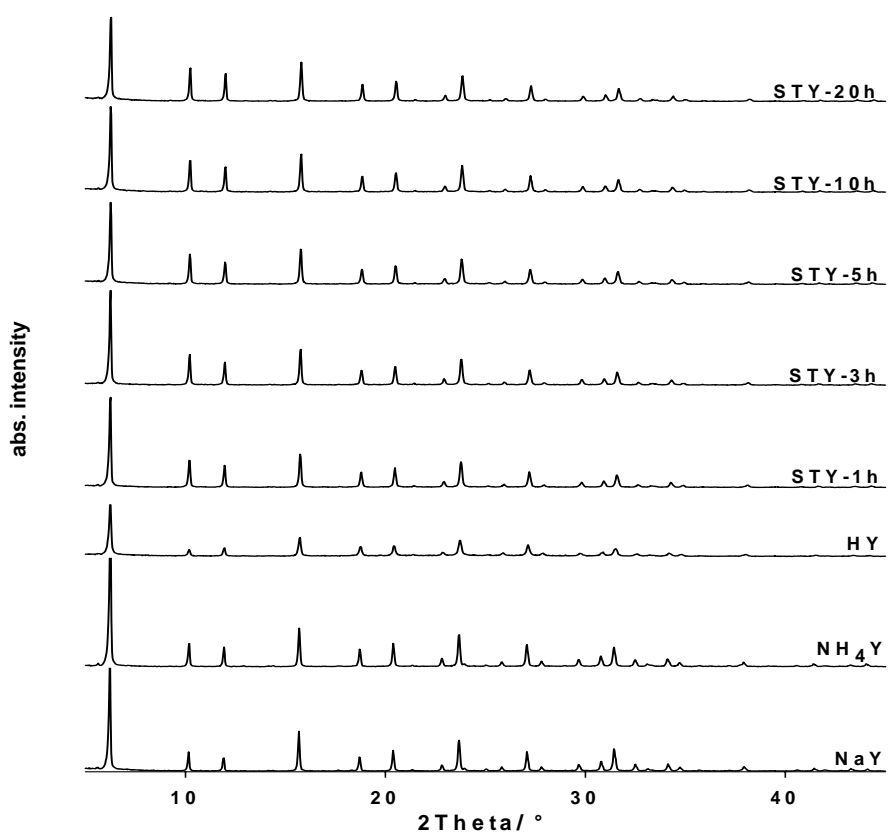Fig. 83. IR spectra of steamed samples for different times at 473 K.

Fig. 84. XRD-patterns of steamed samples at 773 K and 1 bar water pressure for different steaming times.
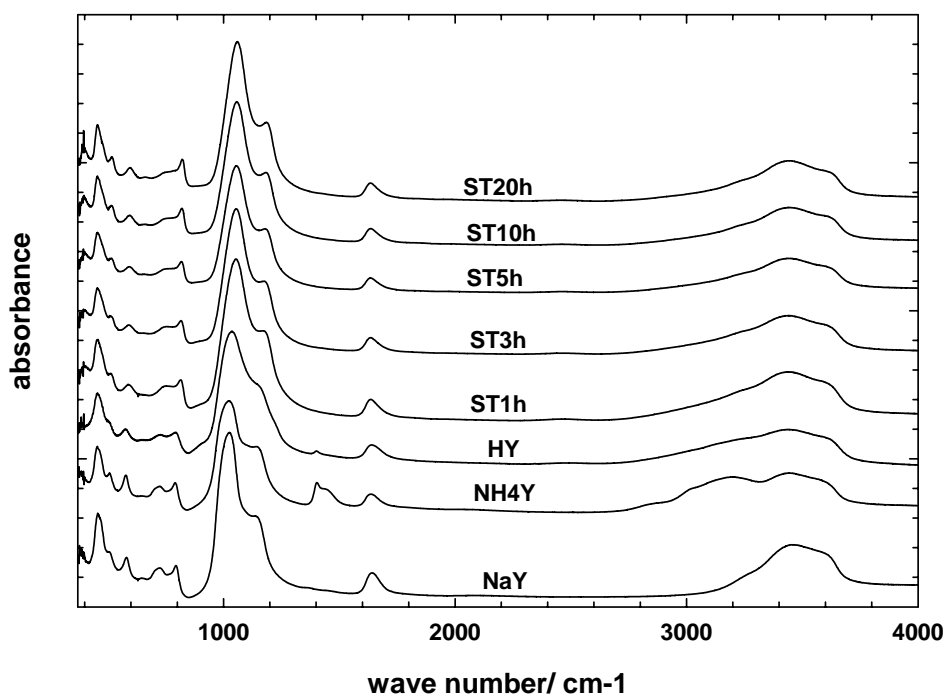

Fig. 85. IR-spectra of steamed samples at 773 K and 1 bar water pressure for different steaming times.
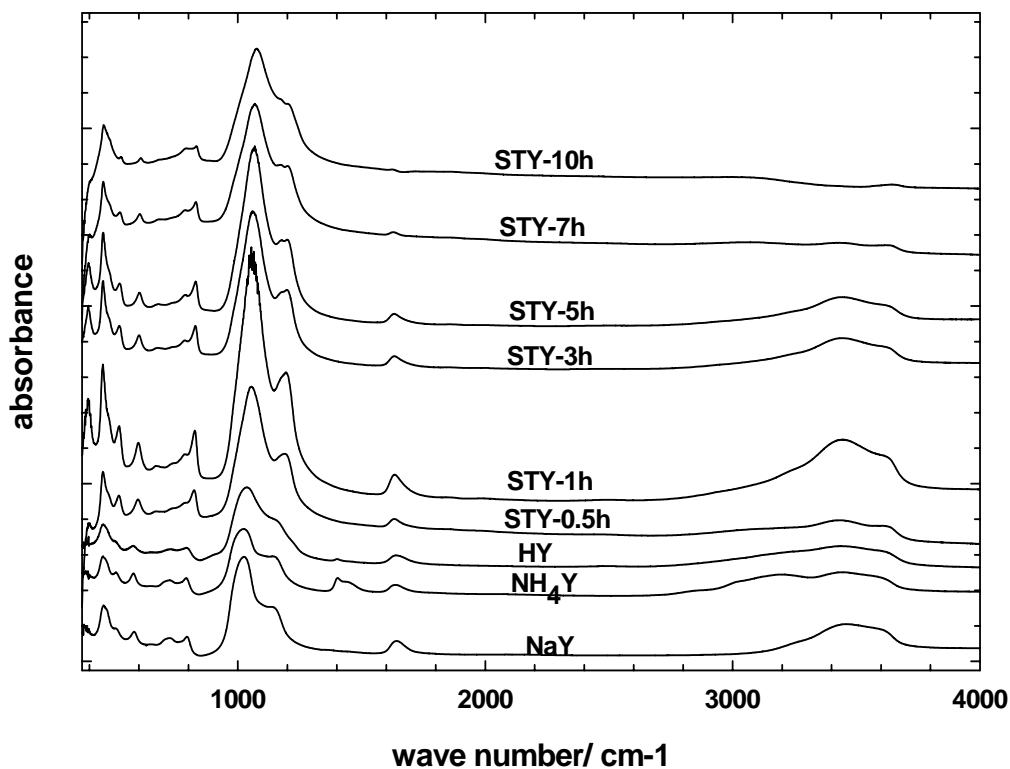
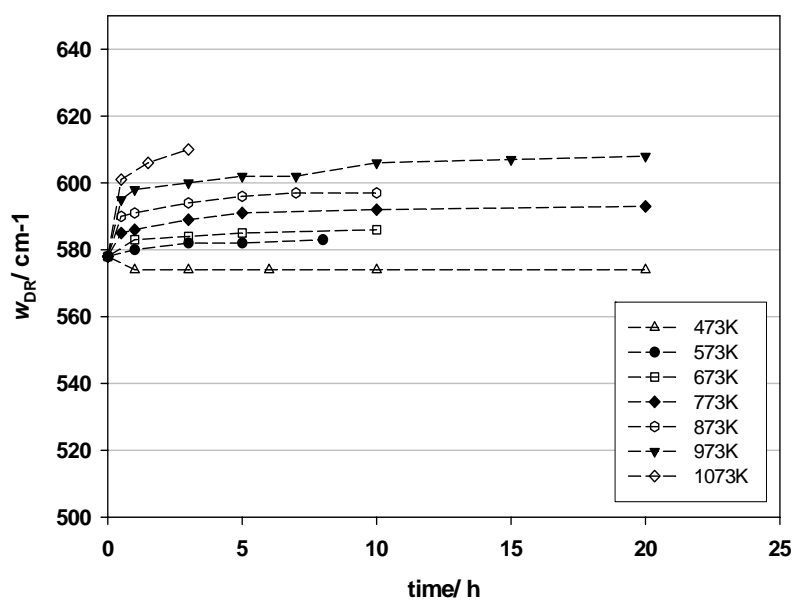Fig. 86. IR spectra of steamed samples for different times at 973 K.

Fig. 87. Change of the double six-ring mode w_{DR} as a function of steaming time variation at selected temperature ranges.
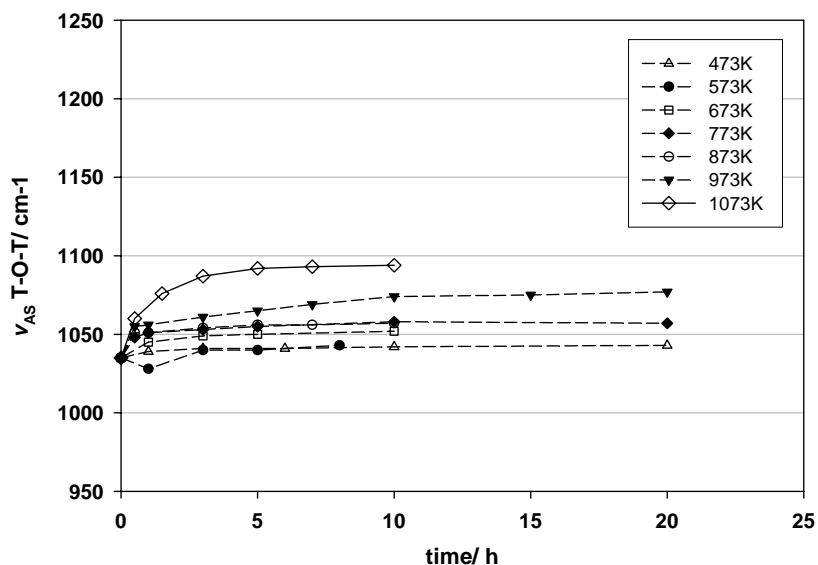
Fig. 88. Change of the asymmetric streching mode v_{AS} T-O-T as a function of steaming time variation at selected temperature steps.

A significant increase of both vibration modes is detected at higher temperature values, i.e. steaming time is more effective at high temperature ranges and reaches the maximum at the highest temperature applied at 1073 K (Fig. 86). Effect of time variation on w_{DR} and vibration modes at all selected temperatures is also revealed in figures 87 and 88. A saturation in n_{Si}/n_{Al} is also observed with increasing steaming time at selected temperatures (Fig. 89). However, with increasing steaming temperature a distinct increase in n_{Si}/n_{Al} values is observed especially at 973 K and 1073 K.
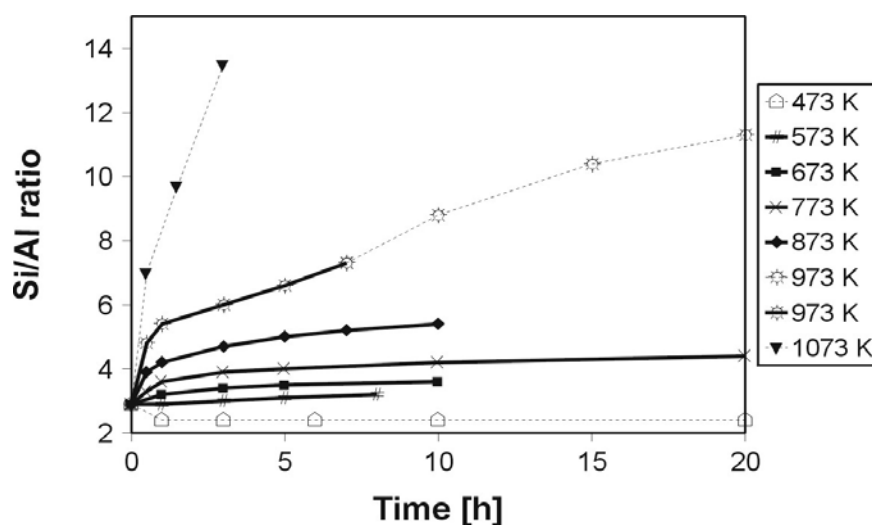

Fig. 89. Si/Al ratio of DAY zeolites steamed as a function of temperature and time (dashed lines: partial to total amorphization).

### 3.4.2.3. determination of extra-framework species by ^{29}Si MAS NMR spectroscopy and molybdate method

The existence of extra-framework species of dealuminated FAU zeolites of parent zeolites with n_{Si}/n_{Al} values between 2.0 and 2.7 (three self-prepared samples after the procedures [7], [39] and [40], and two commercial samples) has been also discussed. These samples were steamed at 873 K for 7 hours under 1 bar water pressure (Tab. 21). According Lutz et al. [65] these extra-framework species are aluminosilicate and silica gel. As discussed above the heterogeneity of FAU zeolite increases with increasing the n_{Si}/n_{Al} of the framework with Al-rich part in the center and Si-rich part in the surface. Both parts are not stable under steaming conditions and they, therefore, dissolved to some extent into aluminosilicate (formed by the hydrolysis of Al-rich parts of the crystal) and silica gel (formed by dissolution of Si-rich parts). These species could be detected using molybdate method and ^{29}Si MAS NMR spectroscopy.

Table 21. n_{Si}/n_{Al} values and degree of crystallinity of the as-prepared and the steamed samples at 873 K, 7 h and 1bar H_2O pressure.

| sample	Synthetic type	As-prepaed samples		Steamed samples	
		n_{Si}/n_{Al}[1]	Amorphization portion[2] %	n_{Si}/n_{Al}	Amorphization portion %
Zeosorb	Y	2.6981	4	4.3	22
CKB	Y	2.4619	1	4.1	23
Fahlke	X/Y	2.3913	4	3.9	26
Ginter	X/Y	2.2240	15	3.2	63
Ferchiche	X/Y	2.4619	8	3.5	32

[1] calculated form a_0 according the relation described by [64]. The a_0 is estimated by using Topas Software (see the experimental part), [2] calculated from the degree of crystallinity which estimated by XRD method.
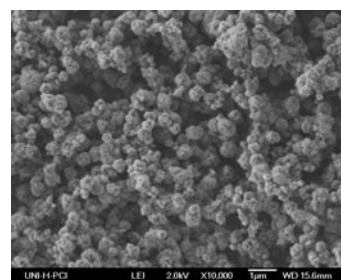
The maximum particle size of these samples is between 0.5 and 2.0 µm estimated from the direct measurement of the crystal diameter of SEM-images (Fig. 90a, 90b, 89c, 90d and 90e).

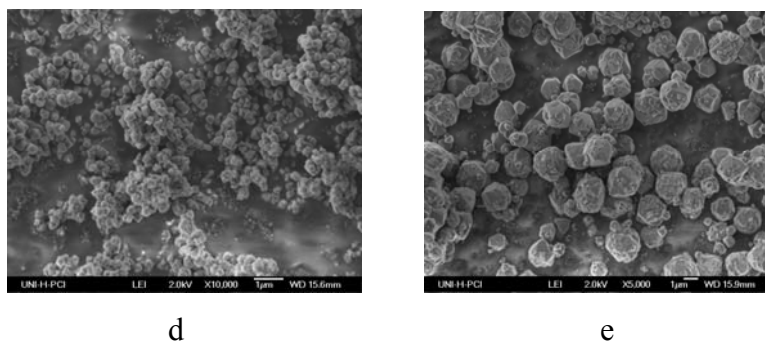a   b   c

d   e
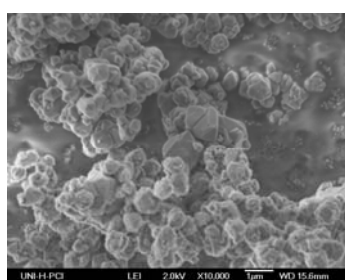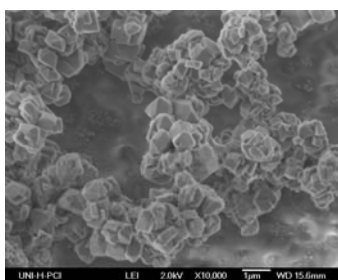
Fig. 90. SEM-images of commercial Y type (Zeosorb) with n_{Si}/n_{Al} of 2.66 (a), commercial Y type (CKB) with n_{Si}/n_{Al} of 2.46 (b), self -prepared X/Y type according Fahlke et al. [74] with n_{Si}/n_{Al} of 2.25 (c), self -prepared X/Y type according [7](Ginter) with n_{Si}/n_{Al} of 2.16 (d) self -prepared X/Y type according [40] (Ferchiche) with n_{Si}/n_{Al} of 2.00 (e). The maximum crystal diameter is 0.5-2.0 µm.

X zeolite of type LSX with n_{Si}/n_{Al} of 1 shows a straight molybdate line resulting from the active monomeric building units of this zeolite type (Fig. 91). For 13X type zeolite of n_{Si}/n_{Al} of 1.2 the molybdate line is shifted slightly to a longer time measurement because of existence of some diameric building units beside the monomeric ones. With increasing n_{Si}/n_{Al} this line is converted to a curve which indicates a longer reactant time with increasing the non-reacted silicate units (oligomeric building units). For Y zeolite ($n_{Si}/n_{Al} \geq 2.428$) only oligomeric and polymeric should be detected referring to no molybdate active material with an infinte silicate chain.
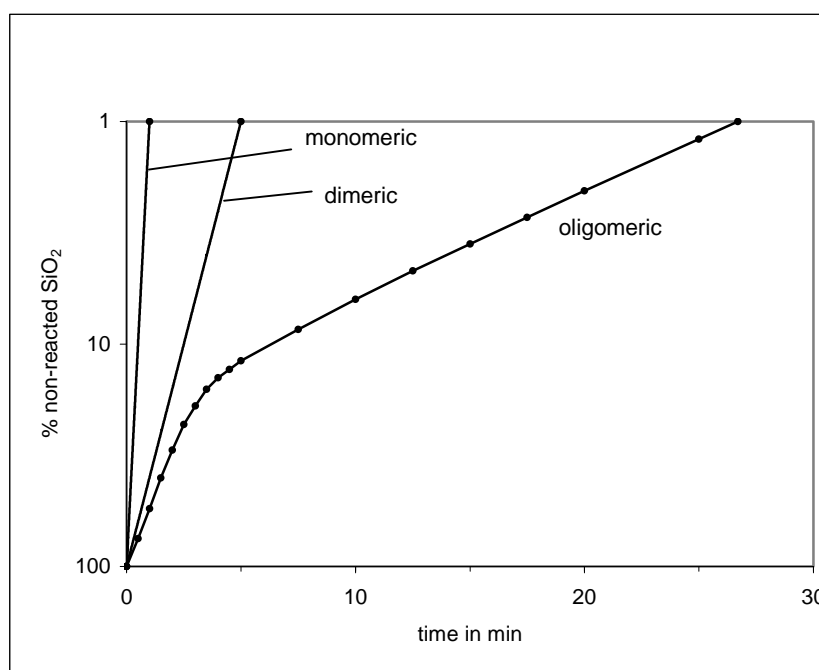

Fig. 91. Standard molybdate measurements of monomeric, diameric and oligomeric building units.

Comparing the standard curves with the molybdate curves of our as-prepared samples a portion of the monomeric building units is observed indicating a molybdate active material in all samples (Fig. 92). This behaviour is explained by Rüscher et al. [77] as the co-existence of X/Y mixtures in the samples with $n_{Si}/n_{Al} = 2.25$ (Fahlke), $n_{Si}/n_{Al} = 2.2$ (Ginter) and $n_{Si}/n_{Al} = 2.0$ (Ferchiche). Zeolites of Y type with $n_{Si}/n_{Al} = 2.46$ (CKB) and $n_{Si}/n_{Al} = 2.66$ (Zeosorb) show also molybdate active curves because of the gradient in n_{Si}/n_{Al} distribution with values of 1 in the center increases gradually to the surface of the crystal.
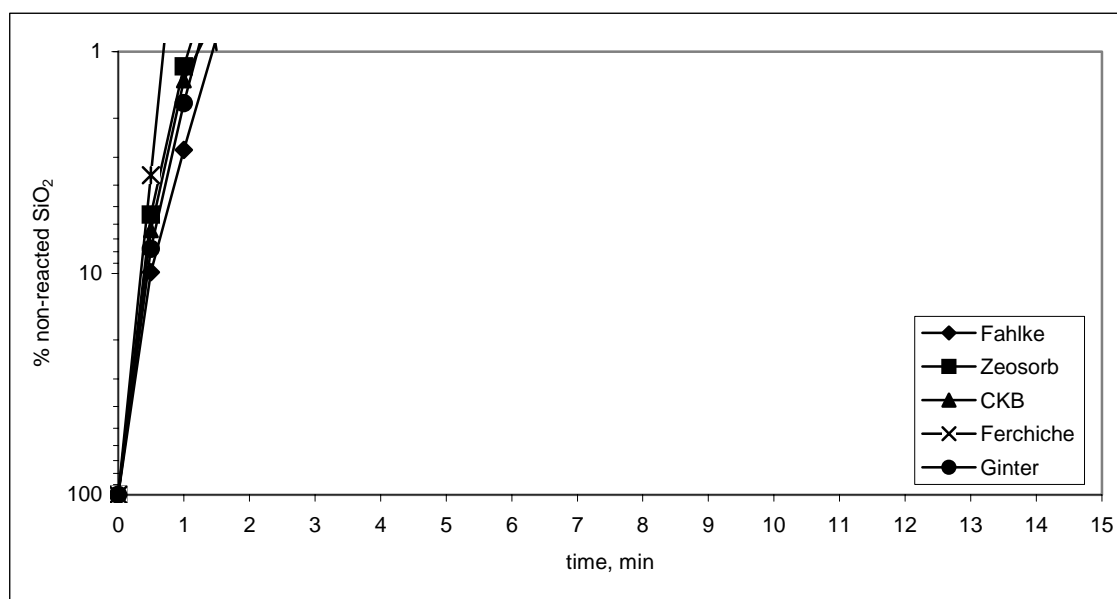

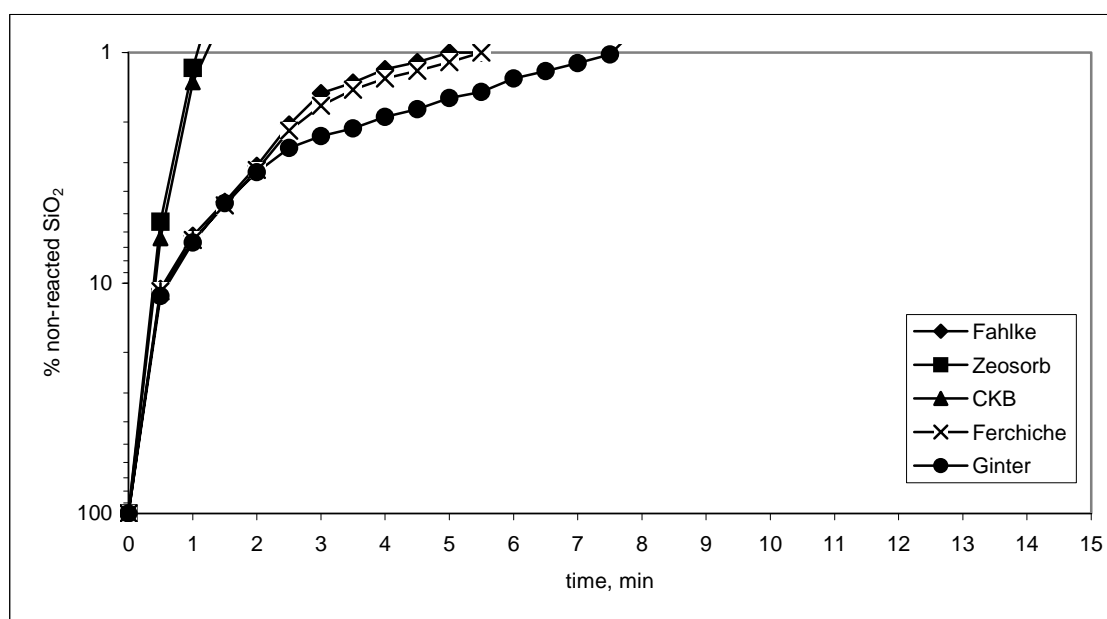Fig. 92. Molybdate curves of the as-prepared samples.

Fig. 93. Molybdate curves of the steamed samples at 873 K, 7 h and 1 bar water pressure.

Whereas the formed aluminosilicate species under steaming conditions could be detected by molybdate method, the formed silica gel can not be detected because of the existence of only polymeric building units which are molybdate inactive (Fig. 93). An amorphous aluminosilicate has a n_{Si}/n_{Al} of 1 which means it consists of monomeric building units. This amorphous part appears in all samples. The framework aluminosilicate after steaming consists of long and middle silicate chains. For the steamed Zeosorb and CKB the aluminosilicate framework consists of infinite silicate chains which could not be detected by molybdate measurement. However, a portion of diameric units is also exist in these two samples and this could be detected. The other three samples of lower n_{Si}/n_{Al} values of the parent zeolites become richer in silicate after steaming with long and middle oligomeric units which are detectable in the molybdate curves of these samples.

The typical five finger prints of FAU type zeolite appear by ^{29}Si MAS NMR measurements with a slight difference of the peak intensities according to their individual framework n_{Si}/n_{Al} with Si(4Al), Si(3Al), Si(2Al), Si(1Al) and Si(0Al) in the range of chemical shift between -84 and -108 ppm (Fig. 94). The very low amount of the amorphization portion of the as-prepared samples do not appear after the deconvolution and simulation of the spectra (III). After steaming at 873 K for 7 hours and 1 bar water pressure higher framework n_{Si}/n_{Al} values occur as a consequence of dealumination. The peak intensities of Si(4Al), Si(3Al) and Si(2Al) decrease, therefore, while the intensity of Si(1Al) and Si(0Al) peaks increases significantly. A partial hydrolysis of zeolite framework takes place and, therefore, non-framework aluminosilicate and silica gel species are formed [65].
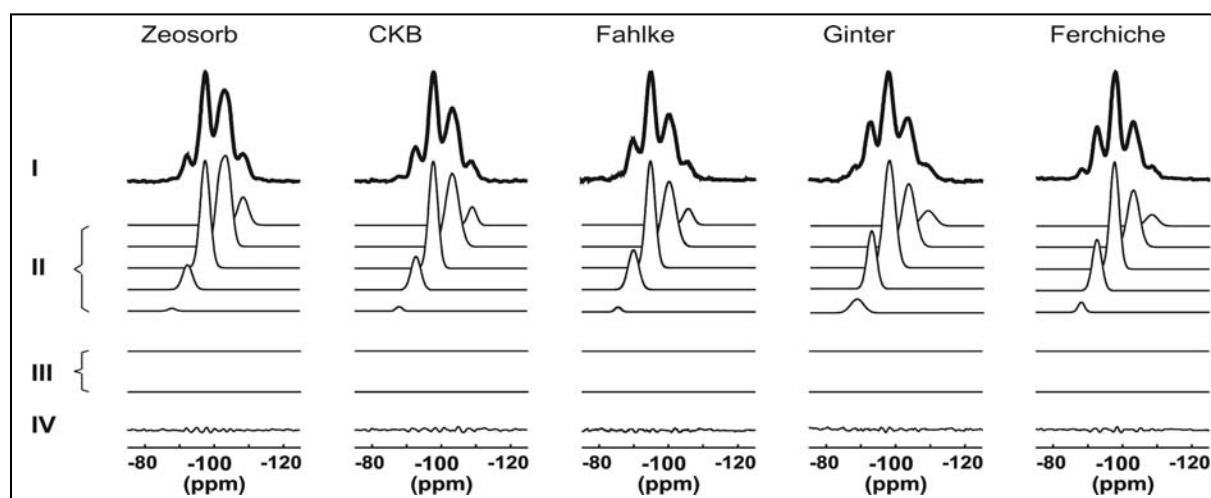

Fig. 94. Measured (I), deconvoluted (II and III) and difference between measured and deconvoluted (IV) ^{29}Si MAS NMR spectra of the as-prepared samples.

The convoluted and simulated NMR spectra refer to an occurrence of two shoulders in the region between -80 and -90 ppm and at about -112 ppm denoted by a (for the extra aluminosilicate species) and s (for the silica gel [81]) (Fig. 95). This means an occurrence of extra non-framework species. The indirect analysis of non-framework aluminosilicate and silica gel is further described in Lutz et al. [81].
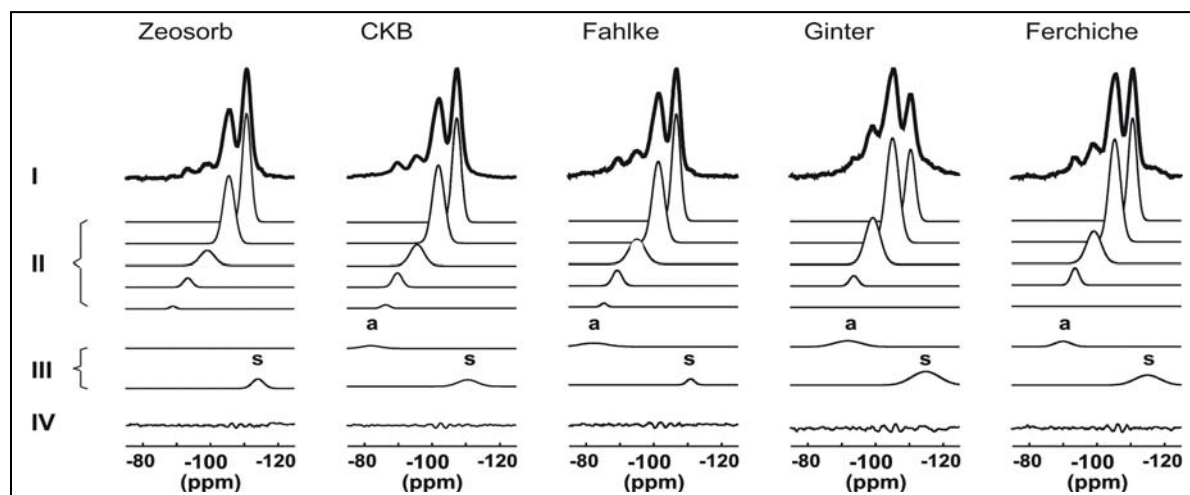

Fig. 95. Measured (I), deconvoluted (II and III) and difference between measured and deconvoluted (IV) ^{29}Si MAS NMR spectra of the steamed samples at 873K, 7h and 1bar H2O.

References:

[1]   A. F. Kronstedt, Konglike Svenska Vetenstapf Academica Handlingar, Vol. 18 (1756) 111.

[2]   Barrer, Hydrothermal Chemistry of Zeolites. Academic Press, London, New York 1982.

[3]   L. Puppe, Chemie in unserer Zeit, 20(4) (1986) 117.

[4]   D. W. Breck, Zeolite Molecular Sieves; structure, chemistry, and use. John Wiley & Sons, New York 1974.

[5]   The zeolite homepage of Volker Betz (http://members.aol.com/vbetz/Zeolites.html), last update Feb. 19, 2005.

[6]   W. M. Meier, D.H. Olson, atlas of zeolite framework types (2001) 132; and database of zeolite structure (http://www.iza-structure.org/databases/); International Zeolite Association (2000).

[7]   D. M. Ginter, A. T. Bell, C. J. Radke, in Synthesis of Microporous Materials, Vol. I, Molecular Aieves, M. L. Occelli, H. E. Robson (eds.), Van Nostrand Reinhold, New York (1992) 6.

[8]   S. P. Zhdanov, S. S. Khvoshchev, N. N. Feokistova, Synthetic Zeolites, vol. 1, Gordon & Breach Science Publishers, New York (1990) 197.

[9]   S. P. Zhdanov, Adv. Chem. Ser., 101 (1971) 20.

[10] B. Fahlke, W. Wieker und E. Thilo, Z. Anorg. Allg. Chem., 347 (1966) 82.

[11] B. Fahlke, P. Starke, V. Seefeld and W. Wieker and K.-P. Wendlandt, Zeolites, 17 (1987) 209.

[12] E. Thilo, W. Wieker, H. Stade, Z. Anorg. Allg. Chem., 340 (1965) 261.

[13] E. M. Flanigen, Molecular sieves, 121 (1973) 119.

[14] H. Lechert, P. Staelin, M. Wrobel, U. Schimmel, Nucleation Gels for the Synthesis of Faujasite Type Zeolites, p. 147, in: J. Weitkamp, H. G. Karge, H. Pfeifer, W. Hölderich (Eds.), Zeolites and Related Microporous Materials: State of the Art 1994, Studies in Surface Science and Catalysis, Vol. 84, Elsevier Science B.V. (1994) 147.

[15] H. Lechert, H. Kacirek, Zeolites, 11 (1991) 720.

[16] H. Lechert, H. Kacirek, Zeolites, 13 (1993) 192.

[17] H. Lechert, Zeolites 17 (1996) 473.

[18] H. Lechert, H. Kacirek, Molecular Sieves, M. Occelli, H. Robson, 1 (1992) 494.

[19] H. Lechert, Verified Syntheses of Zeolitic Materials. H. Robson, (2001) 33.

[20] H. Lechert, H. Robson, Micropor. Mesopor. Mater., 22 (1998) 495.

[21] K. E. Hamilton, E. N. Coker, A. sacco, Jr., A. G. Dixon, R. W. Thompson, Zeolites, 13 (1993) 645.

[22] G. Scott, R.W. Thompson, A.G. Dixon, A. Sacco, Jr., Zeolites, 10 (1990) 44.

[23] J. A. Kostinko, ACS Symposium Series, 218 (1983) 3.

[24] R. W. Thompson, Zeolites, 9 (1989) 496.

[25] J. Warzywoda, N. Baç, A. Sacco Jr., J. Crystal Growth 204 (1999) 539.

[26] V. Valtchev, S. Mintova, V. Dimov, A. Toneva, Zeolites 15 (1995)193.

[27] McMillan, P. Am. Mineral, 69 (1984) 622.

[28] M. Taylor, G. E. Brown, Geochim. Cosmochim. Acta. 43 (1979) 1467.

[29] H. Köroğlu, A. Sarıoğlan, M. Tatlıer, A. Erdem-Şenatalar, Ö. Savaşçi, Crystal Growth 241 (2002) 481.

[30] L. B. Sand, Pure & Appl. Chem., 52 (1980) 2105.

[31] Vega, A. J., *ACS Symp. Ser.,* No. 218 (1983) 217.

[32] Melchior M. T., *ACS Symp. Ser.*, No. 218 (1983) 243.

[33] P. Pichat, R. Beaumont, D. Barthomeuf, J. Chem. Soc. Faraday Trans.**,** 70 (1977) 1402.

[34] C. M. B. Henderson, D. Taylor, Spectrochemica Acta 33 (1977) 283.

[35] P. K. Dutta, D. C. Shieh, M. Puri, Phys. Chem., 91 (1987) 2332.

[36] Chen N Y, Degnan T F. Chem Eng Prog 84(2) (1988) 32.

[37] Venuto P B, Habib Jr. FT. In: Fluid catalytic cracking with zeolite catalysts, New York: Marcel Dekker, 1979, p. 42.

[38] Wojciechowski B W, Corma A. In: Catalytic cracking: catalysis, chemistry, and kinetics, New York: Marcel Dekker (1986) 73.

[39]   J. F. Charnell, J. cryst. growth, 8 (1971) 291.

[40] S. Ferchiche, M. Valcheva-Traykova, D. E. W. Vaughan, J. Warzywoda, A. Sacco Jr., J. cryst. Growth, 222 (2001) 801.

[41] Chr. Berger, R. Gläser, R. A. Rakoczy, J. Weitkamp, Micropor. and Mesopor. Mater. 83 (2005) 333.

[42] H. Kacirek and H. Lechert, J. Phys. Chem., 79 (1975) 1589.

[43] H. Robson, High-Silica Faujasit by Direct Synthesis, in: Zeolite Synthesis, Chapter 30, American Chemical Society (1989) 436.

[44] J. Warzywoda, N. BaÇ, A. Sacco Jr., J. cryst. growth , 204 (1999) 539.

[45] V. N. Bogomolov, V. P. Petranovsky, Zeolites 6 (1986) 418.

[46] K. E. Hamilton, E. N. Coker, A. sacco, Jr., A. G. Dixon, R. W. Thompson, Zeolites, 13 (1993) 645.

[47] S. P. Zhdanov, A. V. Kiselev, V. I. Lygin, T. I. Titova, Zh. Fiz. Chim. 38 (1964) 2408.

[48] A. V. Kiselev, V. I. Lygin, in Infrared Spectra of Adsorbed Species by L. H. Little, Academic Press, New York, (1966) 361.

[49] P. Pichat, R. Beaumont, D. Barthomeuf, Compt. Rend. C 272 (1971) 612.

[50] P. Pichat, R. Beaumont, D. Barthomeuf, J. Chem. Soc. Faraday Trans. 1 70 (1974) 1402.

[51] D. W. Breck, E. M. Flanigen in : Molecular Sieves, Soc. Chem. Indust., London (1968) 47.

[52] E. M. Flanigen, H. Khatami, H. A. Szymanski, Adv. Chem. Ser. 101 (1971) 201.

[53] E. Dempsey, G. H. Kühl, D. H. Olson, J. Chem. Phys. 73 (1969) 387.

[54] U. Lohse, E. Alsdorf, H. Stach, A.V. Kiselev, Z. Anorg. Allg. Chem., 447 (1978) 64.

[55] U. Lohse, E. Alsdorf, H. Stach, H. Thamm, W. Schirmer, A. A. Isirikjan, N.I. Regent, M. M. Dubinin, Z. Anorg. Allg. Chem., 460 (1980) 179.

[56] U. Lohse, M. Mildebrath, Z. Anorg. Allg. Chem., 476 (1981) 126.

[57] G. Engelhardt, U. Lohse, E. Lippmaa, M. Tarmak, M. Mägi, Z. Anorg. Allg. Chem., 482 (1981) 49.

[58] G. Engelhardt, U. Lohse, V. Patzelova, M. Mägi, E. Lippmaa, Zeolites 3 (1983) 233.

[59] K. Sato, Y. Nishimura, N. Matsubayashi, M. Imamura, H. Shimada, Micropor. Mesopor. Mater., 59 (2003) 133.

[60] J. Datka, B. Gil, T. Domatala, K. Góra-Marek, Micropor. Mesopor. Mater., 47 (2001) 61.

[61] G. Weber, M. Simonot-Grange, Zeolites 14 (1994) 433.

[62] D. P. Siantar, W. S. Millman, J. J. Fripiat, Zeolites 15 (1995) 556.

[63] C. H. Rüscher, J.-Chr. Buhl, W. Lutz, in: A. Galarneau, F. Di Renzo, F. Fajula, J. Vedrine (Eds.), Zeolite and Mesoporous Materials at the Dawn of the 21st Century, Stud. Surf. Sci. Cat., Vol. 135, Eelsevier, Amsterdam (2001) 1.

[64] H. Fichtner-Schmittler, U. Llohse, H. Miessner, H.-E. Maneck, Z. phys. Chem. Leipzig 271 (1990) 69.

[65] W. Lutz, C. H. Rüscher, D. Heidemann, Microporous and Mesoporous Materials 55 (2002) 193.

[66] G. Engelhardt, U. Lohse, A. Samoson, M. Mägi, M. Tarmak, E. Lippmaa, Zeolites 2 (1982) 59.

[67] G. Engelhardt, U. Lohse, V. Patzelova, M. Mägi, E. Lippmaa, Zeolites 3 (1983) 239.

[68] J. Klinowski, C. A. Fyfe, G. C. Gobbi, J. Chem. Soc., Farady Trans. 1, 81 (1985) 3003.

[69] M. W. Anderson, J. Klinowski, J. Chem. Soc., Faraday Trans. 1, 82 (1986) 1449.

[70] H. Hamdan, B. Sulikowski, J. Klinowski, J- Phys. Chem. 93 (1989) 350.

[71] G. Zi, T. Yi, Zeolites 8 (1988) 232.

[72] A. Gola, B. Rebours, E. Milazzo, J. Lynch, E. Benazzi, S. Lacombe, L. Delevoye, C. Fernandez, Micropor. Mesopor. Mater., 40 (2000) 73.

[73] B. A. Holmberg, H. Wang, Y. Yan, Micropor. Mesopor. Mater., 74 (2004) 189.

[74] B. Fahlke, W. Wieker, H. Fürtig, W. Roscher, R. Seidel, Z. Anorg. Allg. Chem., 439 (1978) 95.

[75] D. Massiot, H. Thiele, A. Germanus, Bruker Report 140 (1994) 43.

[76] N. Salman, C. H. Rüscher, J.-Chr. Buhl, W. Lutz, H. Toufar, M. Stöcker, Micropor. and Mesopor. Mater. 90 (2006) 339.

[77] C. H. Rüscher, N. Salman, J.-Chr. Buhl, W. Lutz, Micropor. and Mesopor. Mater. 92 (2006) 309.

[78] K. Ehrhardt, M. Suckow, W. Lutz, in: H.K. Beyer, H.G. Karge, I. Kirici, J.B. Nagy (Eds.), Catalysis by Microporous Materials, Stud. Surf. Sci. Catal., Vol. 94, Elsevier, London (1995) 179.

[79] C. H. Rüscher, J.-Chr. Buhl, W. Lutz, in: D. Rammlmair, J. Mederer, Th. Oberthür, R.B. Heimann, H. Pentighaus (Eds.), Applied Mineralogy in Research, Economy, Technology, Ecology and Culture, Vol.1, Balkema, Rotterdam (2000) 225.

[80] R. Beaumont, D. Barthomeuf, Catal., 27 (1072) 45.

[81] W. Lutz, H. Toufar, D. Heidemann, N. Salman, C.H. Rüscher, T.M. Gesing, J.-Chr. Buhl, R. Bertram, Micropor. and Mesopor. Mater. (2006) submitted.

ACKNOWLEDGEMENTS

Lebenslauf

Persönliche Daten   Nada Salman, geboren am 21.10.1976 in Hreissoun/ Syrien

Schulausbildung

1982-1988	Volksschule, Banias/ Syrien
1988-1991	Mittelschule, Banias/ Syrien
1991-1995	Gymnasium, Banias/ Syrien, (Abitur)

Studium

1995-1999	Studium der Geologie an der Tishreen –Universität, Lattakia/ Syrien
1999-2000	Postgraduiertenstudium an der Universität Damaskus (Diplom im Bereich Geologie-Hydrogeologie)

Tätigkeiten

04/2001	Assistentin an der Naturwissenschaftlichen Fakultät der Tishreen Universität, Lattakia/ Syrien
10/2002	Promotionsstudium in Mineralogie-Kristallographie, Institut für Mineralogie, Leibniz Universität Hannover